ICEM2022 VALENCIA

XXV International Conference on Electrical Machines

Valencia Conference Centre
Valencia - SPAIN

September 5-8, 2022

Design, Identification and Simulation of PM Synchronous Machines for Traction

gianmario.pellegrino@polito.it and simone.ferrari@polito.it

Politecnico di Torino, Turin, Italy

About the speakers

Gianmario Pellegrino (F' 22, SM '13, M'06) is Professor of Power Converters, Electrical Machines and Drives at Politecnico di Torino. Dr. Pellegrino is constantly engaged in research projects with the industry, and the co-founder of the open-source project SyR-e. He was a visiting fellow at Aalborg University, the University of Nottingham, and the University of Wisconsin-Madison. He has 60 IEEE journal papers, five patents and nine Best Paper Awards. He is an IEEE Fellow and the recipient of the 8th Grand Nagamori Award in 2022.

Simone Ferrari (S'17-M'20) received the Ph.D. degree "cum laude" in 2020 from Politecnico di Torino, where he is currently a Research Fellow. He was a Visiting Scholar at the NC State University in Raleigh, NC, USA. He leads the team of developers of the open-source project SyR-e. Since 2021 he is also the responsible of the testing infrastructure TEST-eDRIVE of the Energy Department and the Power Electronics Innovation Center of Politecnico di Torino.

SyR-e team

Gratitude goes to the **SyR-e team** of the PEIC at PoliTO, as per the papers cited throughout the presentation

Mr. Gaetano Dilevrano and Mr. Paolo Ragazzo, PhD students, helped preparing the material presented today, besides their direct contributions to SyR-e

G. Dilevrano, PhD candidate

P. Ragazzo, PhD candidate

Today’s Content

Introduction (20 min)

- **Politecnico di Torino and the Power Electronics Innovation Center (PEIC)**
- **Permanent magnet machines used in traction**

Overview of SyR-e (40 min)

- SyR-e geography
- Main tools for design and modelling
- Magnetics
- Thermal
- Structural
- PWM waveforms and loss

Design of the IPM machine (60 min)

- Case study: Tesla Model 3 rear axle IPM machine
- FEAfix-corrected (x,b) design plane
- Design procedure
- Number of turns determination
- Stack length minimization
- Structural and Thermal aspects
- syreDrive: Control simulation

Conclusion

Politecnico di Torino

Technical School for Engineers founded in 1959, Politecnico di Torino since 1906

Home to **Galileo Ferraris**, pioneer of electrical engineering

35000 BSc and MSc, 800 PhD students

1000 Faculty members
900 Administrative and Technical staff

Budget (2020): 263 M€
(62% State, 12% student fees, 26% projects)

Tuition fee: 0 - 2600€,
depending on family income and merit

1859

Galileo Ferraris
(1847 – 1897)

Research Revenues of PoliTO in FY 2020

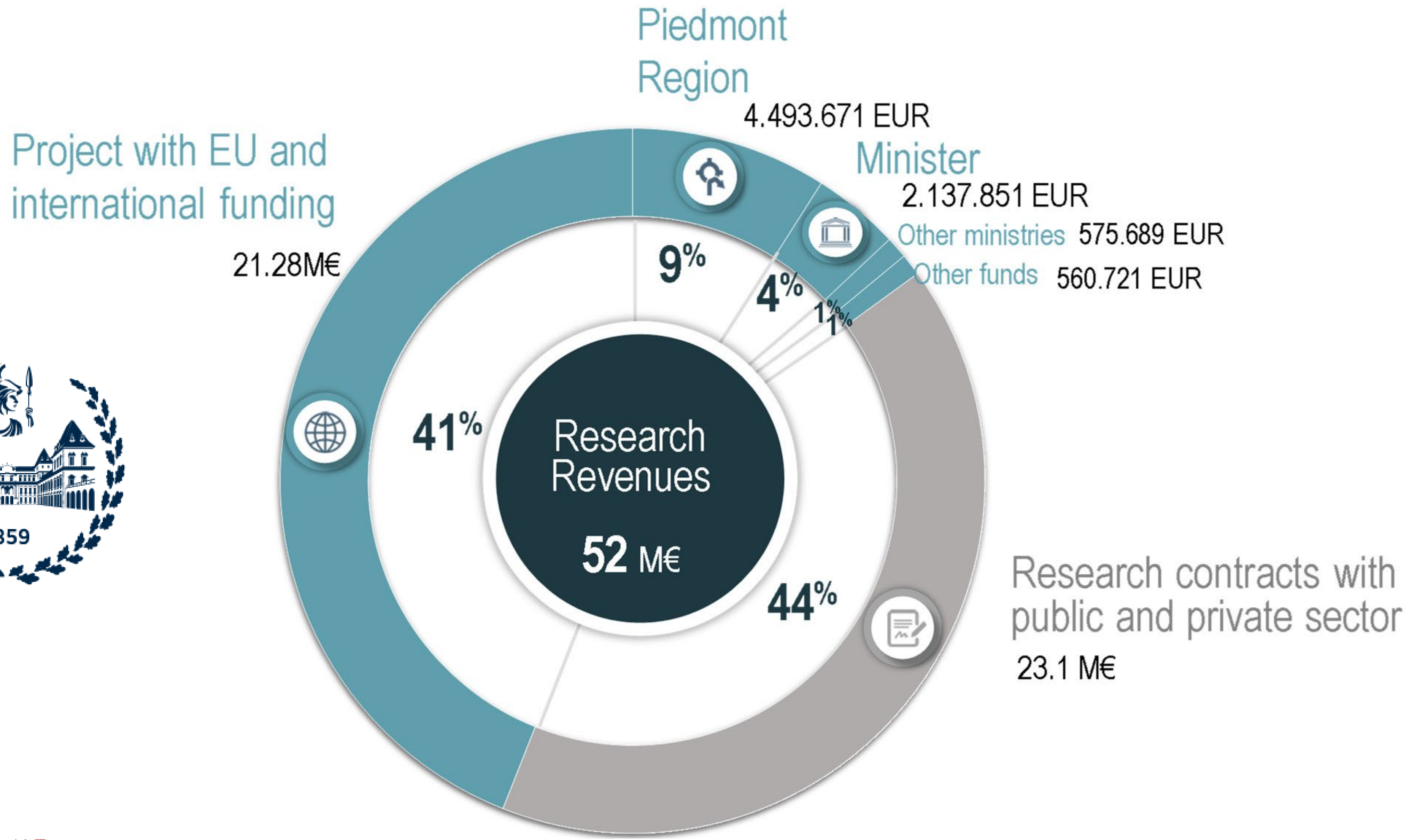

Departments of PoliTO

INDUSTRIAL ENGINEERING

DENERG
Energy

DIMEAS
Mechanical and Aerospace Engineering

DISAT
Applied Science and Technology

INFORMATION TECHNOLOGIES

DAUIN
Control and Computer Engineering

DET
Electronics and Telecommunications

INDUSTRIAL ENGINEERING AND MANAGEMENT AND MATHEMATICS FOR ENG.

DIGEP
Management and Production Engineering

DISMA
Mathematical Sciences

CIVIL AND ENVIRONMENTAL ENG., ARCHITECTURE AND DESIGN

DAD
Architecture and Design

DIATI
Environment, Land and Infrastructure Engineering

DISEG
Structural, Geotechnical and Building Engineering

DIST
Regional and Urban Studies and Planning

1859

Interdepartmental Centers of PoliTO

CARS@PoliTO
Center for Automotive Research and Sustainable mobility

CWC
CleanWater Center@PoliTO

Ec-L
Energy Center Lab

FULL
The Future Urban Legacy Lab

IAM@PoliTO
Integrated Additive Manufacturing

J-Tech@PoliTO
Advanced Joining Technology

PEIC
Power Electronics Innovation Center

PhotoNext

PIC4SeR | PoliTO Interdepartmental Centre for Service Robotics

PoliTo^{BIO}Med Lab
Biomedical Engineering Lab

R3C
Responsible Risk Resilience Centre

SISCON
Safety of Infrastructures and Constructions

SmartData@PoliTO
Big Data and Data Science Laboratory

1859

PEIC: the Power Electronics Innovation Center

The **Inter-Departmental Center** dedicated to Power Electronics, from the Si-SiC-GaN device to the final application, established in 2017

- 20+ faculty, 2 technicians, 25 PhD students
- Main fields of application:
  Transportation, Energy, Industry and Home App.
- TRL4 demonstrators, support to higher-TRL prototypes
- E-motor drive tests up to 20.000 rpm, 500 kW pk

http://www.peic.polito.it/

PEIC: the Power Electronics Innovation Center

Since 2017

- 2 new IEEE Fellows, 2 Nagamori-award awardees
- Several best paper awards
- 10 patent applications

Opportunities of collaboration

- Funded and co-funder PhD grants
- Research contracts
- EU funded projects: Horizon Europe. MSCA, Clean Aviation

http://www.peic.polito.it/

eDrives testing

TEST -e DRIVE

Test -eDrive facility (video)

- Experimental flux maps, cold and hot motor operating conditions (PoliTo benchmark methods)
- Efficiency maps
- HBM Data recorders and torque sensor T12HP
- Automotive test rig: 150 kW, 200Nm, 20,000 rpm, controlled cooling conditions (0-85 °C)

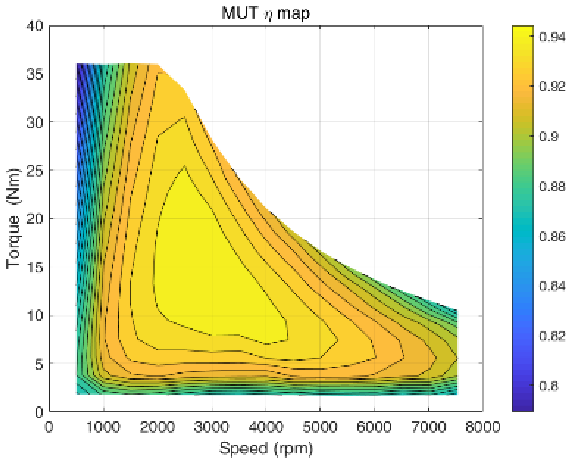

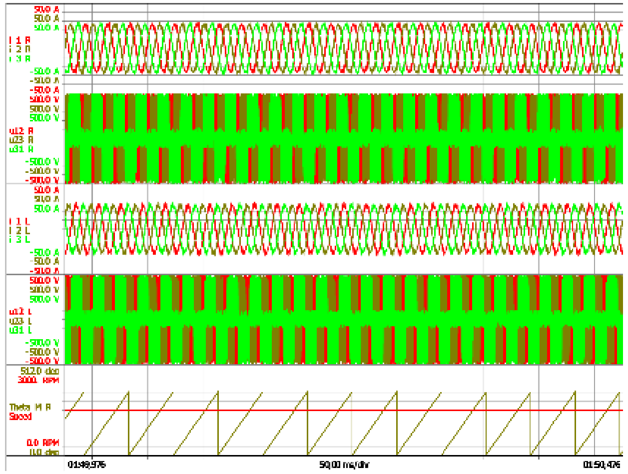

HBM

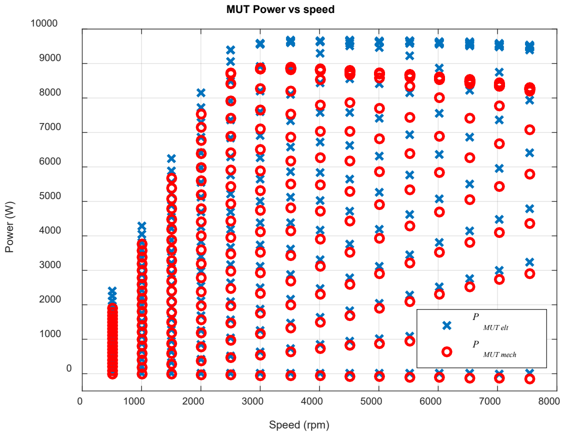

Overview of e-Motors for traction

PM and Reluctance torque tradeoff

PMSMs with increasing rate of Reluctance torque

- peak of rare-earth (RE) metals in 2011 → RE-free trend
- Reluctance torque maximization reduces the RE-PM content

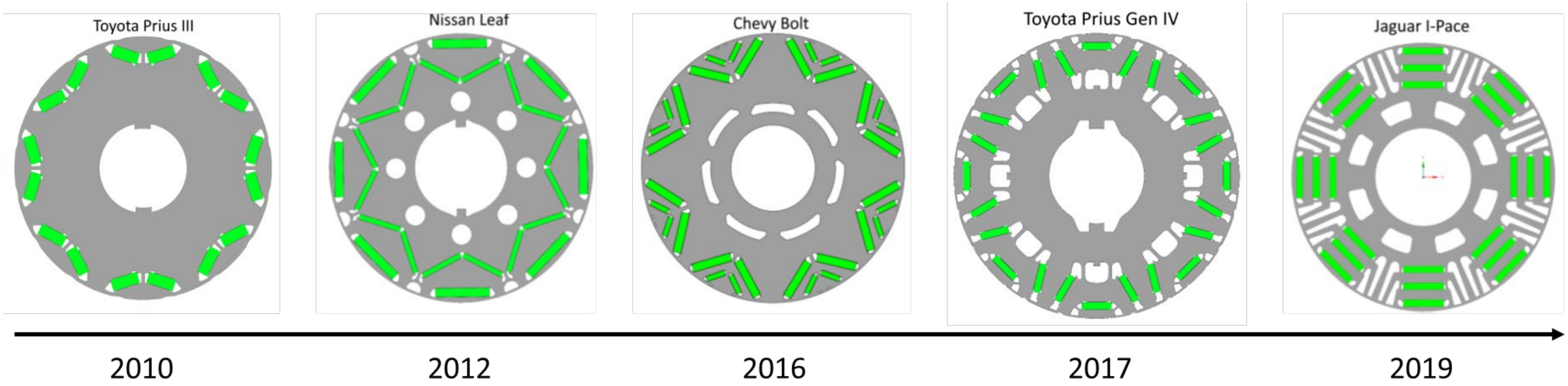

[1] A. Krings and C. Monissen, "Review and Trends in Electric Traction Motors for Battery Electric and Hybrid Vehicles," in *2020 International Conference on Electrical Machines (ICEM)*, 2020

Hairpin windings

Reluctance torque maximization needs distributed windings

Hairpin windings are today's standard for distributed winding-interior PM machines

Pressed-wire solutions exist, both for distributed- and concentrated-winding motors, but tend to show a worse tradeoff between loss minimization and heat extraction

Manufacturability of hairpin on large volumes seems to be established

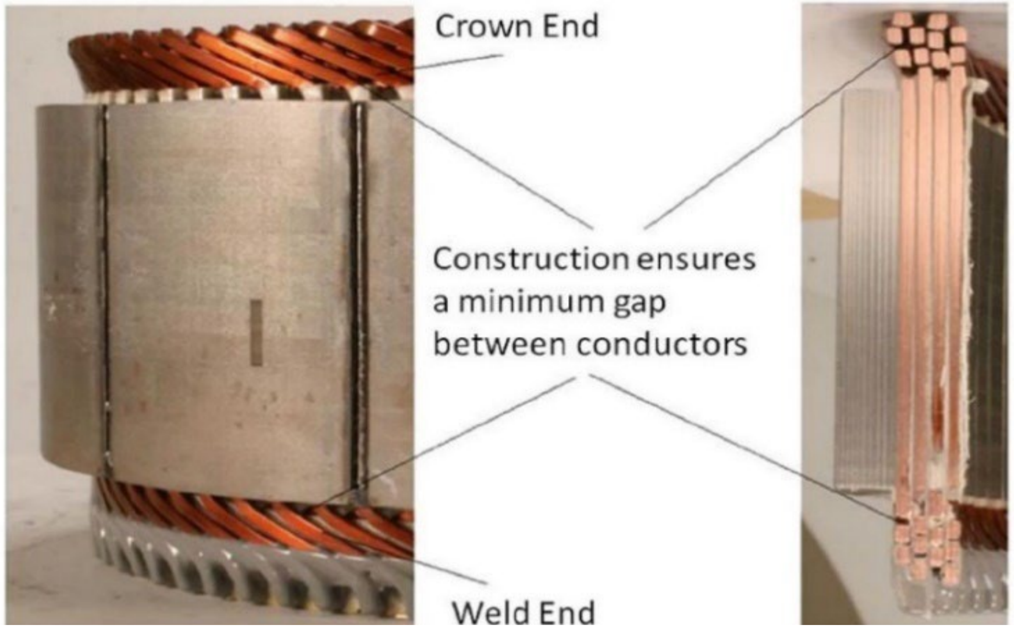

Fill factor 85%
(source: Mitsubishi)

Fill factor 40%
(source: Brusa)

Concentrated windings

Concentrated-winding motors cannot minimize the RE-PM content via reluctance torque [2]

They remain competitive in axial-flux PMSM solutions and high-end radial-flux applications

We focus today on the design of radial-flux, distributed-winding IPM machines for traction

[2] M. Gamba, G. Pellegrino and A. Vagati, "A new PM-assisted Synchronous Reluctance machine with a nonconventional fractional slot per pole combination," 2014 OPTIM, Brasov, Romania

(source: Yasa)

Torque and power density targets

Torque and power density targets are steadily increasing

Torque density requires
- strong **magnets**
- high current density, thus **advanced cooling**

Power density increase is pursued via higher speed

[3] Electric Machines Roadmap 2020 – Advanced Propulsion Center UK www.apcuk.co.uk/app/uploads/2021/09/https___www.apcuk_.co_.uk_app_uploads_2021_02_Exec-summary-Technology-Roadmap-Electric-Machines-final.pdf

	2020	2025	2035
Cost ($/kW)	6	4.8	3.3
Volumetric Power Density (kW/l)	8	25	30
Gravimetric Power Density (kW/kg)	4	8	10
WLTP Average Efficiency	93%	95%	97%

Higher speed trend

[1] A. Krings and C. Monissen, "Review and Trends in Electric Traction Motors for Battery Electric and Hybrid Vehicles," in *2020 International Conference on Electrical Machines (ICEM)*, 2020

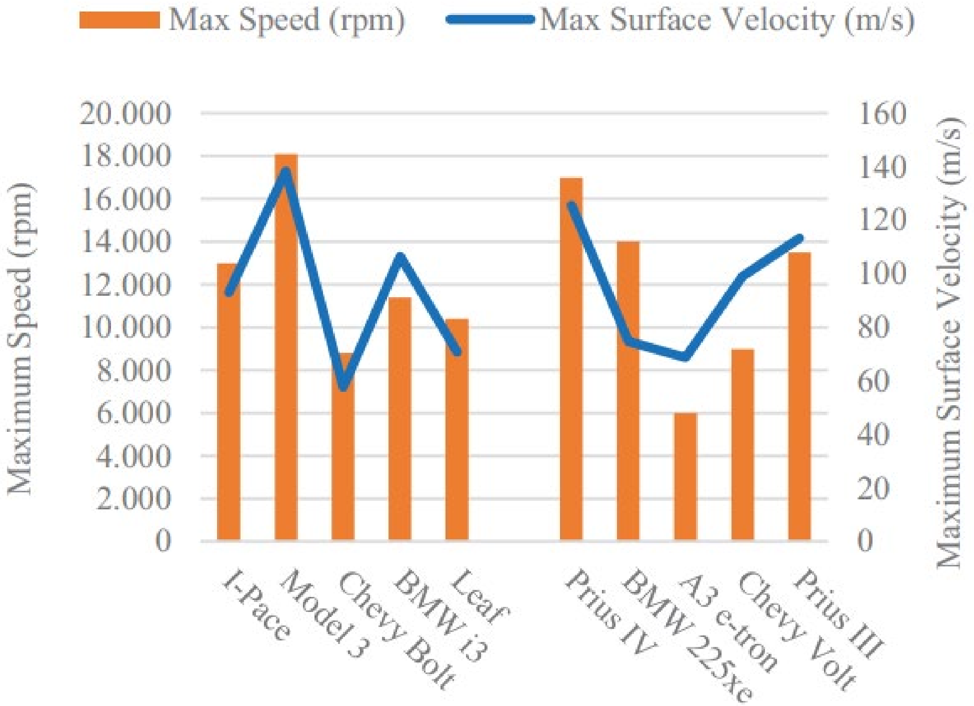

Speed increase is the most direct measure for increasing peak power density

Operating speeds are currently in the 20.000 rpm range, **30.000 rpm is the new target**

The carbon-sleeved rotor of the Tesla Model S Plaid can sustain the maximum speed of 23.300 rpm (source insideevs)

Increasing importance of structural optimization

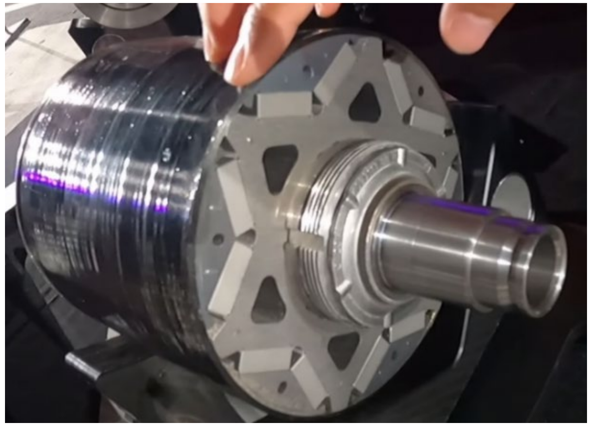

Carbon-sleeved rotor of Tesla Model S Plaid e-motors

Advanced cooling

[4] K. Bennion, G. Moreno, “Convective Heat Transfer Coefficients of Automatic Transmission Fluid Jets with implications for Electric Machine Thermal Management”, International Technical Conference and Exhibition on Packaging and Integration of Electronic and Photonic Microsystems, San Francisco, 2015

Oil cooling tends to replace water cooling

The standard water-glycol cooling jacket, with potted windings is being replaced by advanced solutions such as:

- End-winding oil spray cooling
- Direct stator cooling
- Rotor cooling

Yet, today we refer to standard back iron, as per a water-glycol cooling jacket

The focus today is magnetic design

Tesla Model 3 stator oil channels

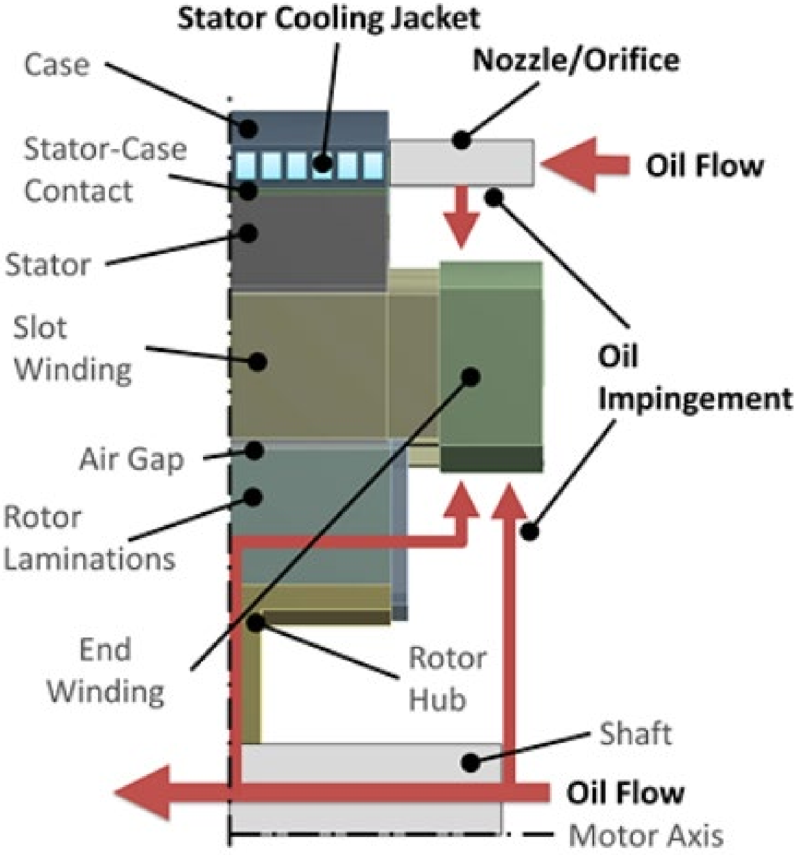

Oil spray cooling principle [4]

Today's Content

Introduction (20 min)
- Politecnico di Torino and the Power Electronics Innovation Center (PEIC)
- Permanent magnet machines used in traction

Overview of SyR-e (40 min)
- **SyR-e geography**
- **Main tools for design and modelling**
- **Magnetics**
- **Thermal**
- **Structural**
- **PWM waveforms and loss**

Design of the IPM machine (60 min)
- Case study: Tesla Model 3 rear axle IPM machine
- FEAfix-corrected (x,b) design plane
- Design procedure
- Number of turns determination
- Stack length minimization
- Structural and Thermal aspects
- syreDrive: Control simulation

Conclusion

syre

https://github.com/SyR-e

SyR-e Geography

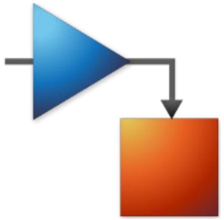

GUI_Syre

Motor design and simulation

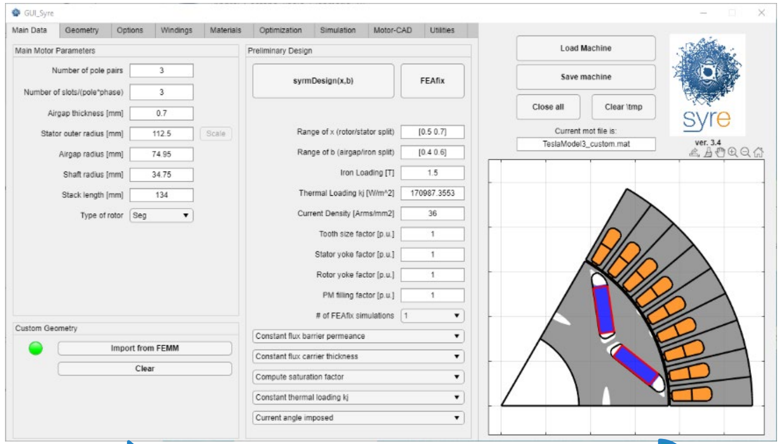

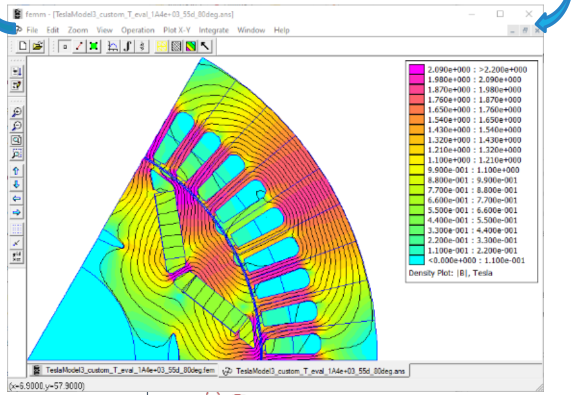

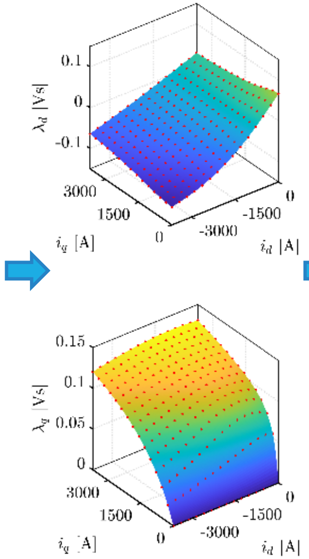

GUI_Syre_MMM

Magnetic Model Manipulation

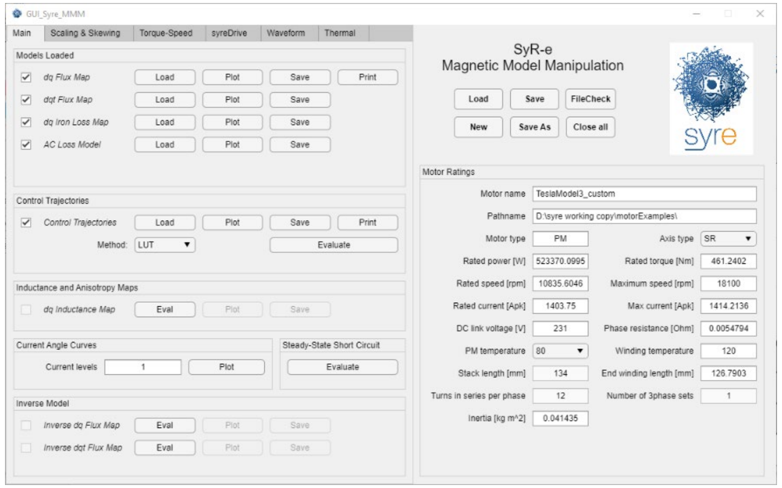

Efficiency Map

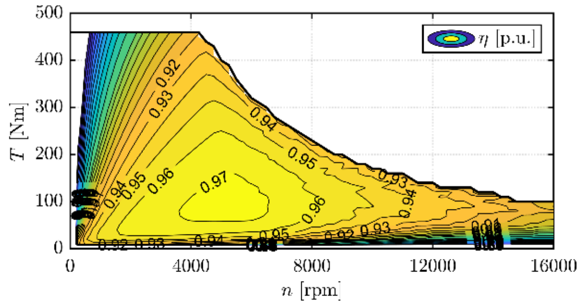

Phase currents with PWM ripple

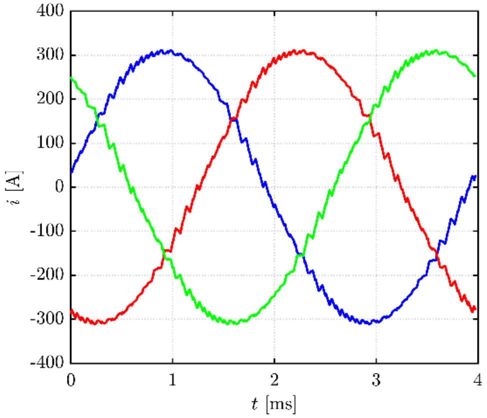

GUI_SyRe: initial GUI for design and FEA simulation

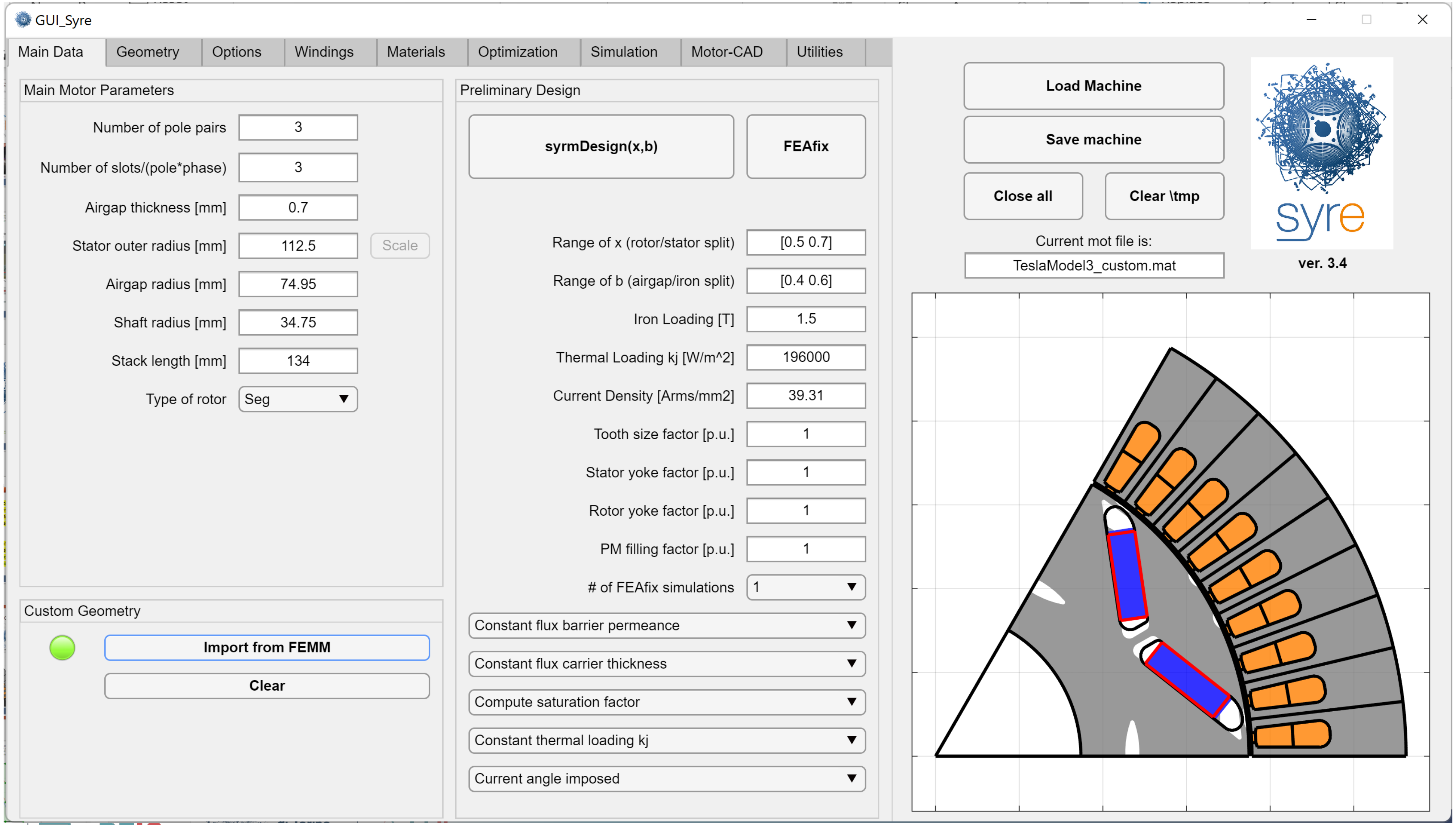

syrmDesign and FEAfix

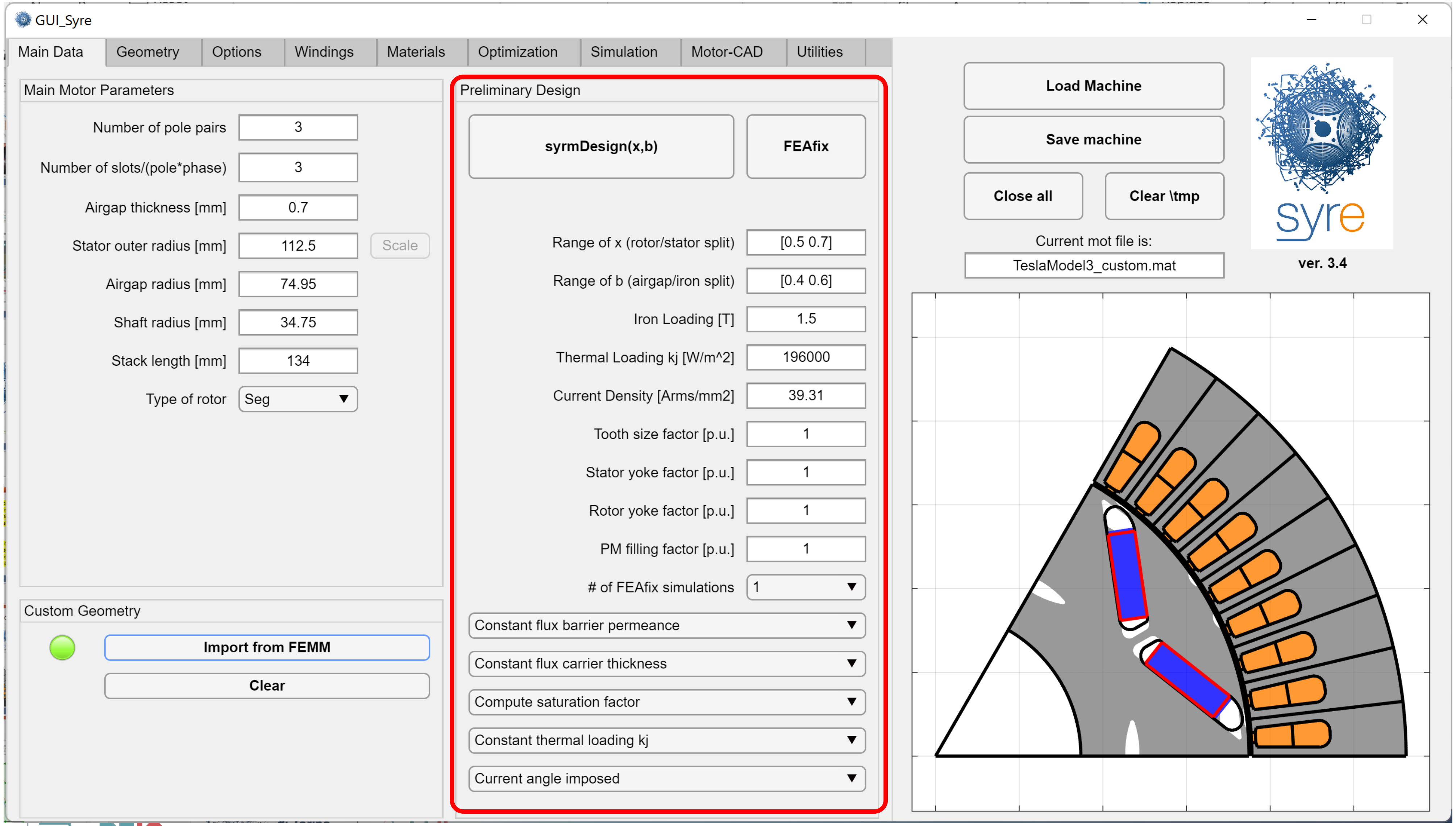

FEAfix Motor Design

[5] S. Ferrari and G. Pellegrino, "FEAfix: FEA Refinement of Design Equations for Synchronous Reluctance Machines," in *IEEE Transactions on Industry Applications*, vol. 56, no. 1, pp. 256-266, Jan.-Feb. 2020.
[6] P. Ragazzo, G. Dilevrano, S. Ferrari and G. Pellegrino, «Design of IPM Synchronous Machines Using Fast-FEA Corrected Design Equations," presented at *2022 XXV International Conference on Electrical Machines (ICEM)*, Valencia, Spain, 2022

Parametric design plane

Torque and PF curves function of the cross-sectional geometry are pre-calculated via equations

The **16 FEAfix simulated designs** calibrate the results of the equations and make the contour curves **exact in the entire design space**

The FEAfix plane is the design tool presented at ICEM'22

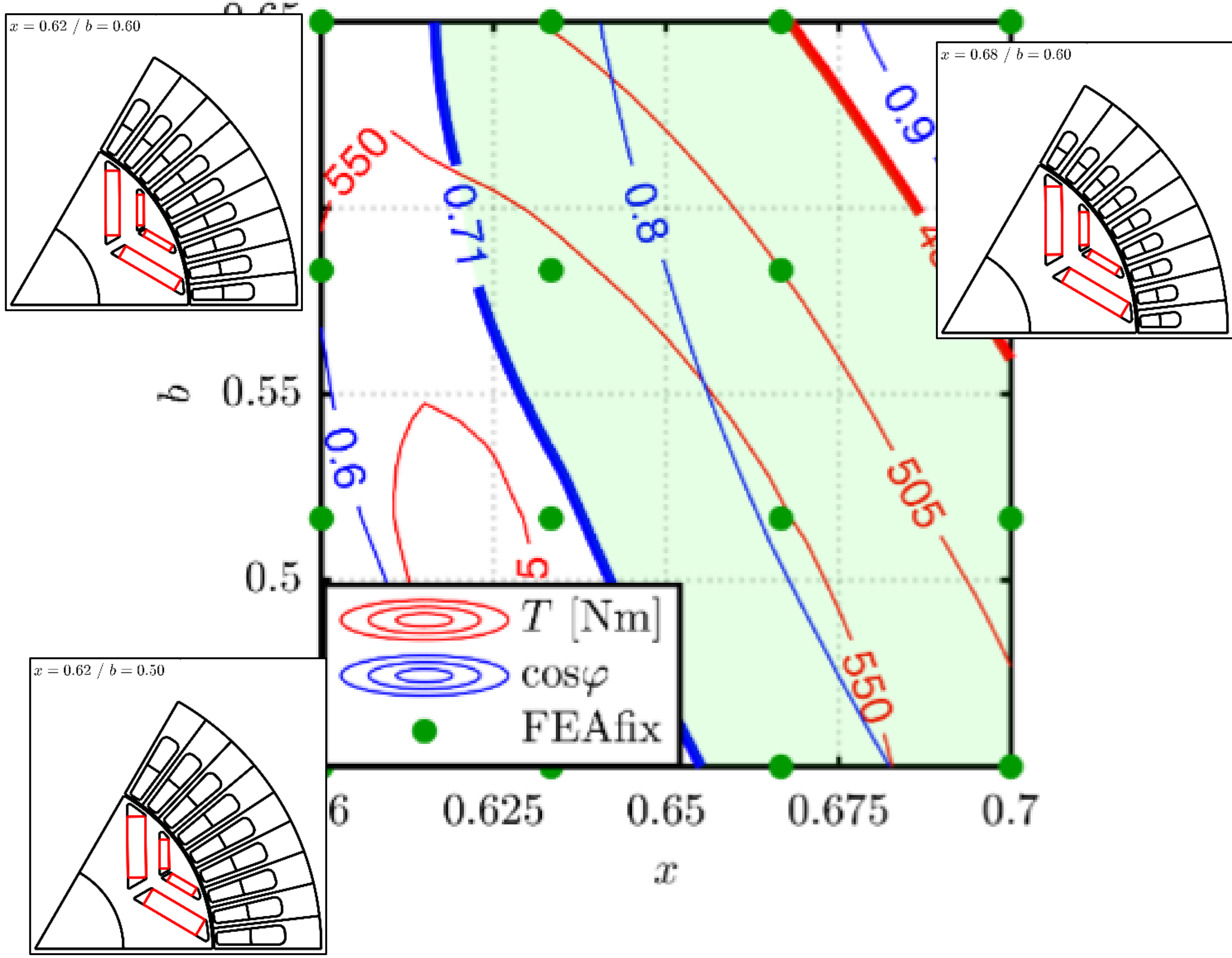

Optimization tab

MODE settings

Input

Goals

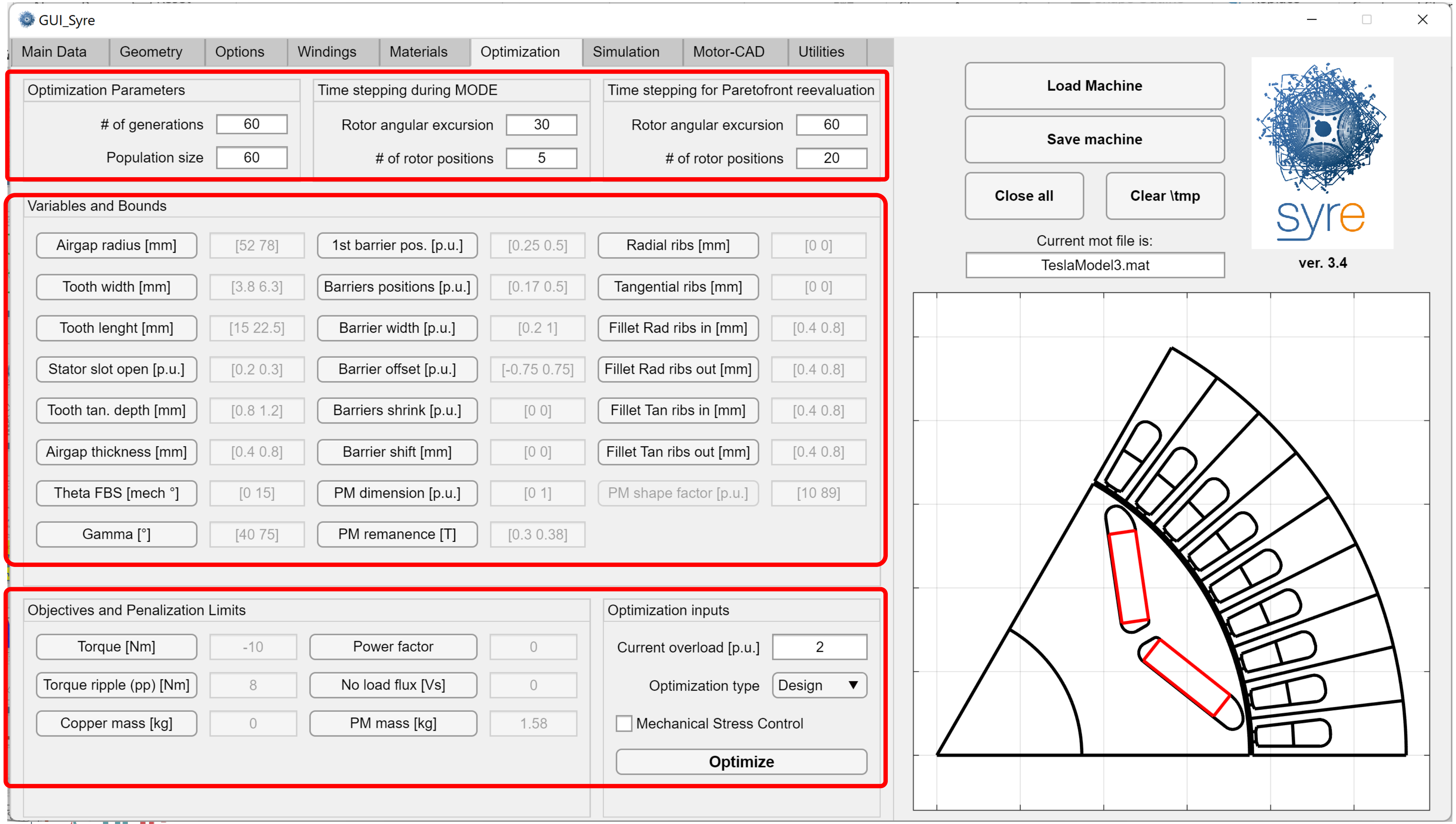

Design Optimization

[7] G. Pellegrino, F. Cupertino and C. Gerada, "Automatic Design of Synchronous Reluctance Motors Focusing on Barrier Shape Optimization," in IEEE Transactions on Industry Applications, vol. 51, no. 2.
[8] F. Cupertino, G. Pellegrino and C. Gerada, "Design of Synchronous Reluctance Motors With Multiobjective Optimization Algorithms," in IEEE Transactions on Industry Applications, vol. 50, no. 6

MODE (Multi-Objective Differential Evolution) is usable in SyR-e to optimize motor cross-section

Selectable optimization goals are

- Torque and torque ripple
- PM and copper mass
- Power Factor
- Open-circuit flux linkage

Optimization was used for design from scratch of Synchronous Reluctance motors

Use for design refinement is recommended for IPM machines

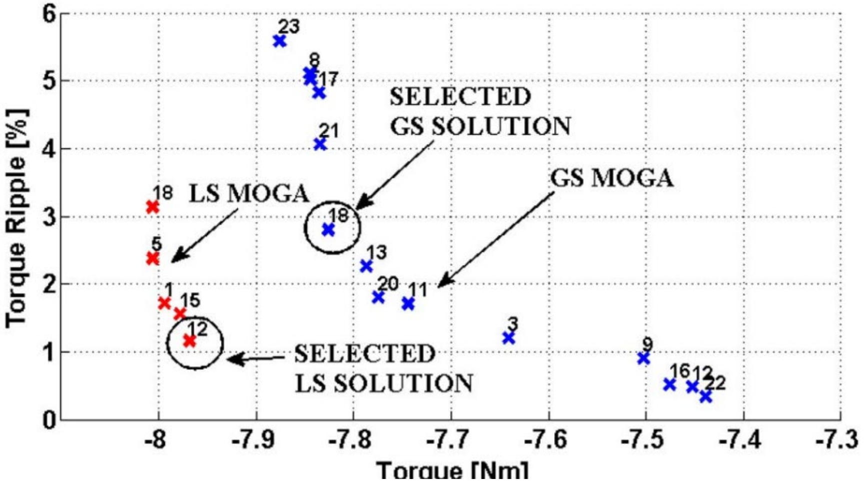

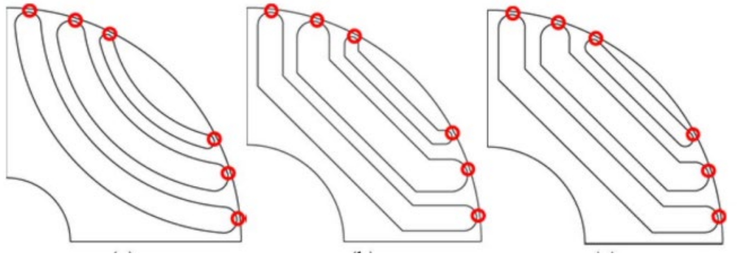

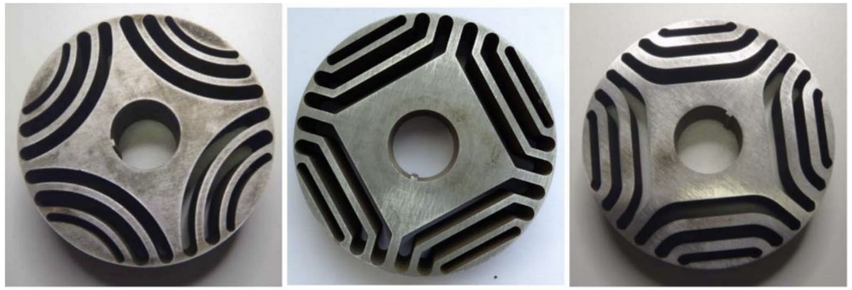

Structural co-design

The overspeed (rpm) input field determines the size of the additional internal rib

Analytical

- Center post evaluated automatically according to max speed

FEA

- Centrifugal stress analysis included, using the **PDE Toolbox of Matlab**

Mesh for structural FEA, PDE Toolbox

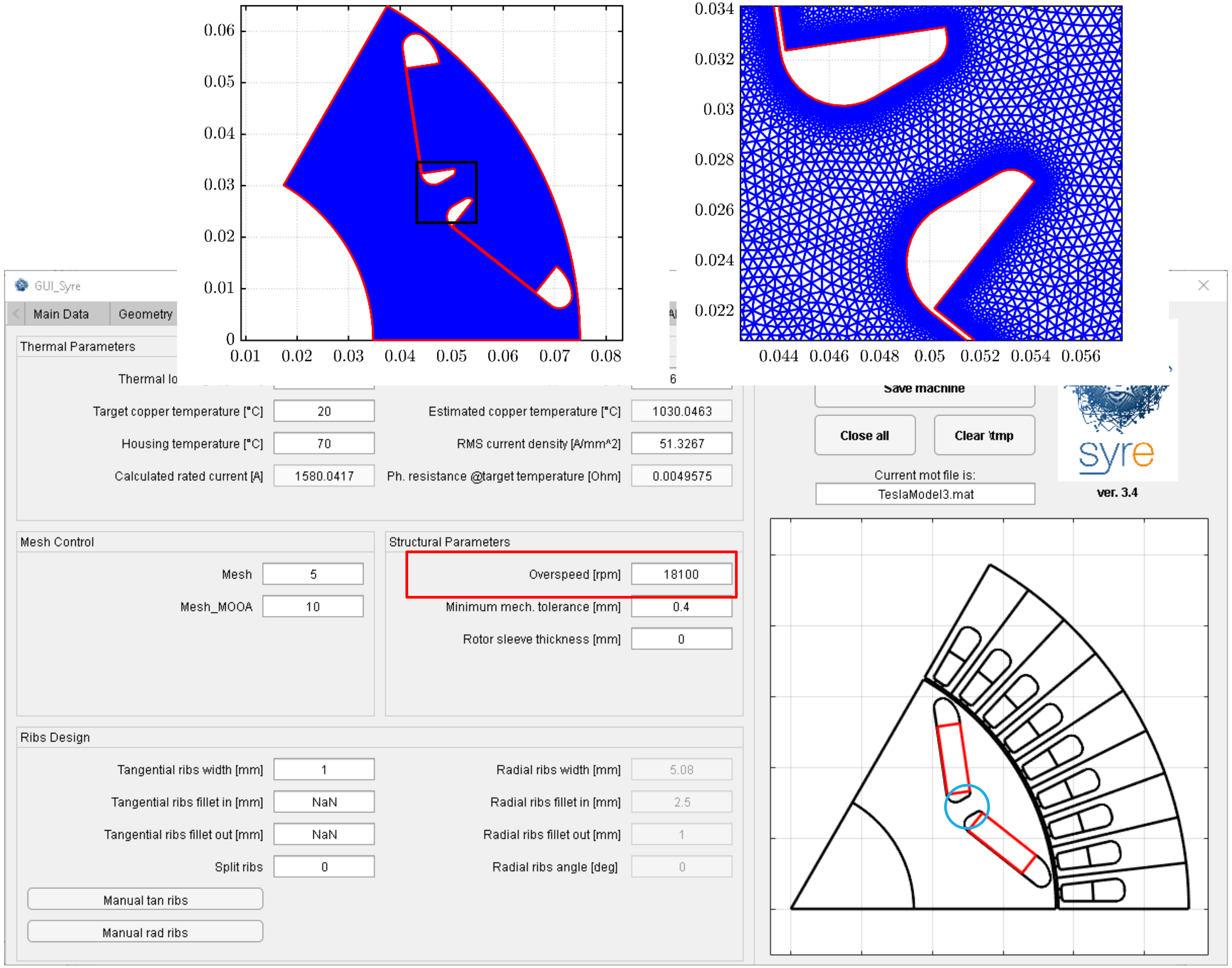

Slot model for AC loss

[9] S. Ferrari, P. Ragazzo, G. Dilevrano and G. Pellegrino, "Flux-Map Based FEA Evaluation of Synchronous Machine Efficiency Maps," 2021 IEEE Workshop on Electrical Machines Design, Control and Diagnosis (WEMDCD), 2021

AC loss is FEA evaluated using AC analysis in FEMM

The AC loss vs frequency characteristic contributes to the **efficiency map** evaluation

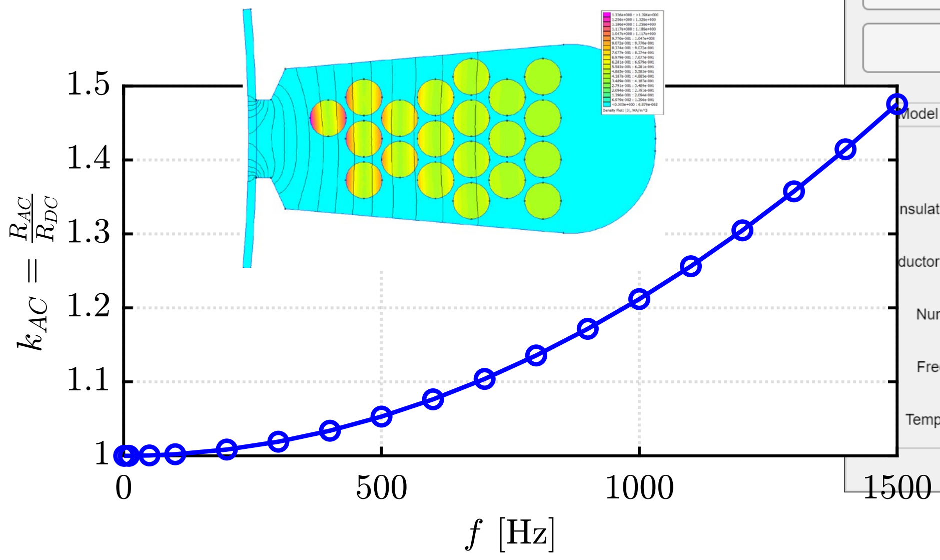

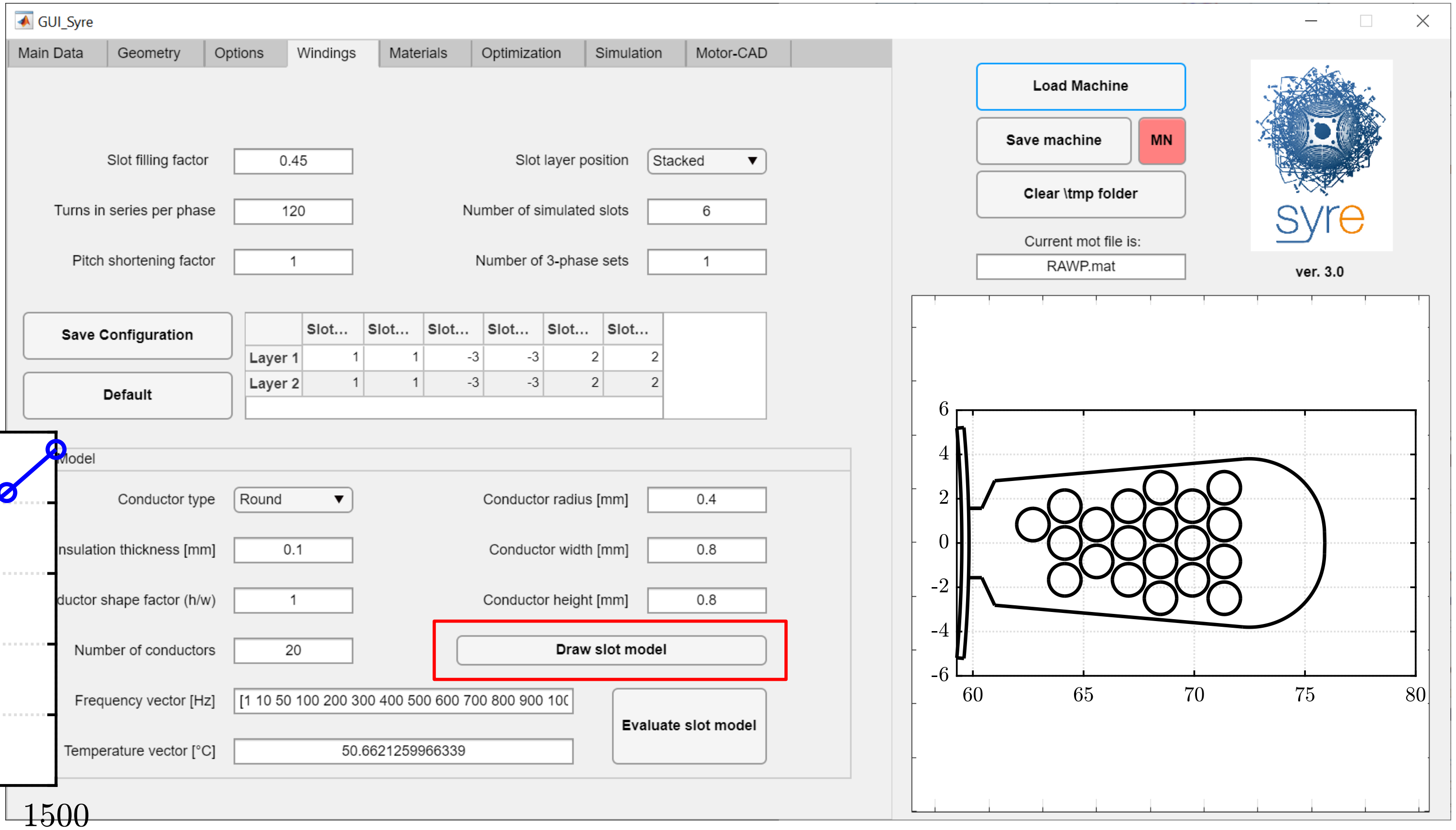

Hairpin Windings

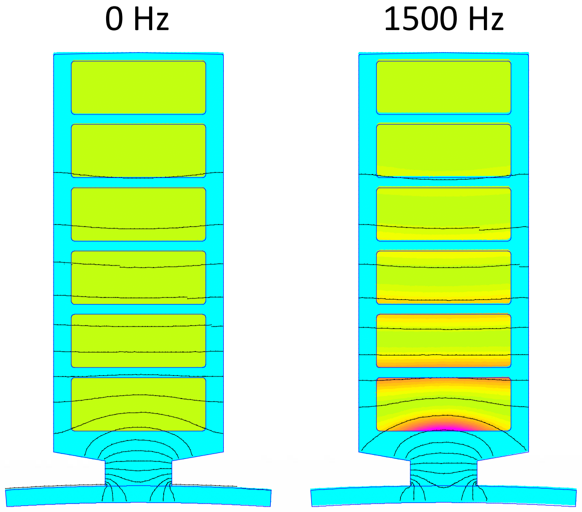

The case of bar conductors is covered, relevant for traction motors

Effects of **frequency** (fundamental and PWM spectrum) and **temperature** are accounted for

End-turns contribute to DC resistance

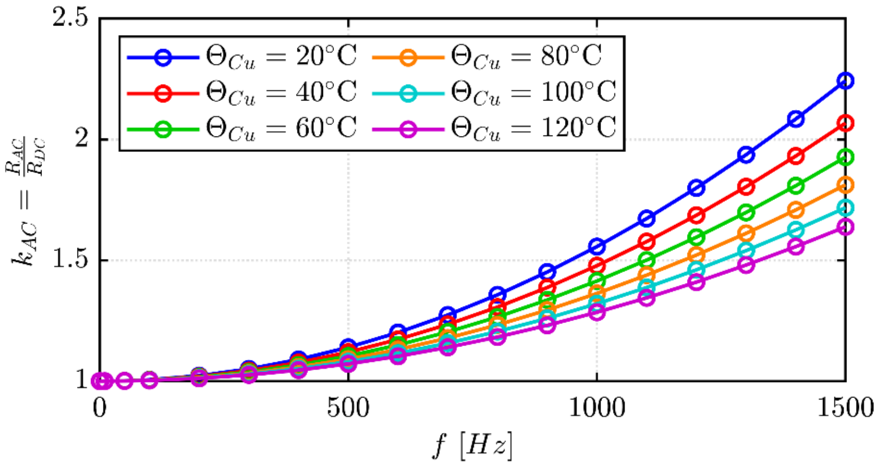

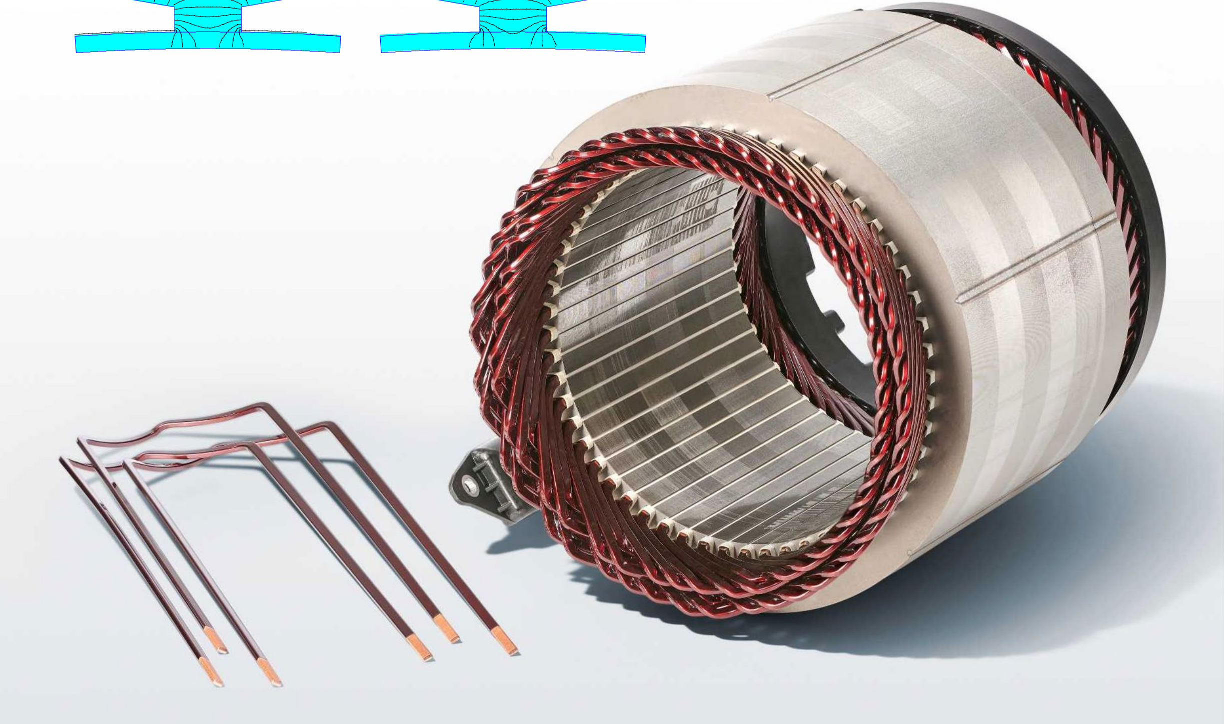

(source: BMW)

FEA Simulation tab

Type of simulation

Simulator

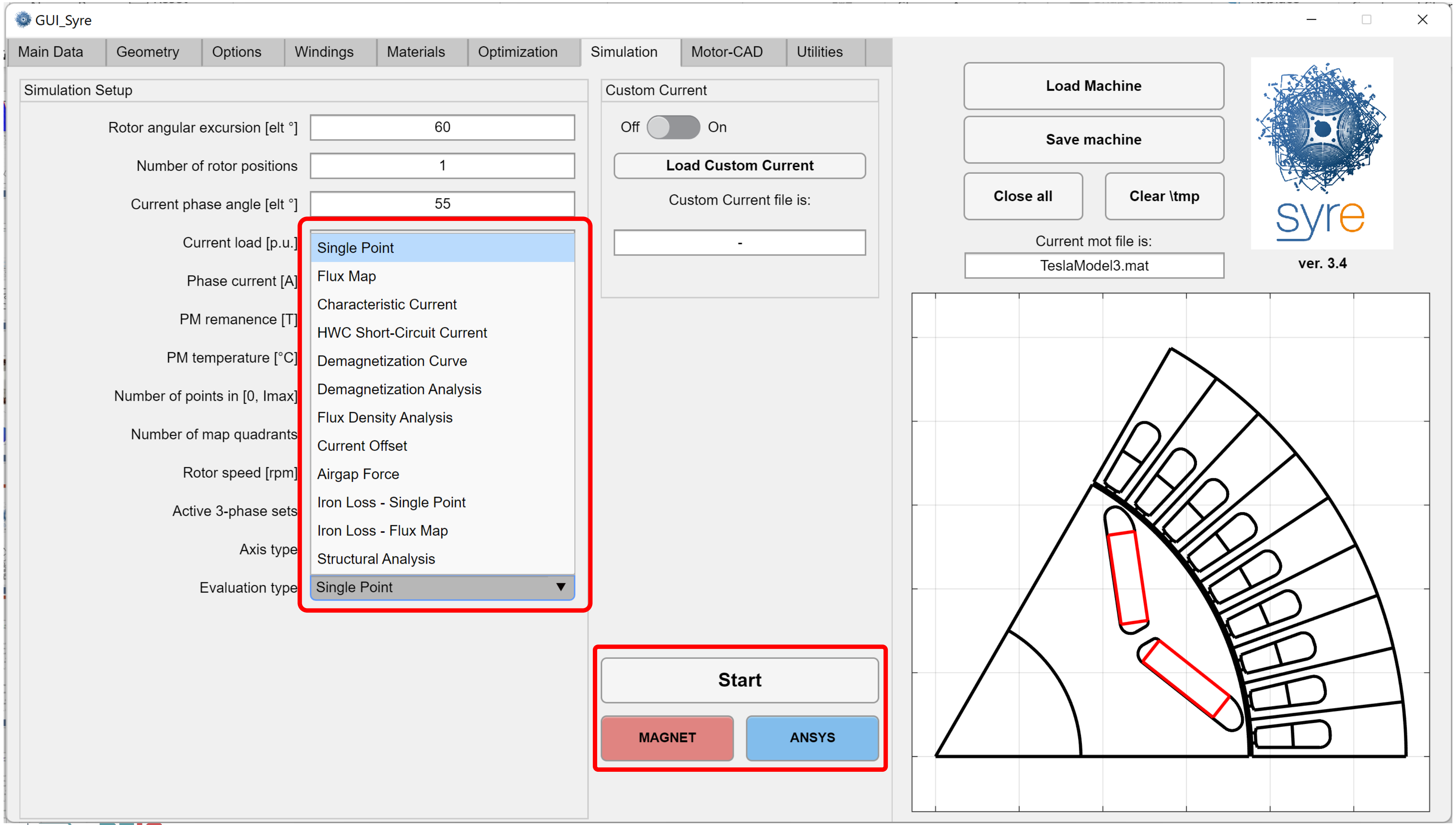

Flux maps

[10] S. Ferrari, G. Dilevrano, P. Ragazzo and G. Pellegrino, "The dq-theta Flux Map Model of Synchronous Machines," *2021 IEEE Energy Conversion Congress and Exposition (ECCE)*, Vancouver, BC, Canada, 2021

The flux maps are calculated with magnetostatic FEMM runs*

$$\lambda_d = \Lambda_d(i_d, i_q) \qquad \lambda_q = \Lambda_q(i_d, i_q)$$

Torque and torque ripple maps come as a result from the same FEA simulations

The torque map is also the external product of the flux and current maps

$$T(i_d, i_q) = \frac{3}{2} p (\Lambda_d \odot I_q - \Lambda_q \odot I_d)$$

$I_d(i_d, i_q)$ and $I_q(i_d, i_q)$ are the current maps

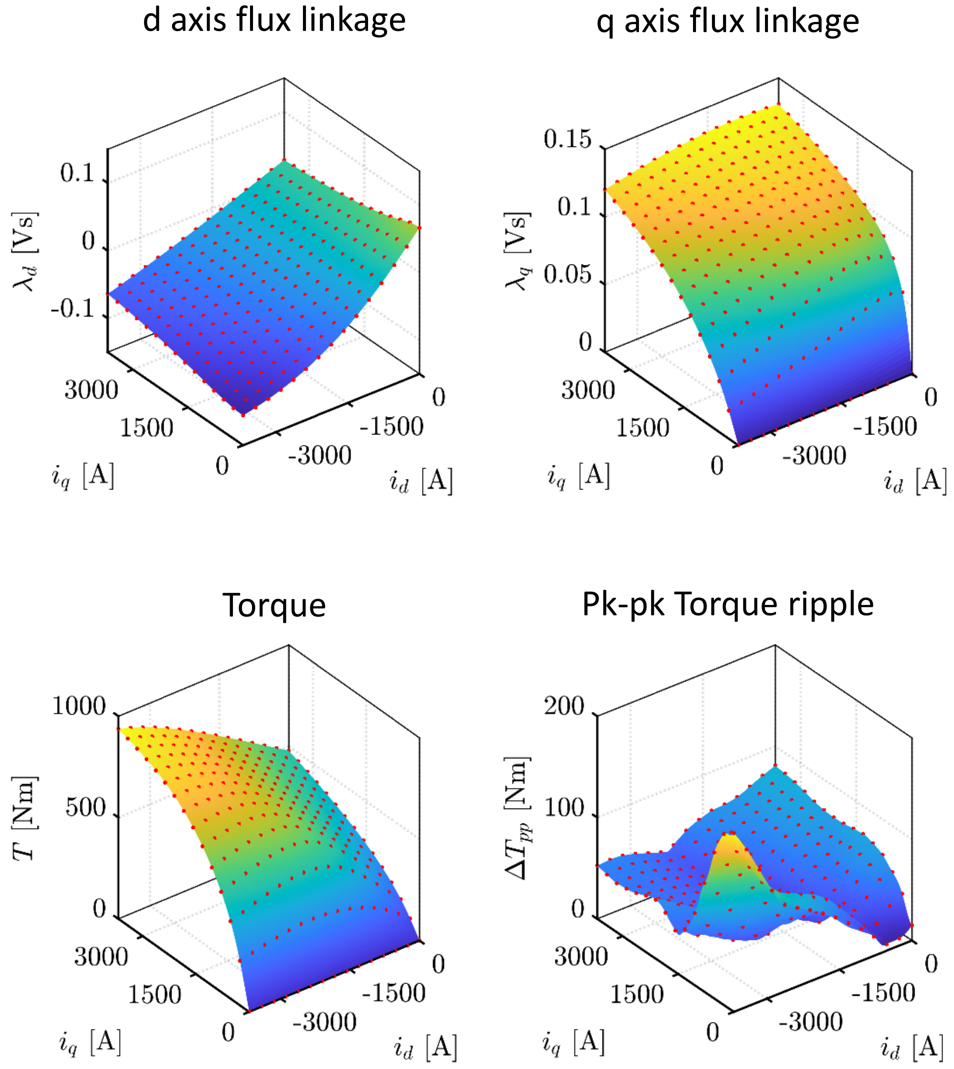

* Red dots are the 15 x 15 grid. Each is 60° rotor excursion on 15 positions
Simulation time ~30 min (14-core workstation)

GUI_SyRe_MMM: magnetic model manipulation

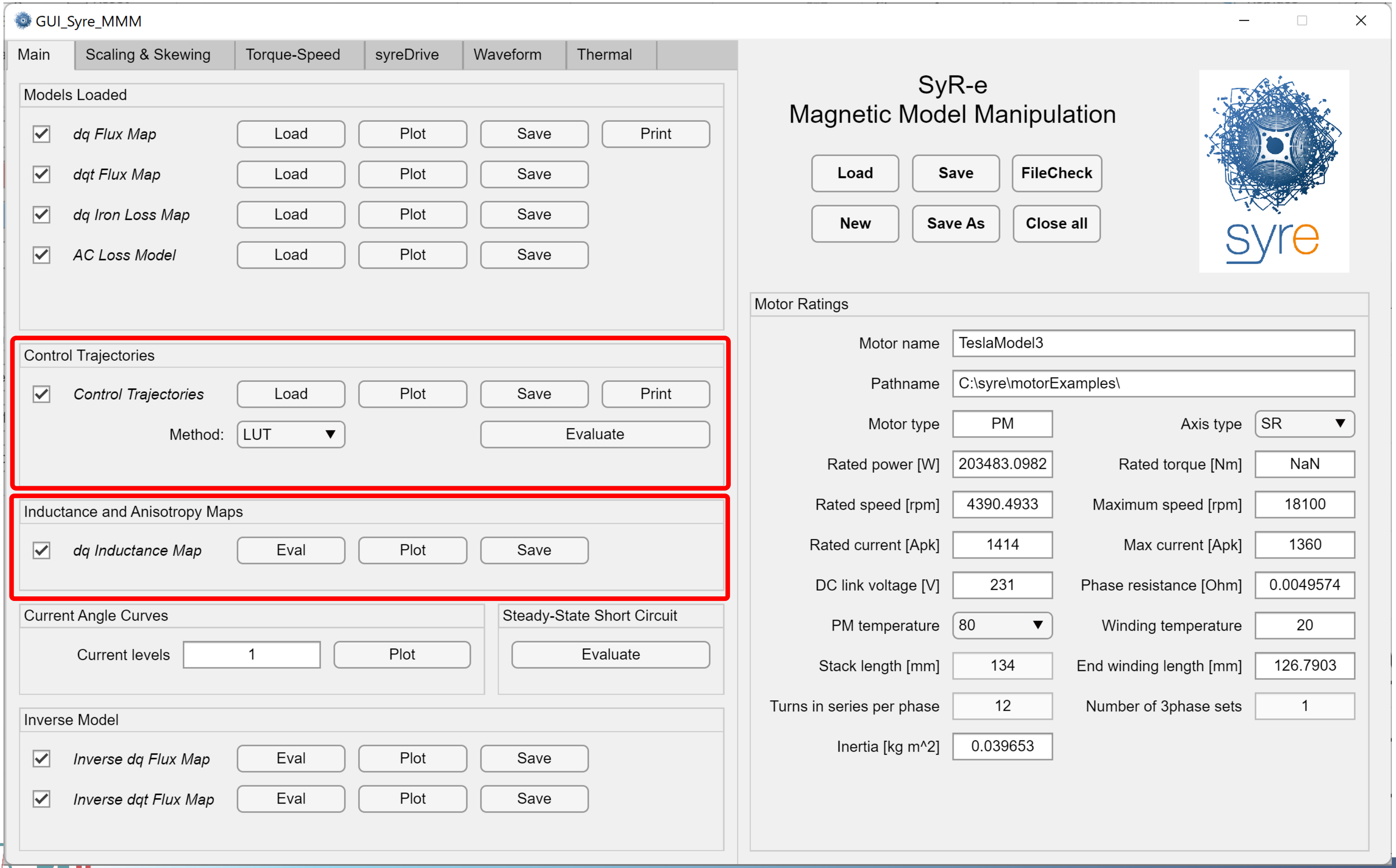

MTPA - MTPV

Inductance maps

Flux maps manipulation

[11] Pellegrino, G., Jahns, T.M., Bianchi, N., Soong, W. and Cupertino, F., The Rediscovery of Synchronous Reluctance and Ferrite Permanent Magnet Motors Tutorial Course Notes.

Flux maps manipulation is used for deriving the inductance maps, where needed (e.g. for Simulink and PLECS models)

Apparent inductance maps, Vs/A division

$$L_d = \frac{\Lambda_d(i_d, i_q)}{i_d}, L_q = \frac{\Lambda_q(i_d, i_q)}{i_q}$$

Incremental inductance maps, differentiation

$$l_d = \frac{\partial\Lambda_d(i_d, i_q)}{\partial i_d}, l_q = \frac{\partial\Lambda_q(i_d, i_q)}{\partial i_q}$$

$$l_{dq} = \frac{\partial\Lambda_d(i_d, i_q)}{\partial i_q} = l_{qd} = \frac{\partial\Lambda_q(i_d, i_q)}{\partial i_d}$$

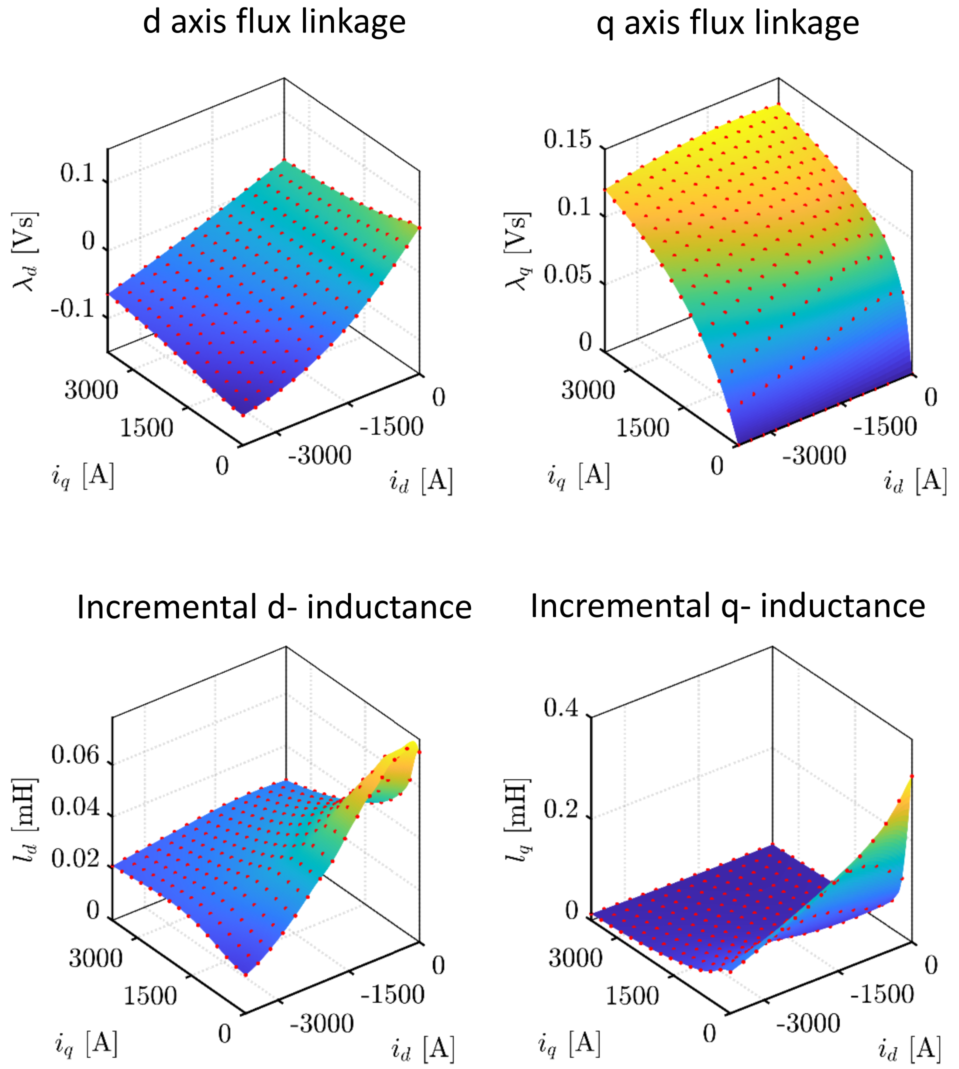

Manipulation for MTPA

Torque and current magnitude contours are defined on the i_d, i_q domain

$$T(i_d, i_q) = \frac{3}{2} p \left(\Lambda_d \odot I_q - \Lambda_q \odot I_d \right)$$

$$I(i_d, i_q) = \left| I_d + j \cdot I_q \right|$$

The MTPA is evaluated by searching the minimum current magnitude for each torque contour

The MTPV (Max Torque per Volt) is retrieved in similar manner

MTPA curve in the dq current plane

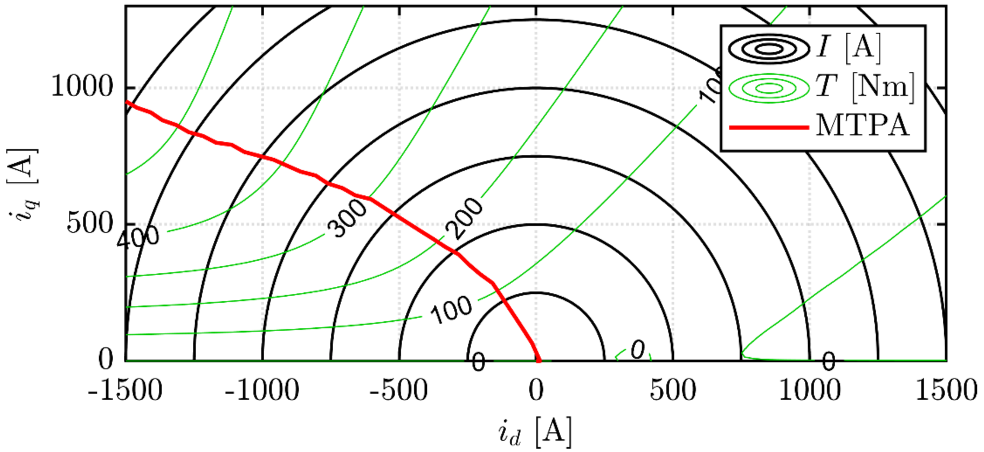

Torque versus ampere in MTPA condition

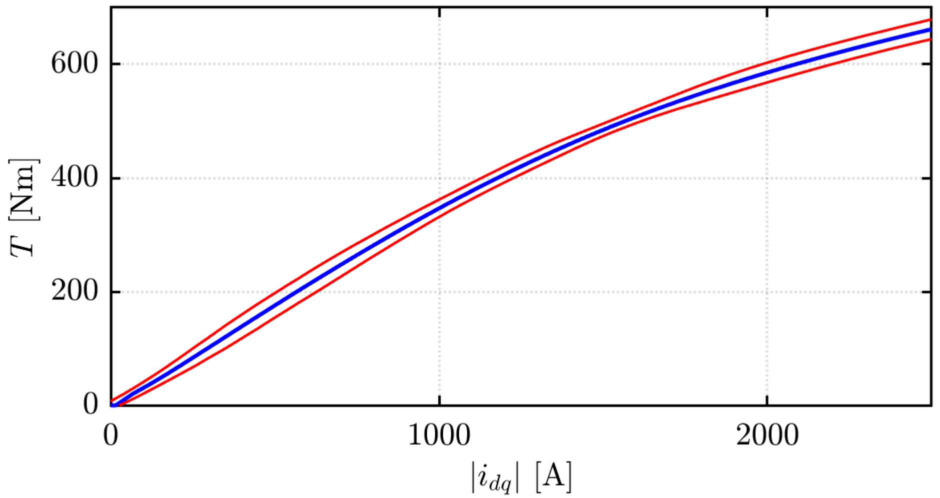

Torque-speed tab

Power curve

Effy map

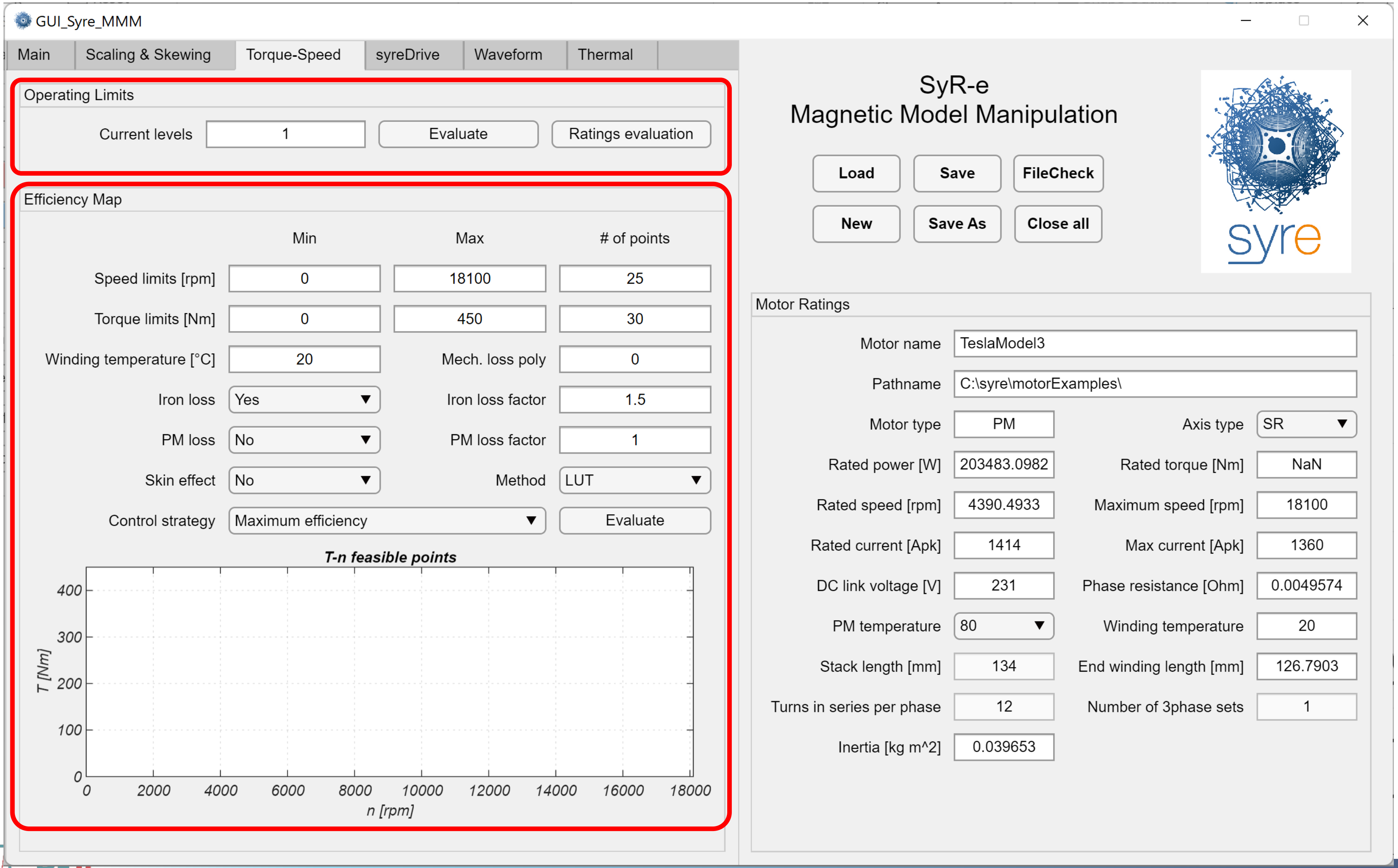

Power vs Speed Curve

Torque and Power versus Speed curves at peak current and maximum voltage conditions

Speed regions:

- MTPA at max current (0 rpm – A)
- Flux weakening at max current (A – B)
- Flux weakening under MTPV limit (B – n_{max})

Control trajectory in the dq current plane

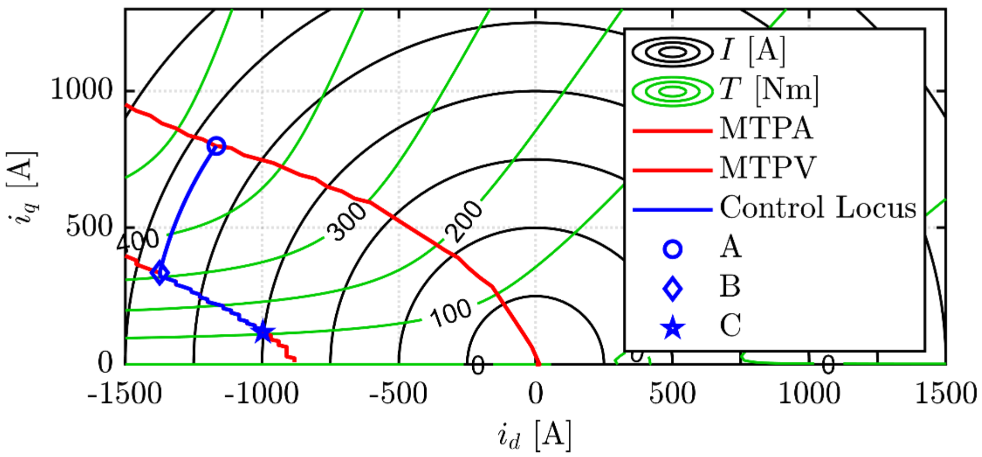

Peak torque-speed and power-speed curves

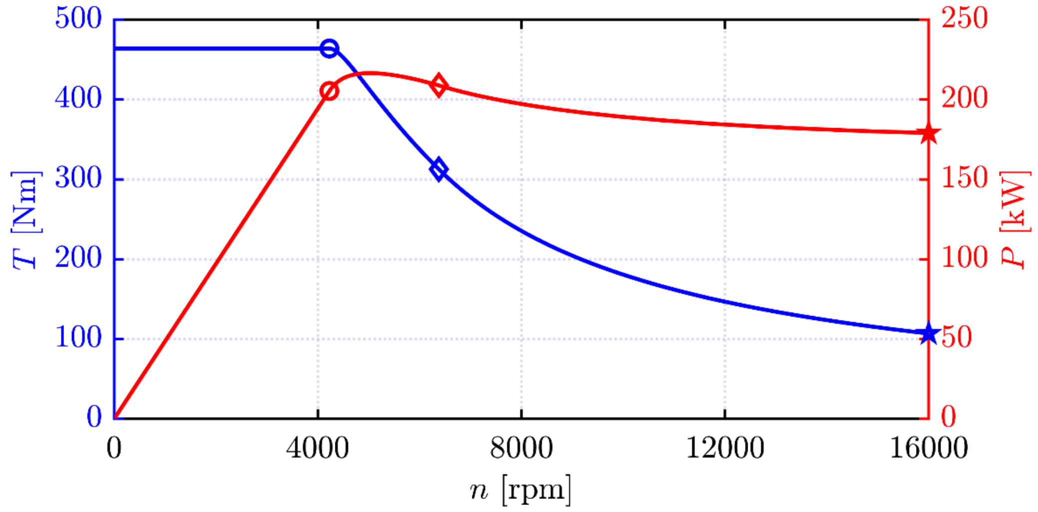

FEA Iron Loss Map

[9] S. Ferrari, P. Ragazzo, G. Dilevrano and G. Pellegrino, "Flux-Map Based FEA Evaluation of Synchronous Machine Efficiency Maps," 2021 IEEE Workshop on Electrical Machines Design, Control and Diagnosis (WEMDCD), 2021, pp. 76-81

The 2-term Steinmetz electric steel loss model is adopted

$$p_{Fe} = k_h f^{\alpha} B^{\beta} + k_e B^2 f^2 \left(\frac{\mathrm{W}}{\mathrm{kg}}\right)$$

The iron loss map is FEA simulated with FEMM (or Magnet, or Maxwell) at a single speed value n_0, with breakdown of hysteresis and eddy-current loss terms

$$P_{Fe,n0}(i_d, i_q) = \underbrace{P_{hs} + P_{es}}_{\text{stator}} + \underbrace{P_{hr} + P_{er}}_{\text{rotor}}$$

(*) Red dots: 9 x 9 grid, 180° of rotor excursion, 90 positions, simulation time ~2 hours (14-core workstation)

Stator loss at reference speed n_0

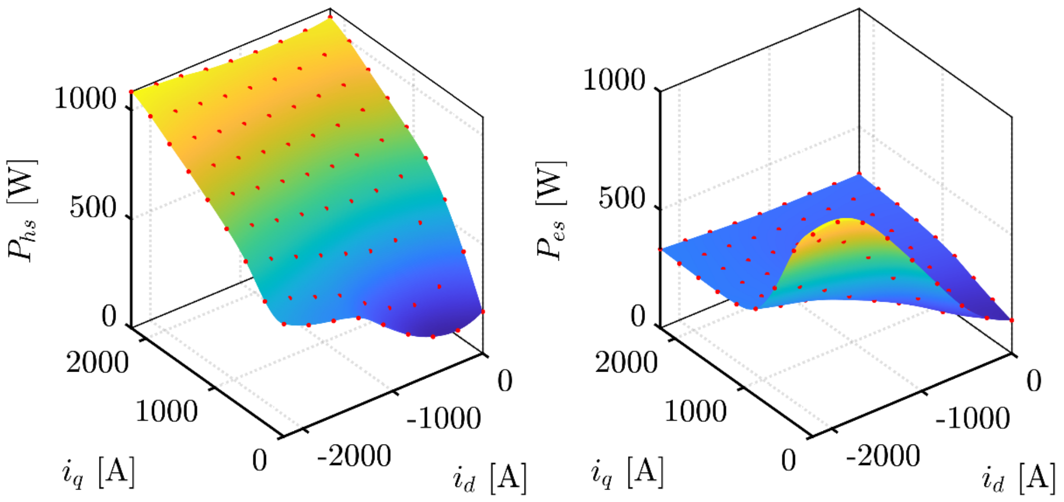

Rotor loss at reference speed n_0

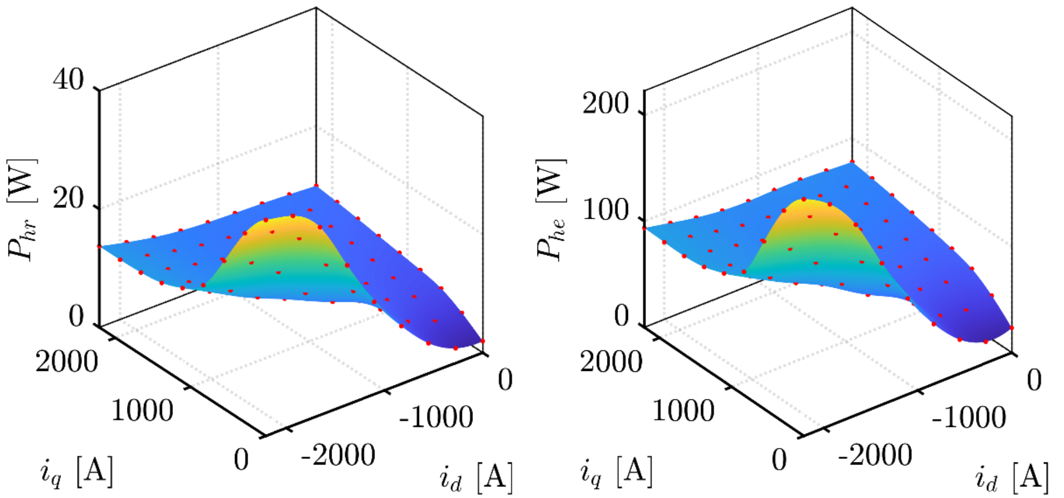

Speed Dependency

[9] S. Ferrari, P. Ragazzo, G. Dilevrano and G. Pellegrino, "Flux-Map Based FEA Evaluation of Synchronous Machine Efficiency Maps," 2021 IEEE Workshop on Electrical Machines Design, Control and Diagnosis (WEMDCD), 2021, pp. 76-81

The loss map is scaled speed-wise using the Steinmetz law

$$P_{Fe}(i_d, i_q, n) =$$

$$(P_{sh} + P_{rh})_{n0} \cdot \left(\frac{n}{n_0}\right)^{\alpha} + (P_{se} + P_{re})_{n0} \cdot \left(\frac{n}{n_0}\right)^{2}$$

FEA calculated PM loss is speed-scaled as the eddy-current loss term, in conservative manner

$$P_{PM}(i_d, i_q, n) = P_{PM,n0} \cdot \left(\frac{n}{n_0}\right)^{2}$$

Iron and PM loss maps function of speed

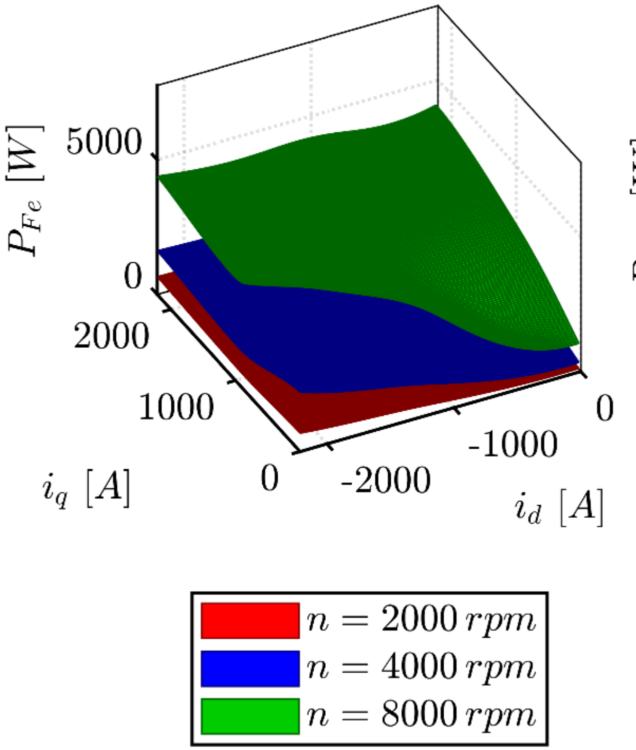

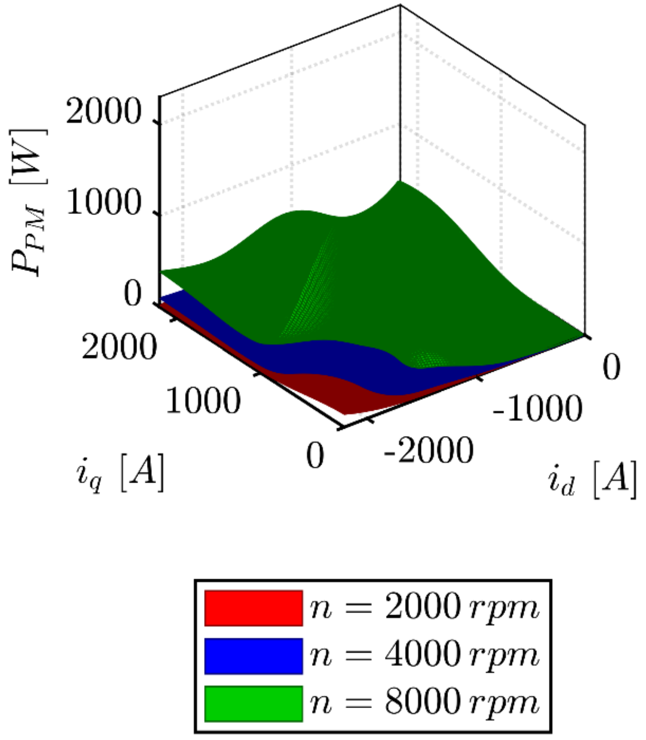

Efficiency Map

[9] S. Ferrari, P. Ragazzo, G. Dilevrano and G. Pellegrino, "Flux-Map Based FEA Evaluation of Synchronous Machine Efficiency Maps," 2021 IEEE Workshop on Electrical Machines Design, Control and Diagnosis (WEMDCD), 2021, pp. 76-81

The efficiency map is calculated from the flux and loss maps, accounting for the inverter limits

A regular (T, n) grid is considered

- For each point, the minimum loss (i_d, i_q) condition is computed, considered the current and voltage limits

Simulation conditions

- Temperature values (Cu and PM) are imposed
- DC and AC copper losses are included
- Sinusoidal supply (no PWM), for now

Computed efficiency map and test points

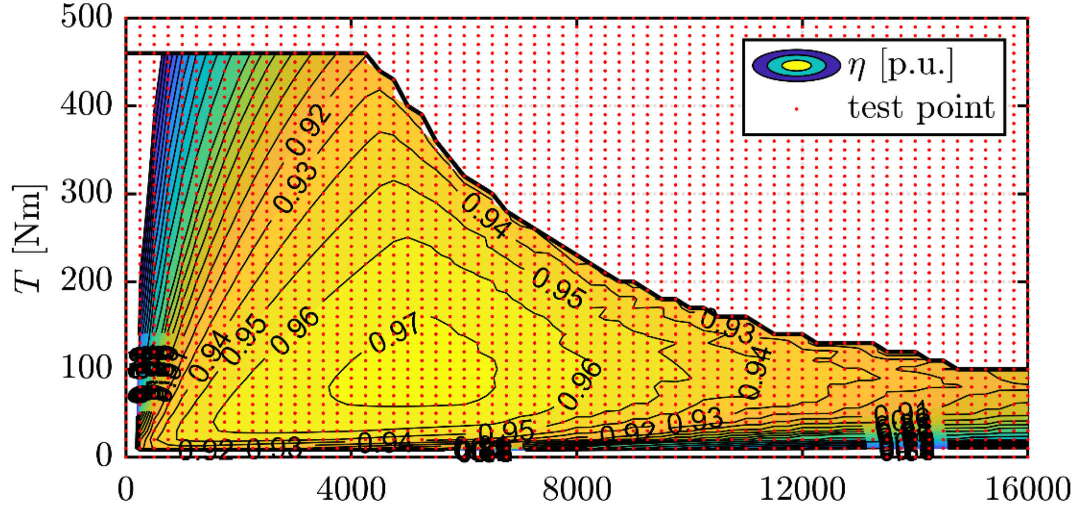

Control trajectories calculated for minimum loss

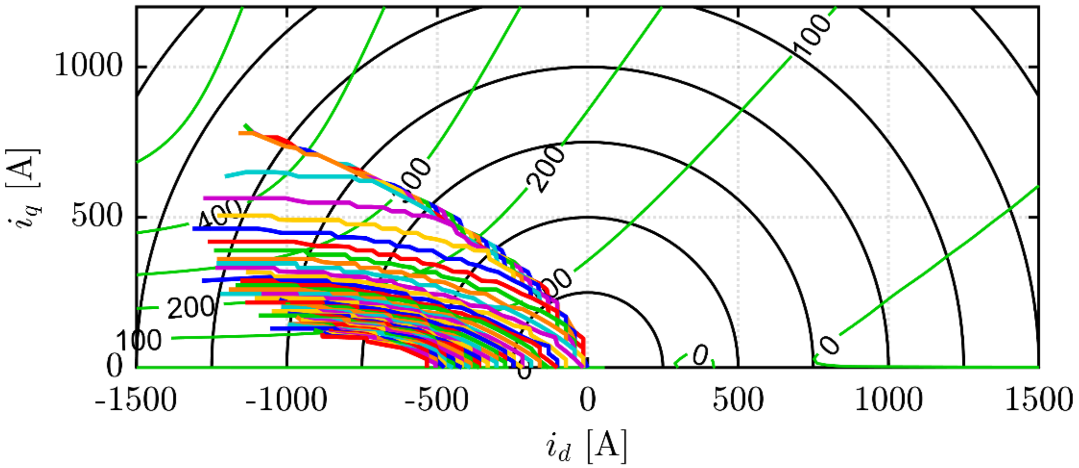

Structural Validation

Integrated method: PDE Toolbox

- 2D linear problem
- Approximated periodic boundary condition (pole sides fixed)
- Single-body model with individual material properties for iron and PM

Benchmark: SolidWorks and Comsol

- SyR-e export to dxf
- 1-pole simulation (periodic boundary)
- Centrifugal force only
- Fine mesh, with finer mesh around the ribs

Comparable results

Conservative linear simulation $(\sigma_{VM} < \sigma_y)$

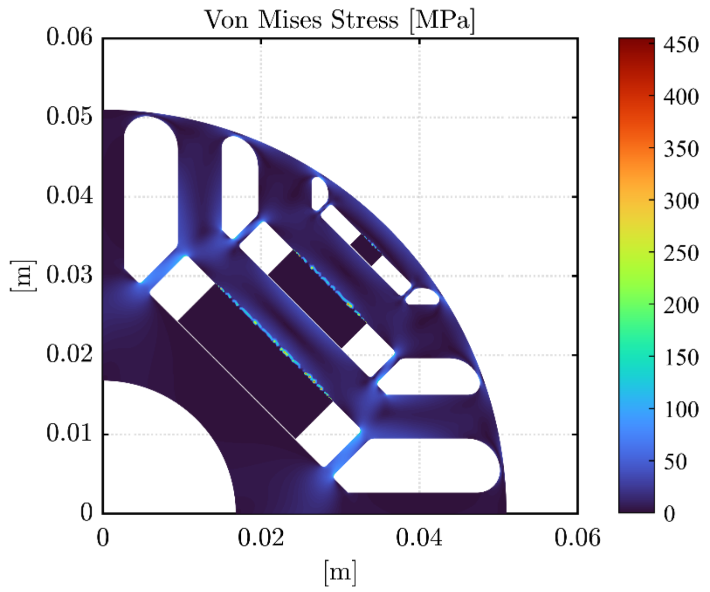

SolidWorks Linear Simulation

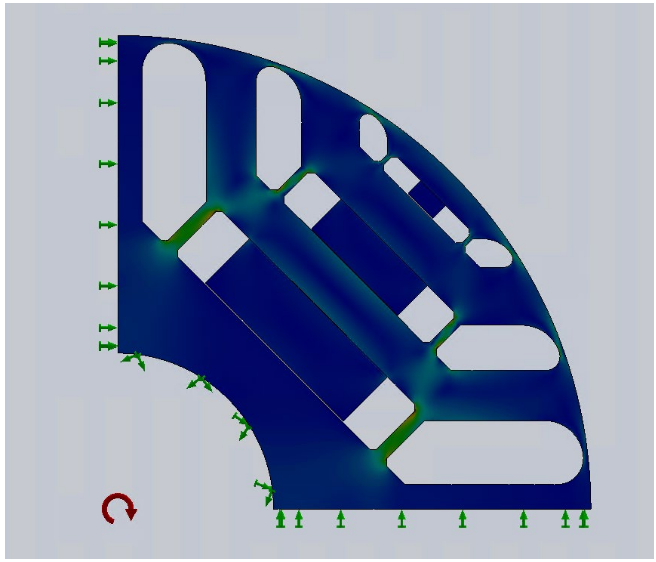

Motor-CAD interface

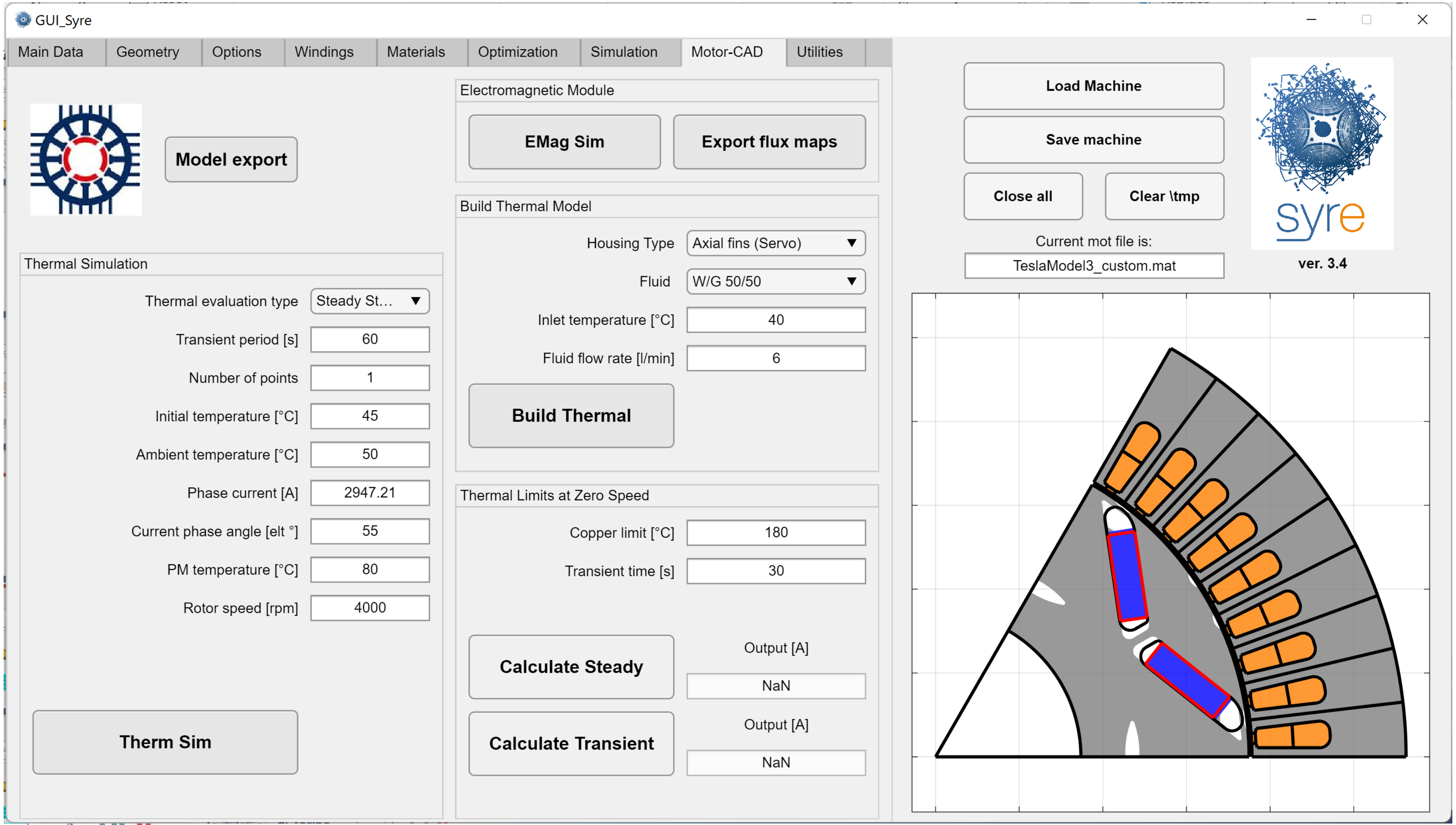

Export to Motor-CAD

[12] P. Ragazzo, S. Ferrari, N. Riviere, M. Popescu, and G. Pellegrino, "Efficient Multiphysics Design Workflow of Synchronous Reluctance Motors," in *2020 International Conference on Electrical Machines (ICEM)*, Gothenburg, Sweden, Aug. 2020

Ansys Motor-CAD is the best-in-class software for thermal validation

The fast preliminary design feature of SyR-e complements very well Motor-CAD

Other software in loop:

- Autocad
- Simcenter Magnet (Infolytica)
- Ansys Maxell

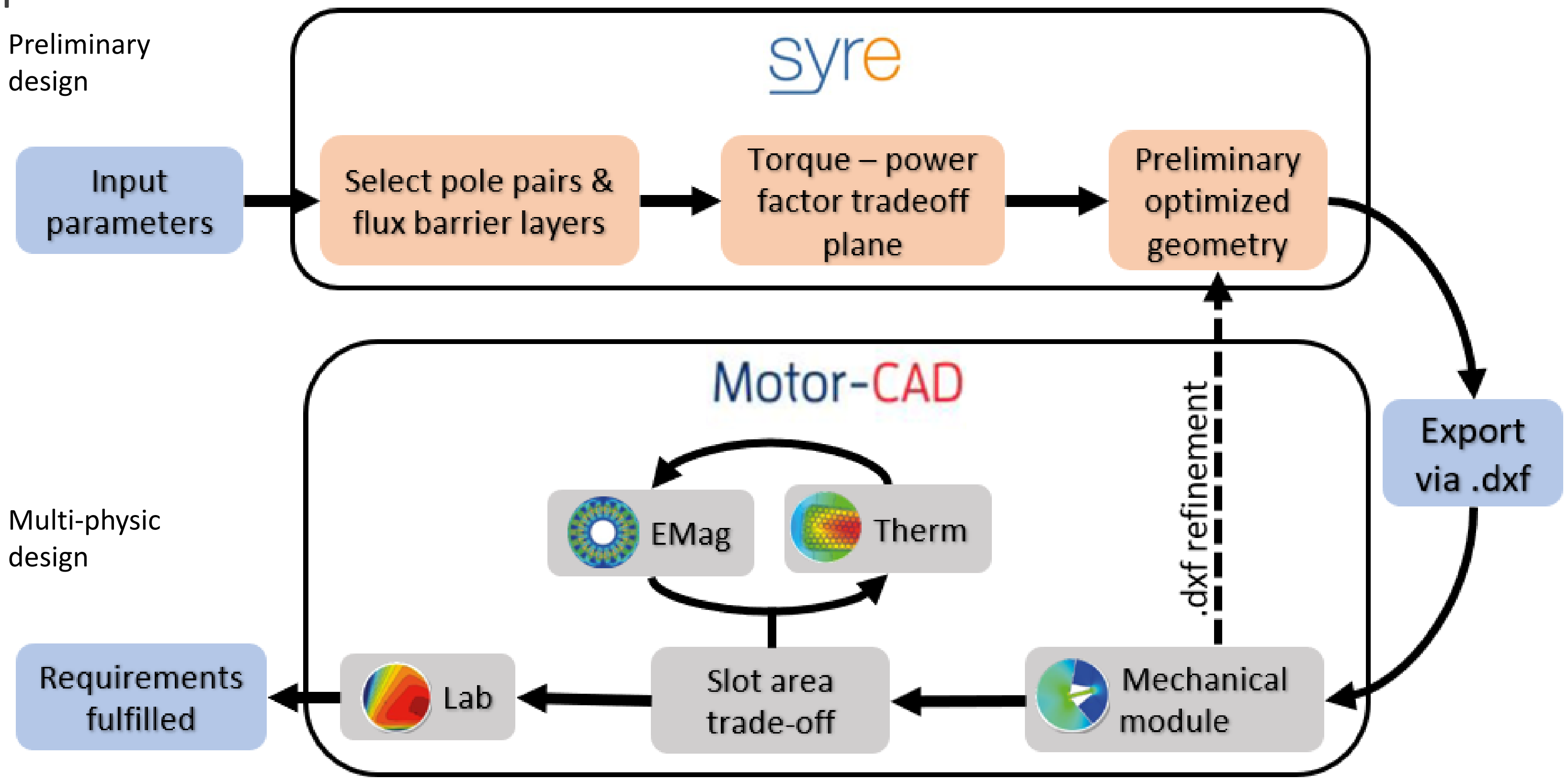

Thermal Limit

This is the continuous curve obtained iterating Motor-CAD under assumptions of 10 liters/min water-glycol, 45°C inlet temperature, full potting 1.9 W/°C/m (end-winding and stack)

Temperature limits: **copper 180°C**, PM 160°C

This shows the co-simulation capability

Transient thermal simulations can be launched directly from SyR-e or in Motor-CAD

Computed efficiency map and thermal limit

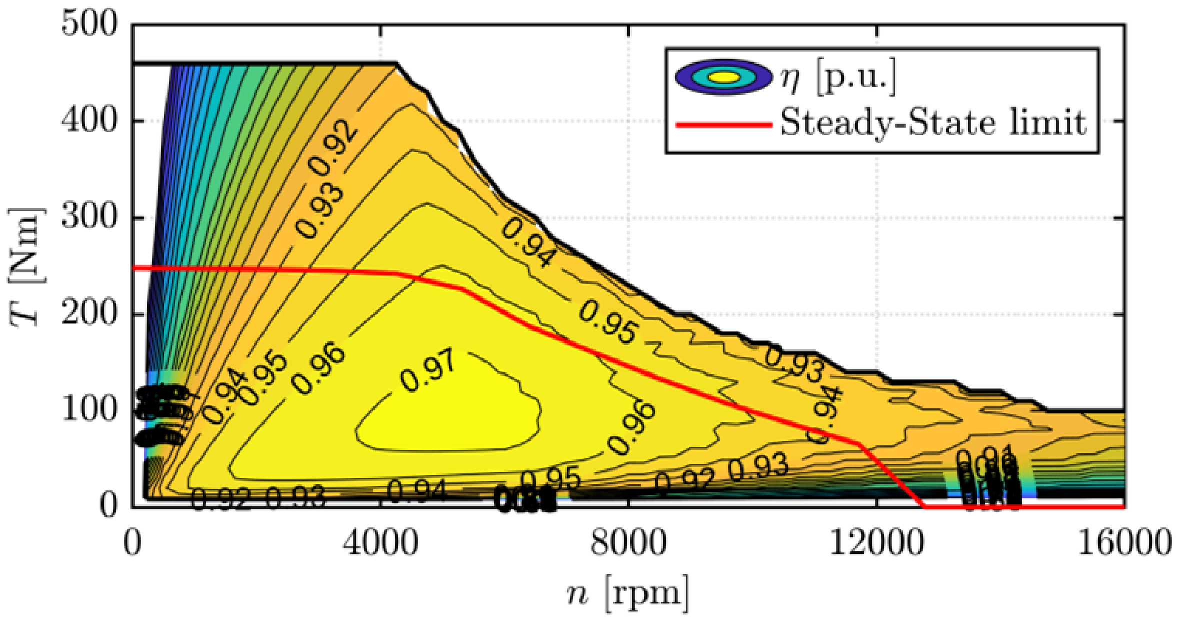

syreDrive tab for control simulation

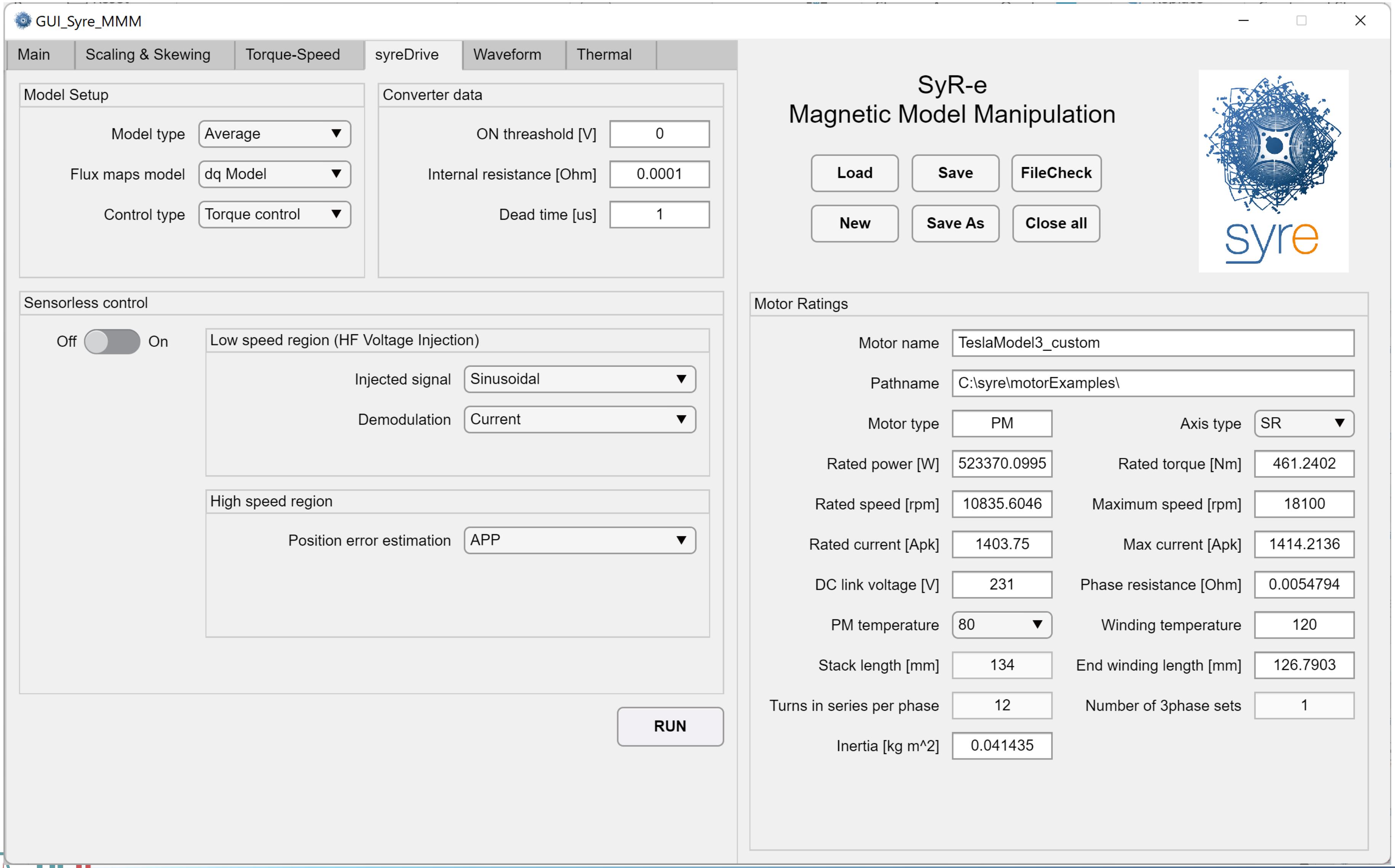

PWM Current Waveforms

[13] S. Ferrari, P. Ragazzo, G. Dilevrano and G. Pellegrino, "Flux and Loss Map Based Evaluation of the Efficiency Map of Synchronous Machines," under review.

PWM loss is calculated in selected points for the sake of time efficiency:

- FEA re-evaluated under PWM current waveforms
- Copper loss corrected via AC loss factor

At 100 Nm, 5.000 rpm:

- +110 W in Cu and Fe
- PM loss explodes

Selected point for PWM loss evaluation

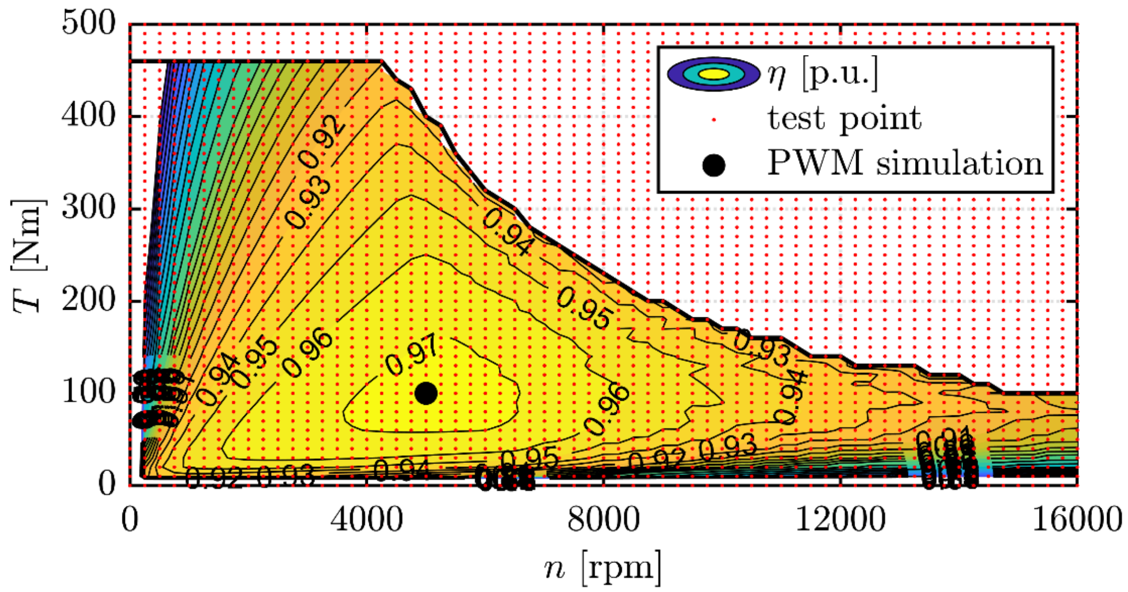

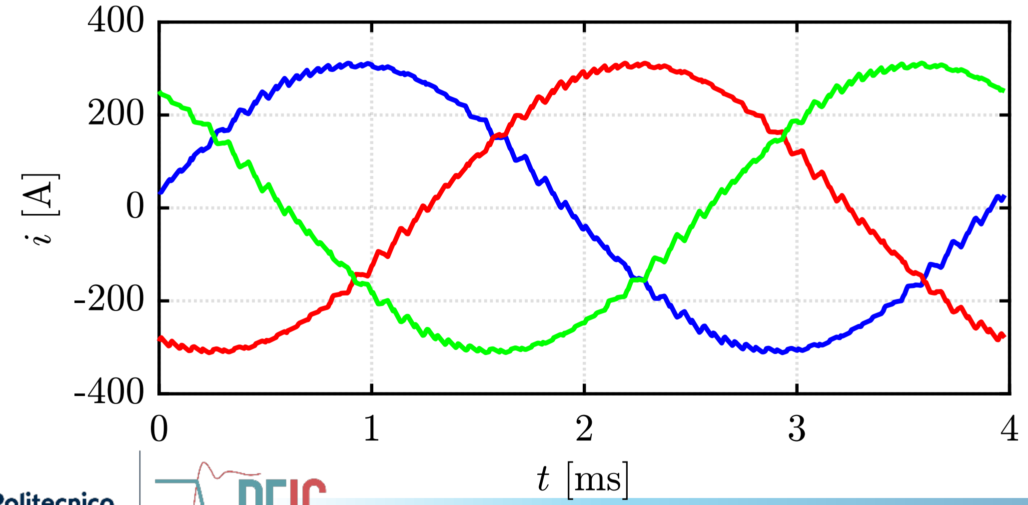

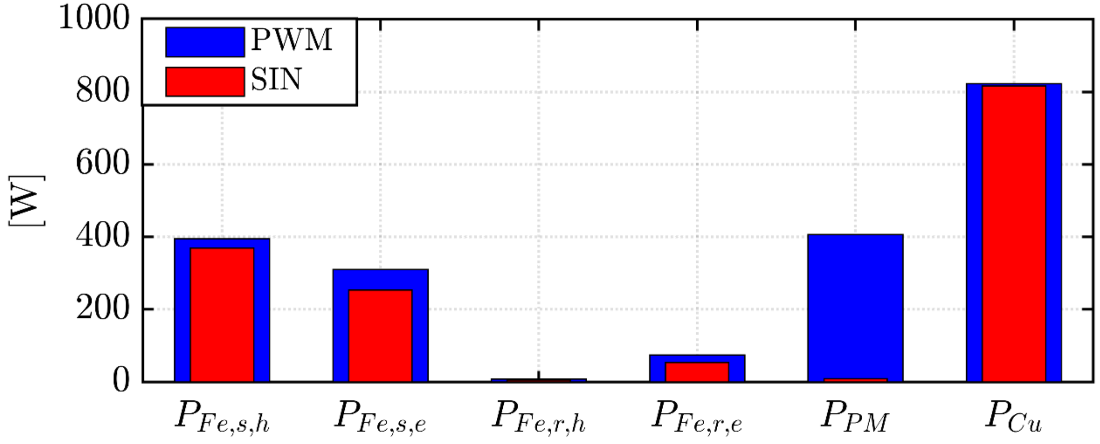

New Public Release

v3.4 on GitHub, September 2022

New SyR-e release with ICEM'22 updates!

- Improved (x,b) design plane (ICEM22 paper)
- Improved scaling rules (ECCE22 paper)
- New demo **TeslaModel3_custom**
- 3rd GUI syrmDesignExplorer
- syreDrive improved
- Improved structural simulation
- Preliminaries of Induction Motor

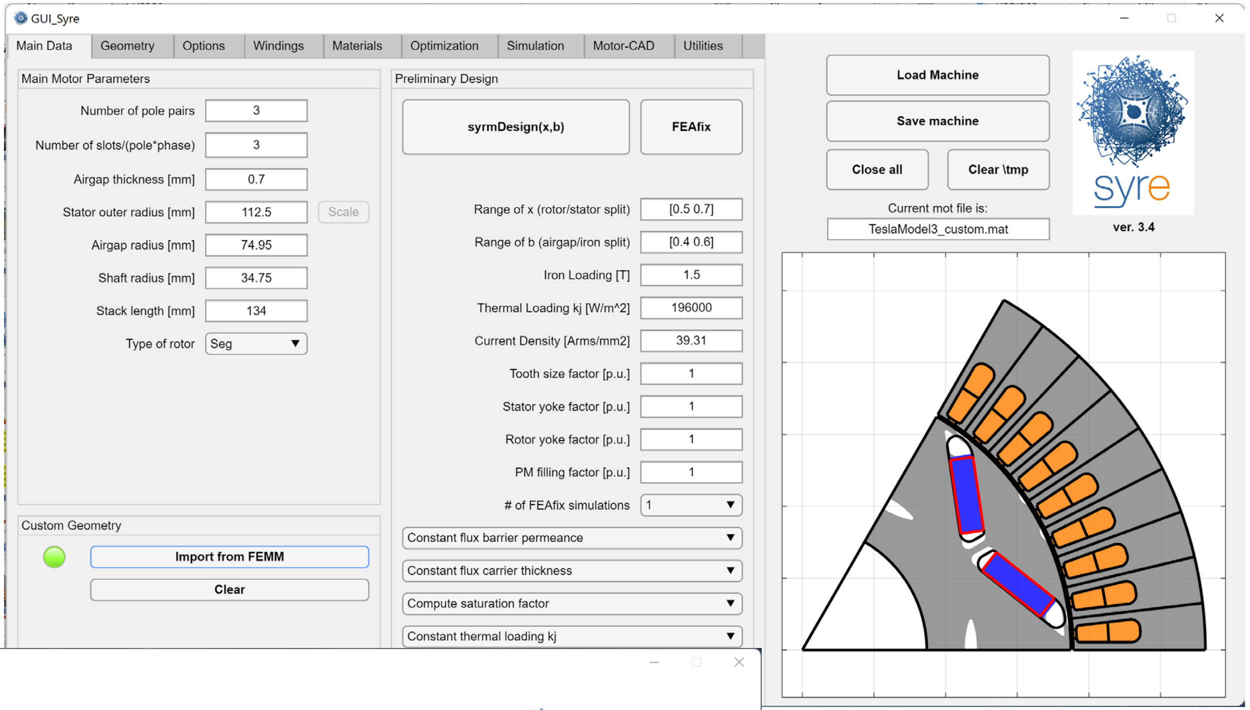

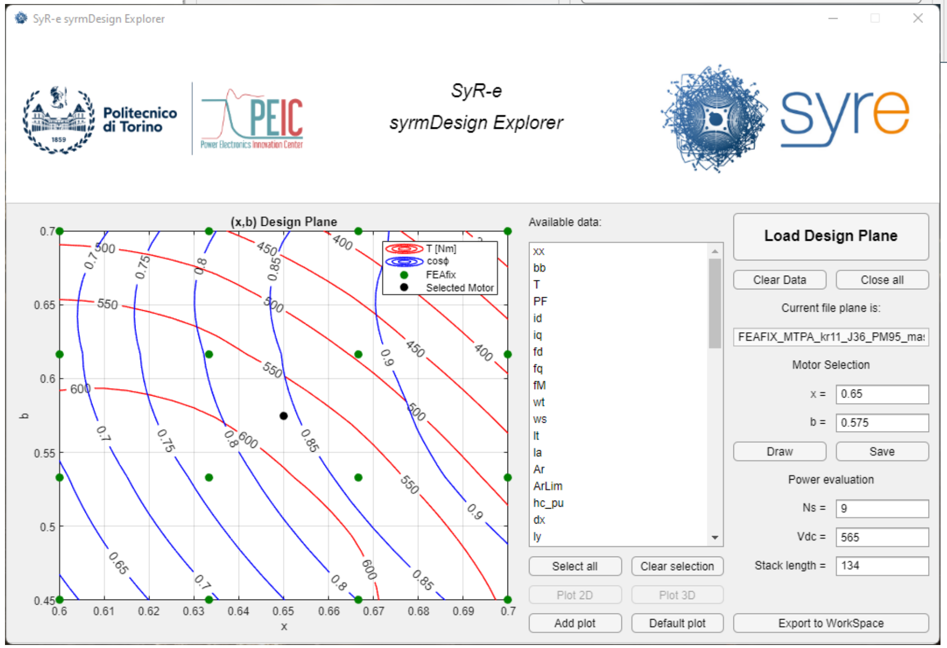

GitHub

Today's Content

Introduction (20 min)

- Politecnico di Torino and the Power Electronics Innovation Center (PEIC)
- Permanent magnet machines used in traction

Overview of SyR-e (40 min)

- SyR-e geography
- Main tools for design and modelling
- Magnetics
- Thermal
- Structural
- PWM waveforms and loss

Design of the IPM machine (60 min)

- **Case study: Tesla Model 3 rear axle IPM machine**
- **FEAfix-corrected (x,b) design plane**
- **Design procedure**
- **Number of turns determination**
- **Stack length minimization**
- **Structural and Thermal aspects**
- **syreDrive: Control simulation**

Conclusion

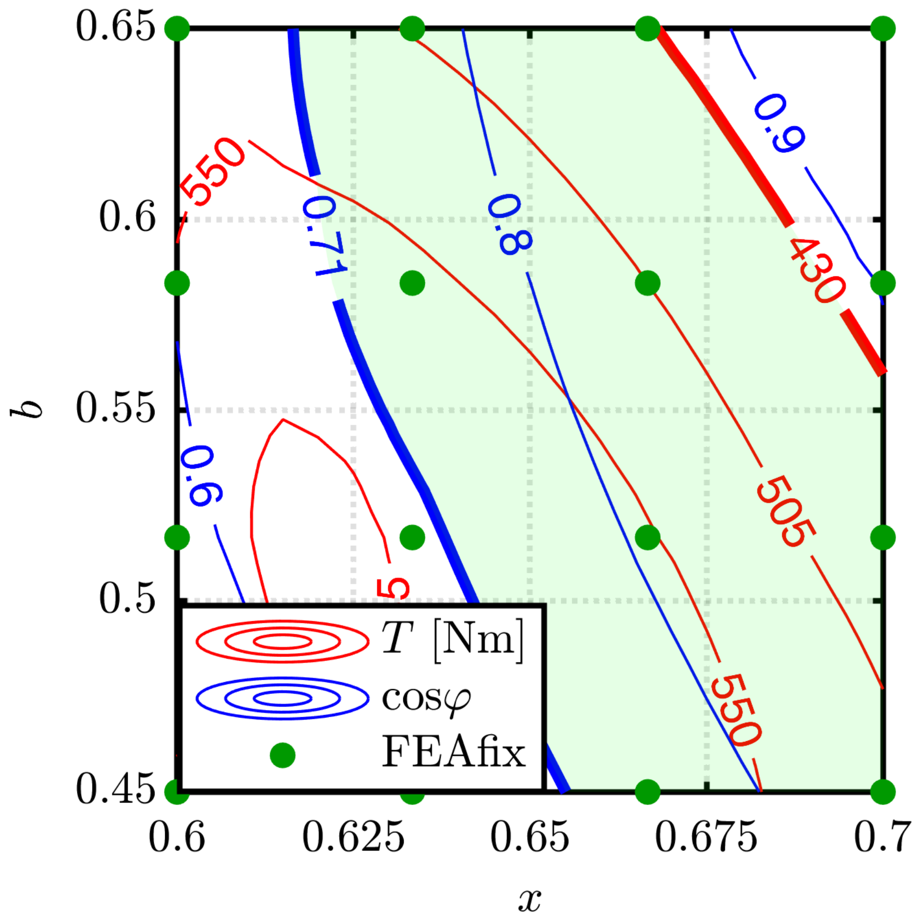

Demo model of SyR-e

Custom version of Model3 rear axle e-motor

TeslaModel3_custom.fem,
TeslaModel3_custom.mat

Main reference is [14], the custom cross-section is derived from pictures available on the internet

Assumptions when data incomplete:

- Slot fill factor: k_{Cu} = 0,38 (net copper/slot area)
- Fe-Si grade: M270-35A
- PM grade: N52UH
- PM temperature: 80°C (avg.)

No direct oil cooling, we focus mostly on magnetic design

Thermal validation refers to water jacket

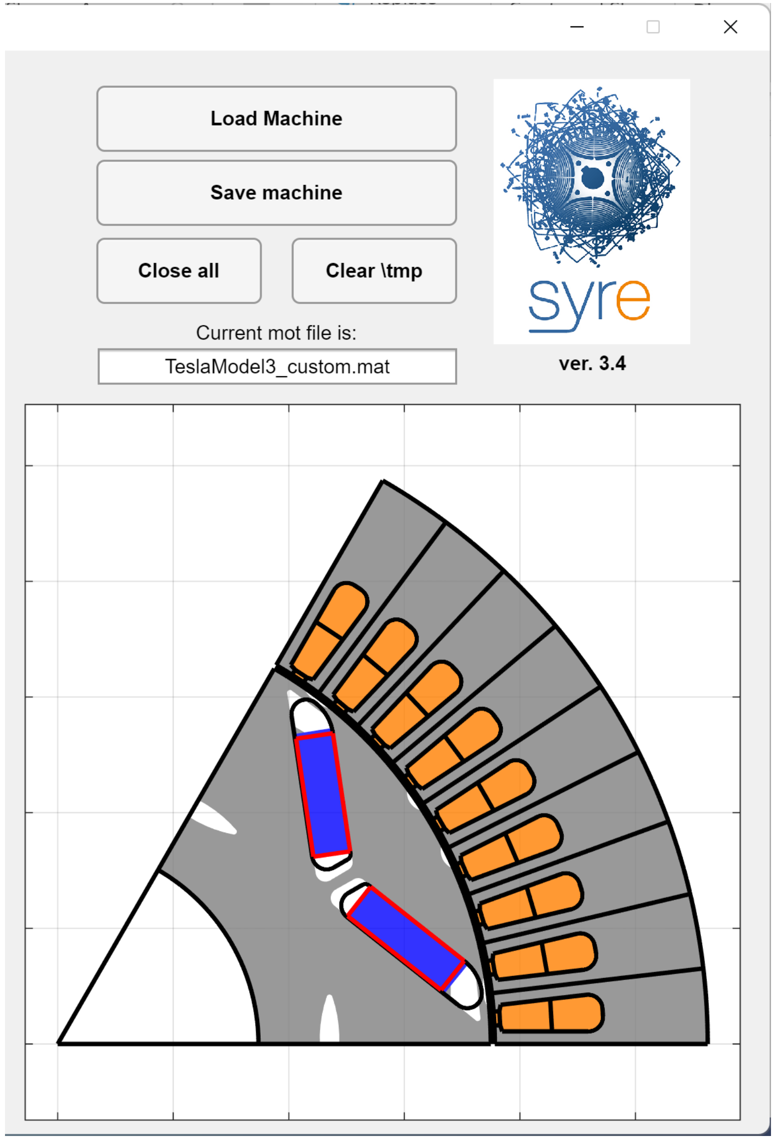

[14] MotorXP, Performance Analysis of the Tesla Model 3 Electric Motor using MotorXP-PM. VEPCO, Jun. 2020, https://motorxp.com/wp-content/uploads/mxp analysis TeslaModel3.pdf

Case Study Specs

[6] P. Ragazzo, G. Dilevrano, S. Ferrari and G. Pellegrino, "Design of IPM Synchronous Machines Using Fast-FEA Corrected Design Equations," presented at *ICEM 2022*, Valencia

2-V IPM rotor type instead of 1-V

The torque and power factor vs (x,b) design plane refers to **a single operating point** per machine, **at MTPA conditions**

Target torque and PF, at MTPA:

- $T_{max} \geq$ **430 Nm**
- $\cos(\varphi_{base}) \geq$ **0.71** (estimated efficiency 95%)

The **PF at MTPA and base speed** replaces the **peak power requirement** in the plane

Model3 custom

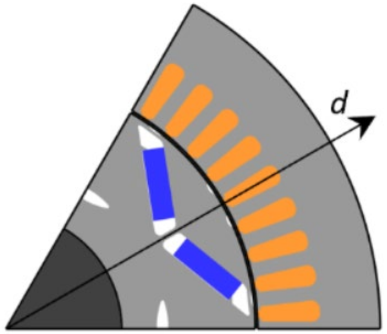

Final design of [13]

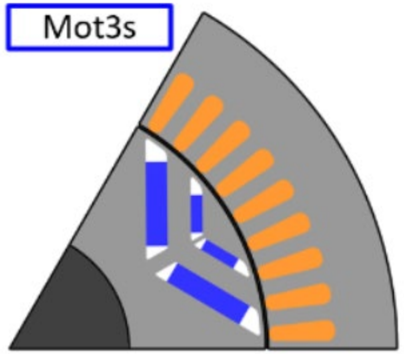

Case study specs		
Peak torque	**[Nm]**	**430**
Peak power	**[kW]**	**192**
Maximum speed	[rpm]	18100
Peak phase current	**[Arms]**	**1000**
DC link voltage (min)	**[V]**	**231**
Peak current density	[Arms/mm2]	36
Stator outer diameter	[mm]	225
Stack length	[mm]	134
Base speed	[rpm]	4200
Target power factor		**0.71**
Number of pole pairs		3
Number of slots		54
PM mass	[kg]	1,8
Cu mass	[kg]	4,7

Peak Torque and Power specs

The magnetic design refers to the indicated point, where the specified **peak torque and power $\boldsymbol{T_{max}}$, $\boldsymbol{P_{max}}$** ideally meet

The base speed value n_{base} is defined, referring to the ideal case

$$n_{base} = \frac{P_{max}}{T_{max}} \cdot \frac{30}{\pi}$$

It is assumed that

- T_{max} is at $\leq I_{max}$ in MTPA conditions
- T_{max} reaches the voltage limit V_{dc} at $\geq n_{base}$

Torque and power specs
and reference design point at base speed

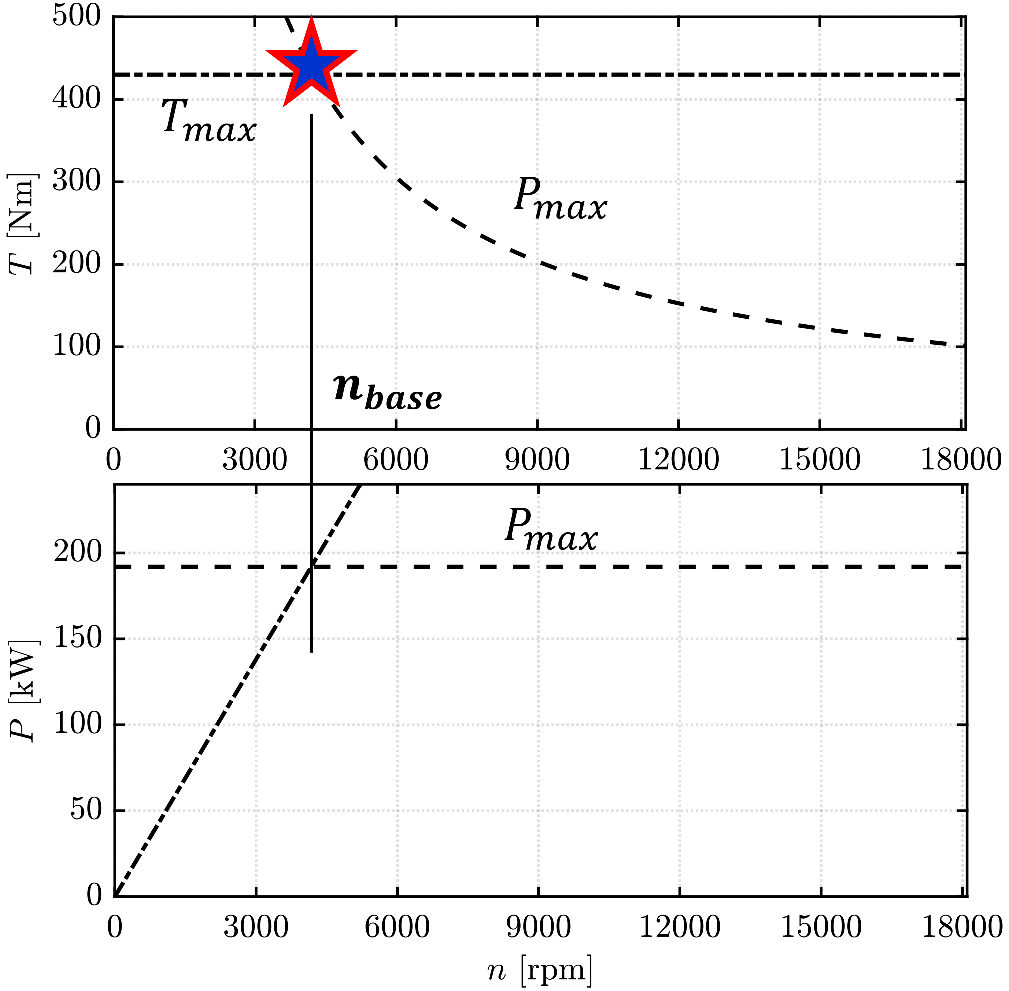

PF in place of Pmax

Considered the inverter limits V_{dc} and I_{max}, and estimated the efficiency at base speed η_{base}, the active power balance at the reference T_{max}, n_{base} point is:

$$\frac{\sqrt{3}}{2} \cdot V_{dc} \cdot I_{max} \cdot \cos(\varphi_{base}) \geq \frac{P_{max}}{\eta_{base}}$$

Therefore

$$\boldsymbol{\cos(\varphi_{base})} \geq \frac{\boldsymbol{P_{max}}}{\eta_{base} \cdot \frac{\sqrt{3}}{2} \cdot V_{dc} I_{max}}$$

The PF constraint represents P_{max}, given the kVA rating

Torque and power specs
and reference design point at base speed

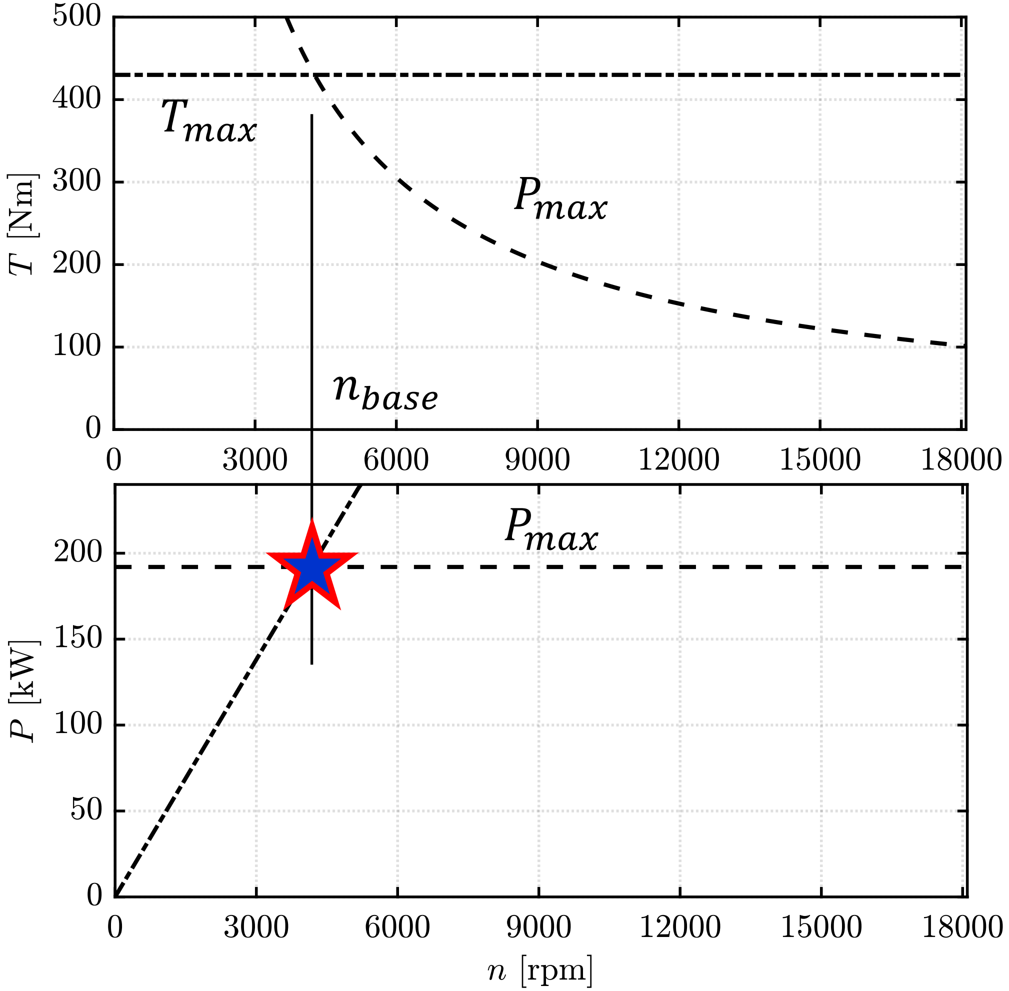

Significance of PF

Considered the inverter limits V_{dc} and I_{max}, and estimated the efficiency at base speed η_{base}, the active power balance at the reference T_{max}, n_{base} point is:

$$\frac{\sqrt{3}}{2} \cdot V_{dc} \cdot I_{max} \cdot \cos(\varphi_{base}) \geq \frac{P_{max}}{\eta_{base}}$$

Therefore

$$\boldsymbol{\cos(\varphi_{base})} \geq \frac{\boldsymbol{P_{max}}}{\eta_{base} \cdot \frac{\sqrt{3}}{2} \cdot V_{dc} I_{max}}$$

The PF constraint represents P_{max}, given the kVA rating

This is a conservative assumption

Case study specs		
Peak torque	**[Nm]**	**430**
Peak power	**[kW]**	**192**
Maximum speed	[rpm]	18100
Peak phase current	**[Arms]**	**1000**
DC link voltage (min)	**[V]**	**231**
Peak current density	[Arms/mm2]	36
Stator outer diameter	[mm]	225
Stack length	[mm]	134
Base speed	**[rpm]**	**4200**
Target power factor		**0.71**
Number of pole pairs		3
Number of slots		54
PM mass	[kg]	1,8
Cu mass	[kg]	4,7

Realistic flux weakening behavior

Conservative assumption

The PF target guarantees meeting the peak power spec **with margin**

$$\cos(\varphi_{base}) \geq \mathbf{0.71} \rightarrow P_{max} > \mathbf{192\ kW}$$

Real-world curves of IPM machines with flux weakening properties have a power increase at early FW stages

Moreover

The higher the PF, the higher the peak power, fixed all other quantities

Real flux-weakening curves

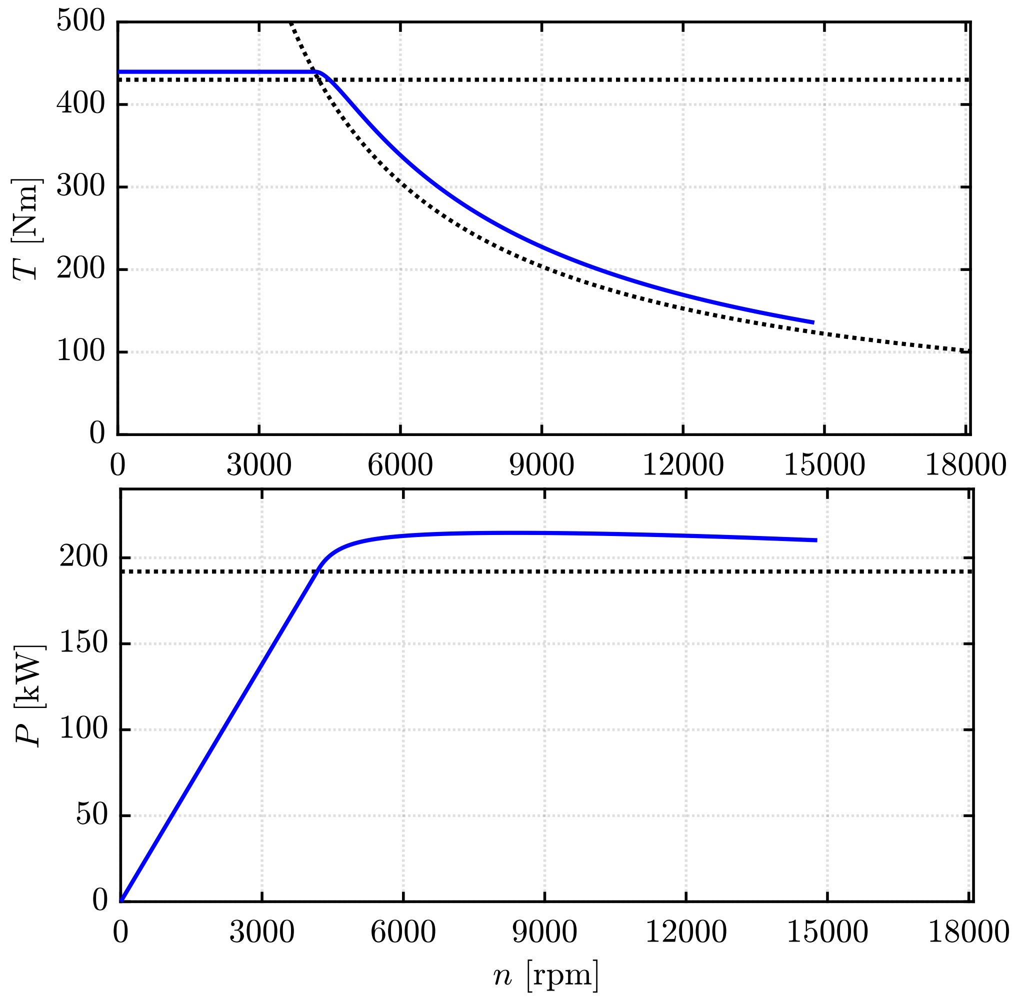

T(x,b) and PF(x,b) design plane

Each point of the plane is one cross-section

The coordinates are:

- Rotor/Stator split ratio $x = \frac{d}{D}$
- Airgap/iron flux density ratio $b = \frac{B_g}{B_{Fe}}$

Common to all designs

- Stack size D = 225 mm, L = 134 mm
- pk current density J_s = 36 A/mm^2 rms

The design equations used to obtain the contours are briefly reviewed

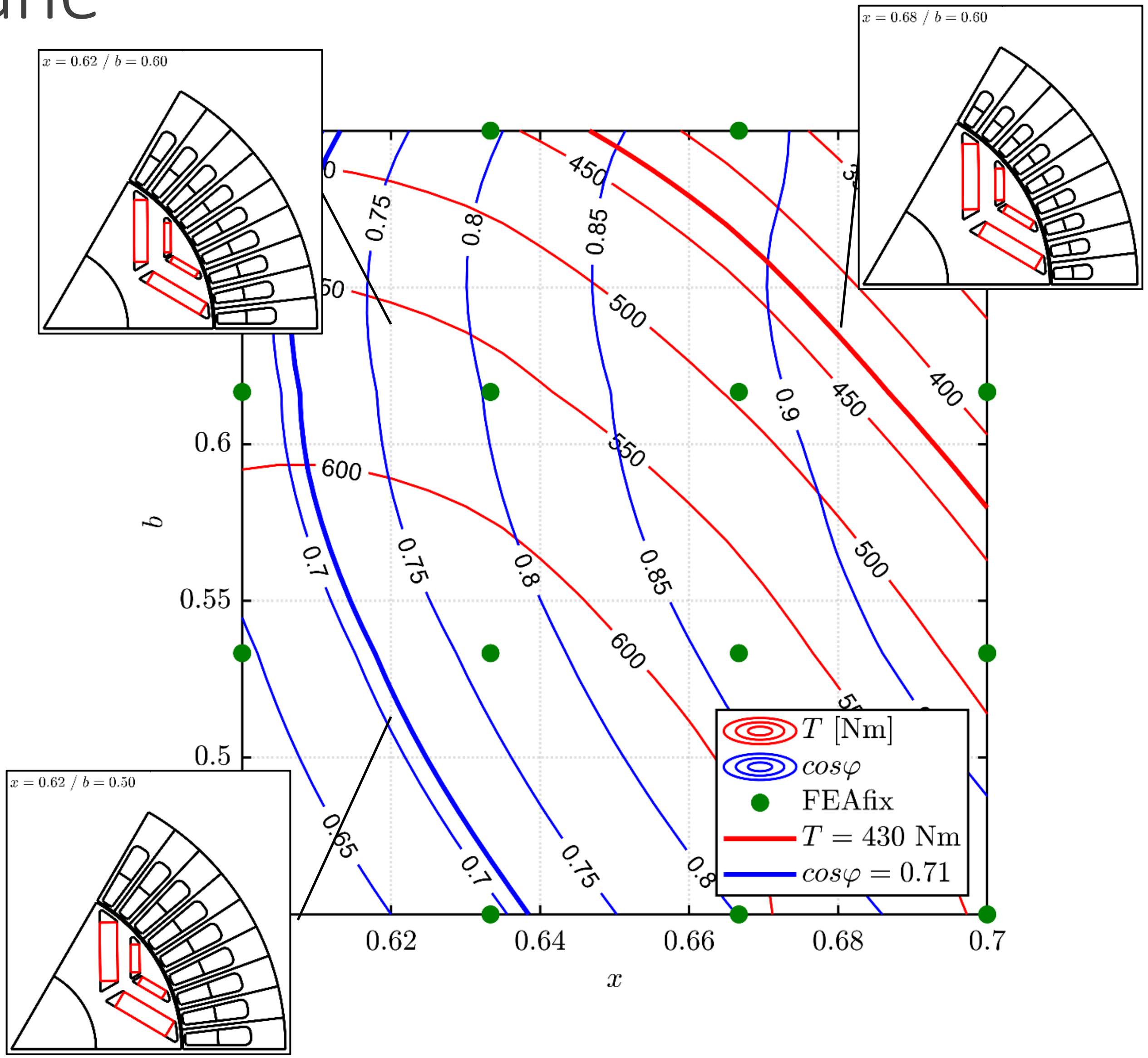

Core dimensions

[6] P. Ragazzo, G. Dilevrano, S. Ferrari and G. Pellegrino, “Design of IPM Synchronous Machines Using Fast-FEA Corrected Design Equations," presented at ICEM 2022, Valencia
[5] S. Ferrari and G. Pellegrino, "FEAfix: FEA Refinement of Design Equations for Synchronous Reluctance Machines," in *IEEE Transactions on Industry Applications*, vol. 56, no. 1, pp. 256-266, Jan.-Feb. 2020.

Core dimensions are function of $x \cdot b$

Stator

- $\boldsymbol{l_y} = \frac{D}{2p} \cdot k_y \cdot xb$
- $\boldsymbol{w_t} = \frac{\pi D}{6pq} \cdot k_t \cdot xb$

Rotor

- $\boldsymbol{l_{y,r}} = \sum h_{Fe} = k_{Fe,r} \cdot l_y$

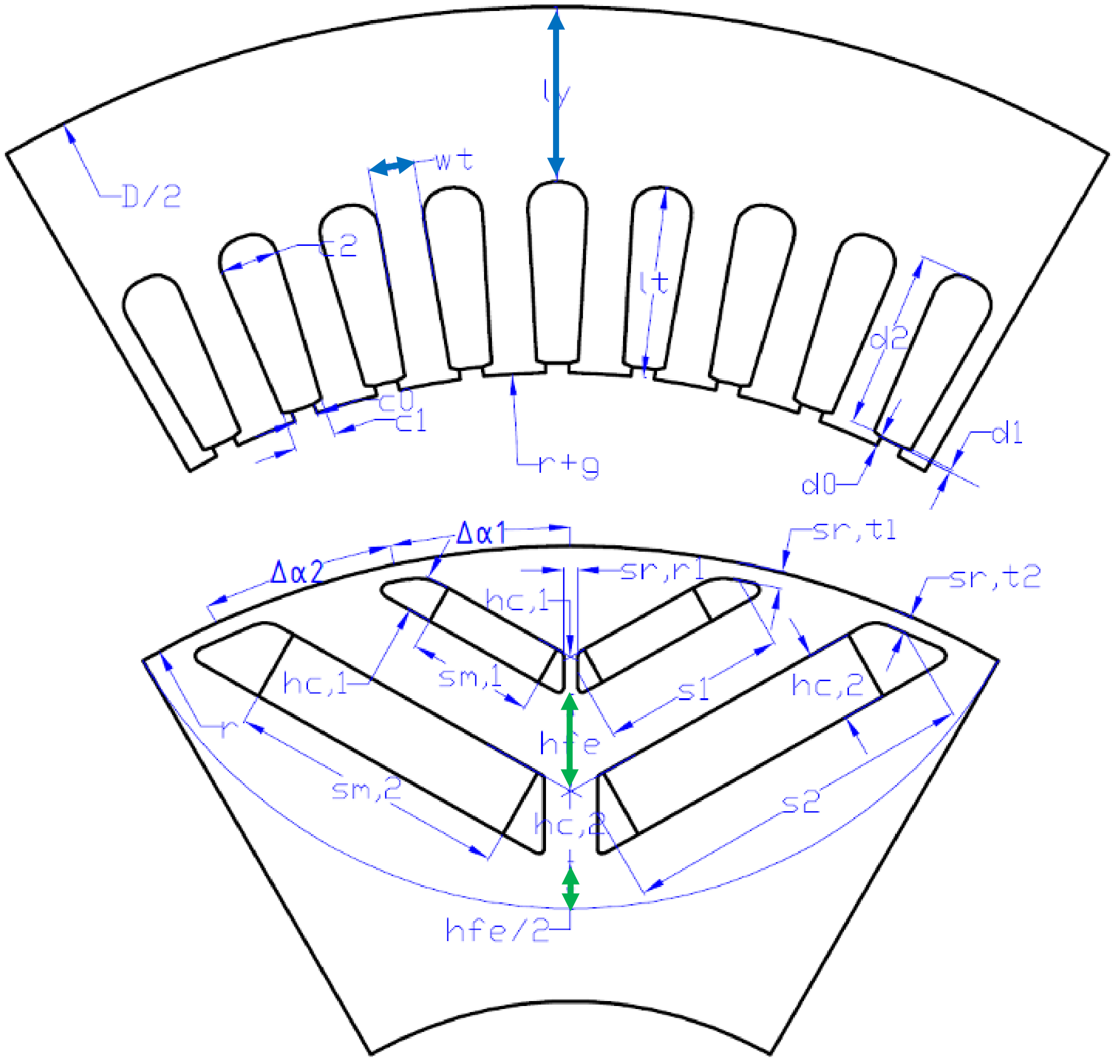

Core dimensions coefficients

Core dimensions are function of $x \cdot b$

Stator

- $l_y = \frac{D}{2p} \cdot \boldsymbol{k_y} \cdot xb$
- $w_t = \frac{\pi D}{6pq} \cdot \boldsymbol{k_t} \cdot xb$

Rotor

- $l_{y,r} = \sum h_{Fe} = \boldsymbol{k_{Fe,r}} \cdot l_y$

Dedicated coefficients further define the stator and rotor iron dimensions

Example

- $k_t = 1$ is equal pk flux density in yoke and tooth
- $k_t < 1$ is a smaller and more saturated tooth

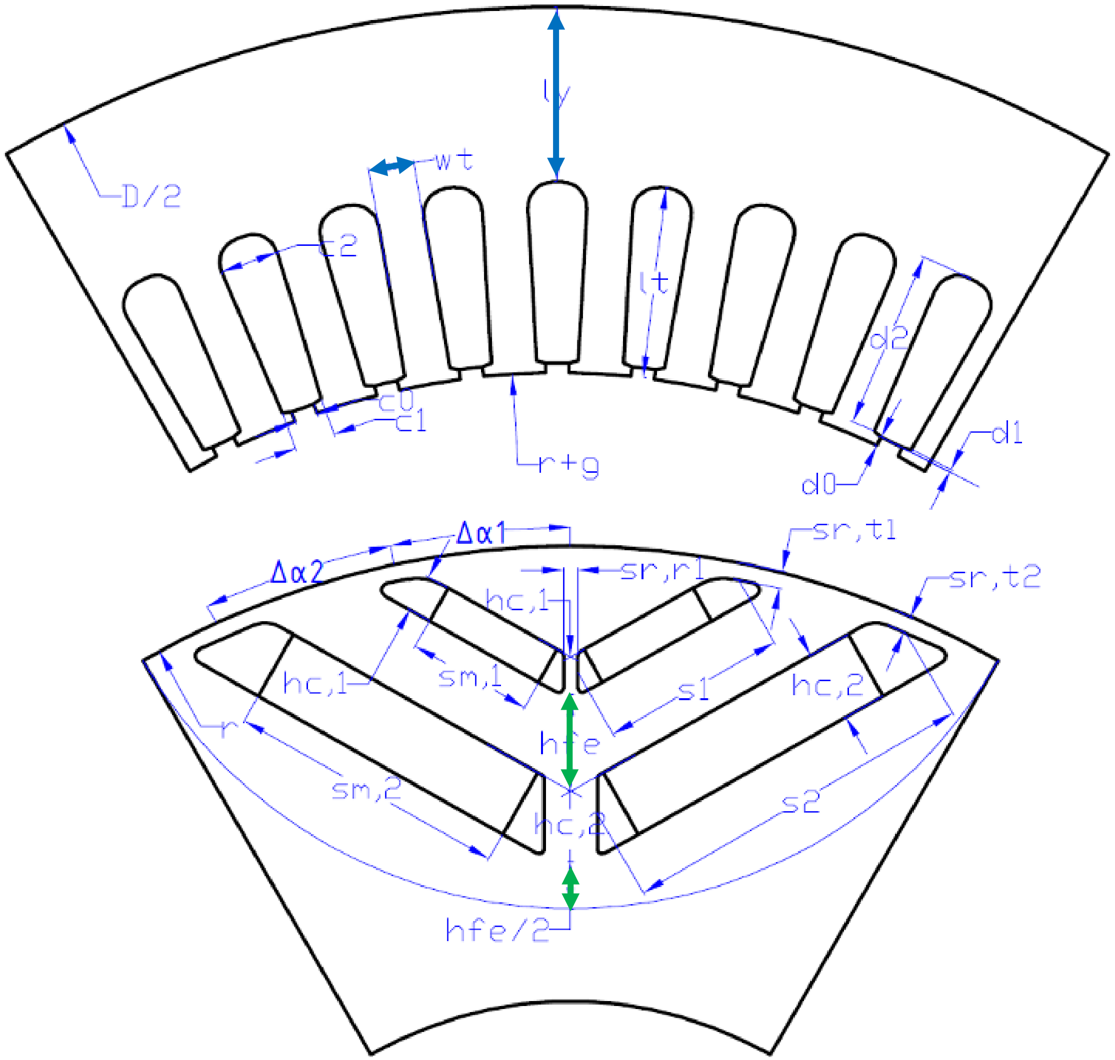

Ampere-turns

The total slot cross-sectional area A_{slots} is function of the coordinates x, b

Fixed the current density J_s $(\mathrm{A/mm^2})$

$$J_s = \frac{6\ N_s I_0}{k_{Cu} A_{slots}}$$

the corresponding phase Ampere-turn value $N_s I_0$ is determined, also function of the coordinates

$$N_s I_0 = \frac{J_s k_{Cu}}{6} A_{slots}(x, b)$$

Each design has a determined $N_s I_0$

The number of turns is not yet defined

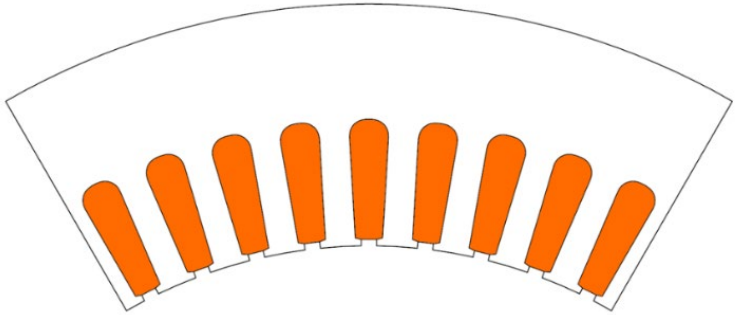

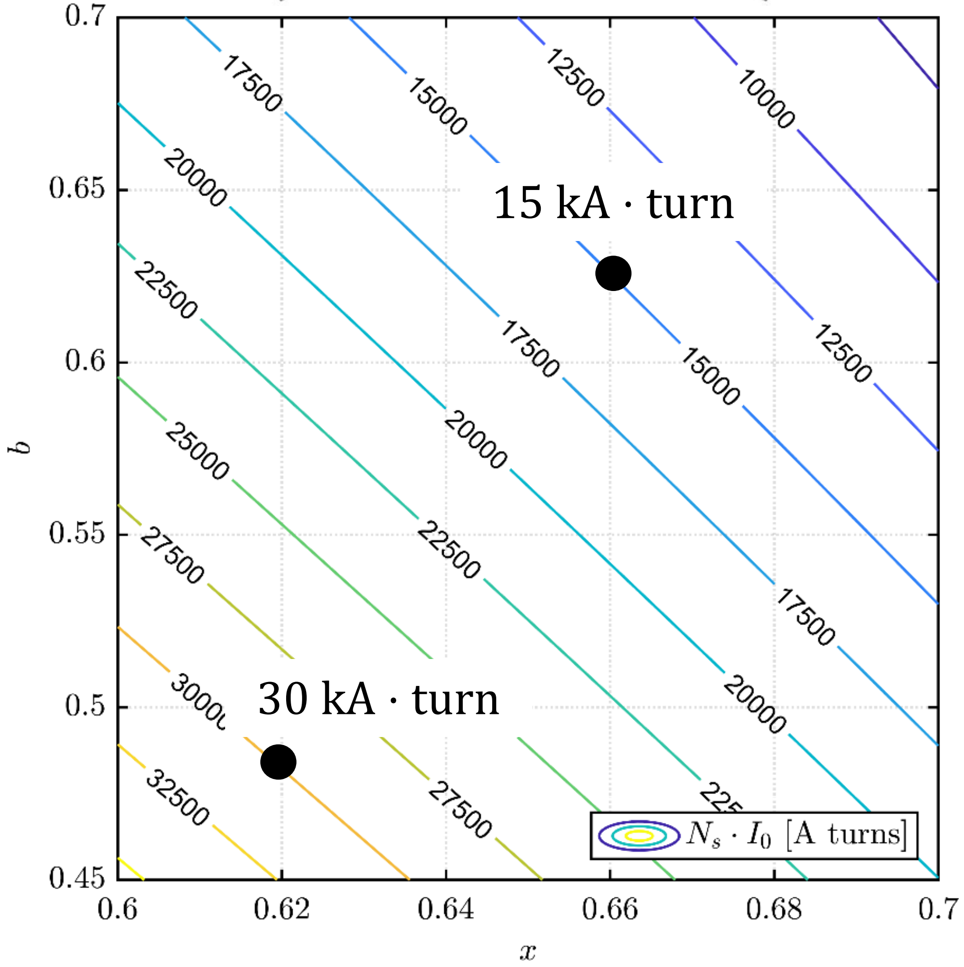

Pole Magnetic Flux

In similar way, the **base flux linkage λ_0** at fixed current density is defined throughout the x, b plane

This is roughly proportional to b, except for the effects of non-idealities such as core saturation, structural ribs, etc ..

The base flux linkage is normalized to the number of turns

Each design has a determined $\frac{\lambda_0}{N_s}$

(Number of turns not yet defined)

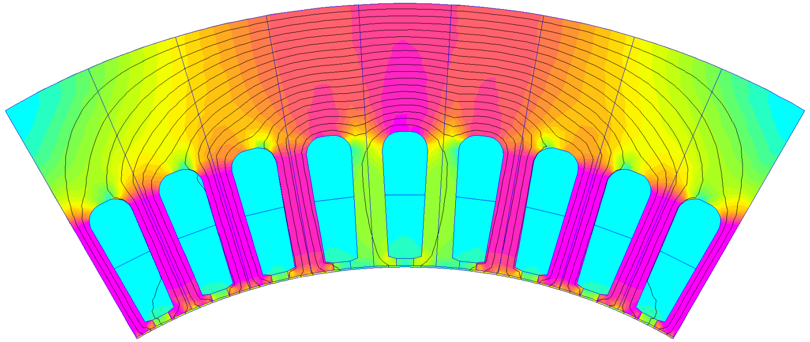

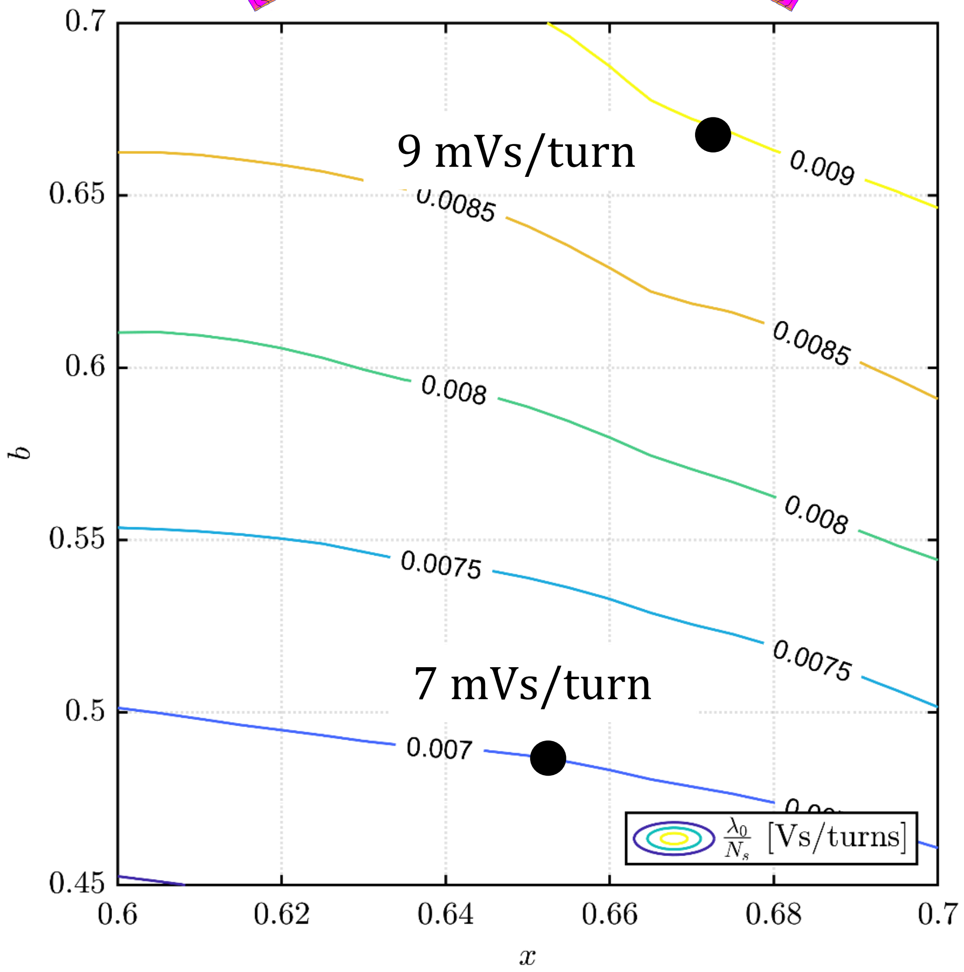

Design Equations Summary

The flux linkages are normalized by the number of turns and defined as:

$$\begin{cases} \dfrac{\lambda_d}{N_s} = \dfrac{(L_{md} + L_\sigma)}{N_s^2} \cdot N_s i_d + \dfrac{\lambda_m}{N_s} \\ \dfrac{\lambda_q}{N_s} = \dfrac{(L_{mq} + L_\sigma)}{N_s^2} \cdot N_s i_q \end{cases}$$

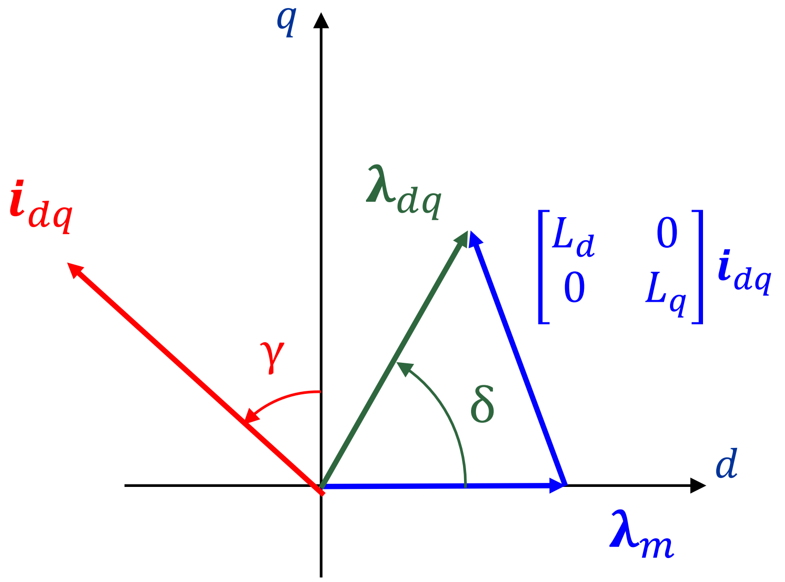

The normalized inductance components L/N_s^2 and the PM flux term $\frac{\lambda_m}{N_s}$ are calculated via dedicated lumped-parameter networks

L_{md}, L_{mq} are magnetizing inductance
L_σ is leakage inductance
λ_m is the PM flux linkage

q axis model

[5] S. Ferrari and G. Pellegrino, "FEAfix: FEA Refinement of Design Equations for Synchronous Reluctance Machines," in *IEEE Transactions on Industry Applications*, vol. 56, no. 1, pp. 256-266, Jan.-Feb. 2020.

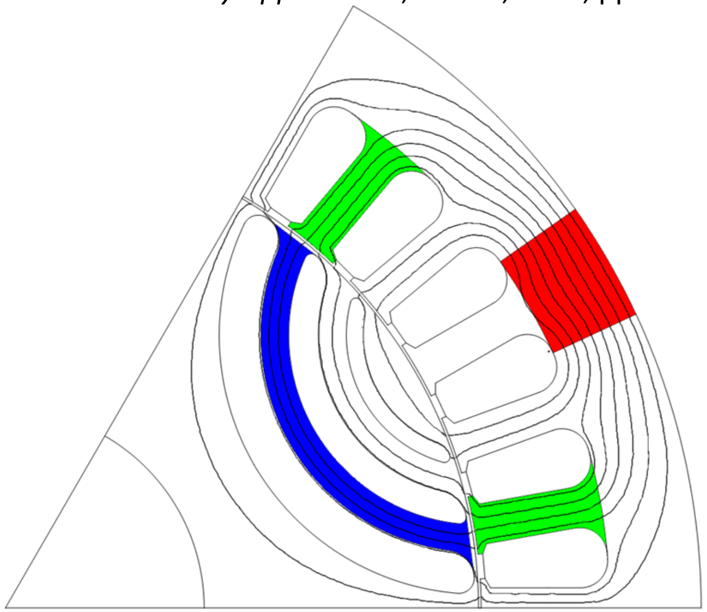

The q inductance is estimated from the solid rotor assumption, considered the **saturation coefficient $\boldsymbol{k_{sat}}$**

$$\frac{L_{mq}}{N_s^2} = \frac{3}{\pi} \cdot \mu_0 \cdot \left(\frac{k_w}{p}\right)^2 \cdot \frac{DL}{k_c g} \cdot \frac{1}{k_{sat}} \cdot \boldsymbol{x}$$

The reference paper [5] covers the SyR machine, and the same equations are used also for the IPM machine.

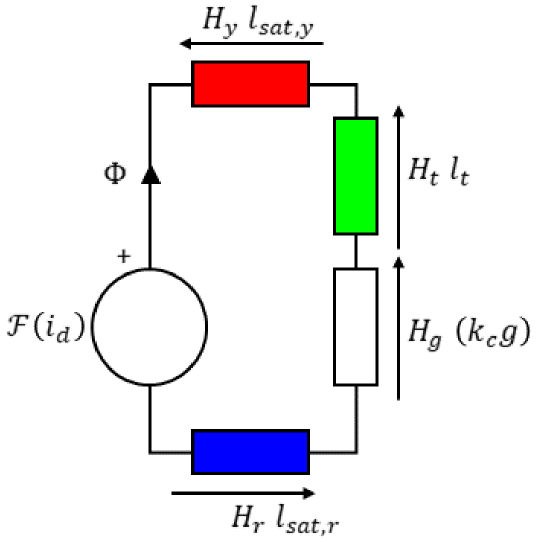

[6] P. Ragazzo, G. Dilevrano, S. Ferrari and G. Pellegrino, “Design of IPM Synchronous Machines Using Fast-FEA Corrected Design Equations," presented at ICEM 2022, Valencia

d axis model

The PM flux linkage is computed with the magnetic equivalent circuit of the pole

The node potentials r_k are solved from the linear system

For example, the PM flux linkage is computed

$$\frac{\lambda_m}{N_s} = 2 \cdot k_w \cdot k_f \cdot \sum_{k=1}^{n_{lay}} \frac{r_k}{R_{g,k}}$$

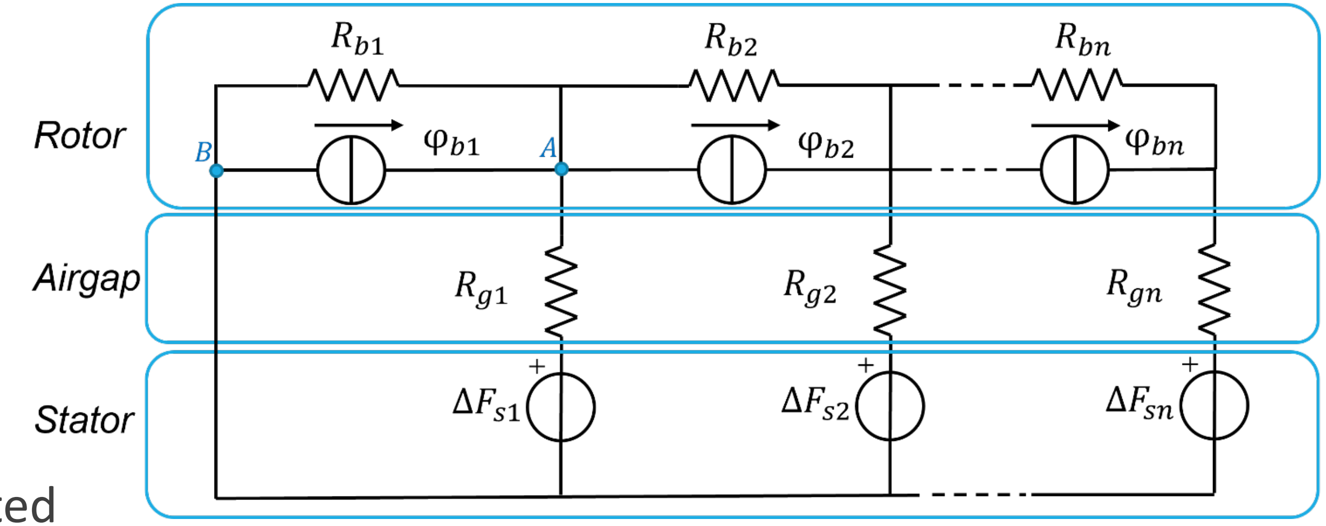

$$\underbrace{\begin{bmatrix} \varphi_{b,k} - \varphi_{b,k+1} \\ \varphi_{b,k} - \varphi_{b,k+1} \\ \vdots \\ \varphi_{b,n} \end{bmatrix}}_{\mathbf{\Phi_b}} = \underbrace{\begin{bmatrix} \mathfrak{R}^{-1}_{k,k} & \mathfrak{R}^{-1}_{k,k+1} & \dots & 0 \\ \mathfrak{R}^{-1}_{k,k-1} & \mathfrak{R}^{-1}_{k,k} & \dots & 0 \\ \vdots & \vdots & \vdots & \vdots \\ 0 & 0 & \dots & \mathfrak{R}^{-1}_{n,n} \end{bmatrix}}_{\mathfrak{R}^{-1}} \underbrace{\begin{bmatrix} r_1 \\ r_2 \\ \vdots \\ r_n \end{bmatrix}}_{\mathbf{r}} \qquad (20)$$

$$\mathfrak{R}^{-1}_{k,k} = \mathfrak{R}^{-1}_{b,k} + \mathfrak{R}^{-1}_{g,k} + \mathfrak{R}^{-1}_{b,k+1} \qquad (21)$$

$$\mathfrak{R}^{-1}_{k,k+1} = -\mathfrak{R}^{-1}_{b,k+1} \qquad (22)$$

$$\mathfrak{R}^{-1}_{k,k-1} = -\mathfrak{R}^{-1}_{b,k} \qquad (23)$$

Torque equation and current components

(electromagnetic) Torque equation:

$$T_e = \frac{3}{2} p \cdot \left(\lambda_d \cdot i_q - \lambda_q \cdot i_d\right)$$

The q-axis MMF is determined so that the peak flux density at the airgap is $b \cdot B_{Fe}$

$$N_s i_q = \frac{\pi}{3} \frac{k_c g}{\mu_0} \frac{p}{k_w} \cdot B_{Fe} \cdot \boldsymbol{b}$$

k_c is the Carter coefficient
g (mm) is the airgap length

The d-axis MMF is derived from $N_s I_0$ (current density input)

$$N_s i_d = \sqrt{(N_s I_0)^2 - \left(N_s i_q\right)^2}$$

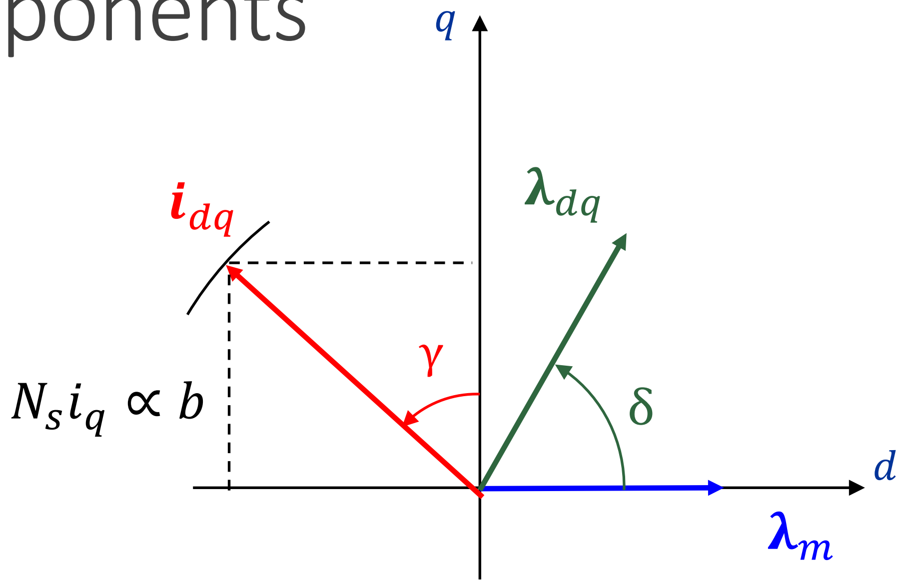

Power Factor equation

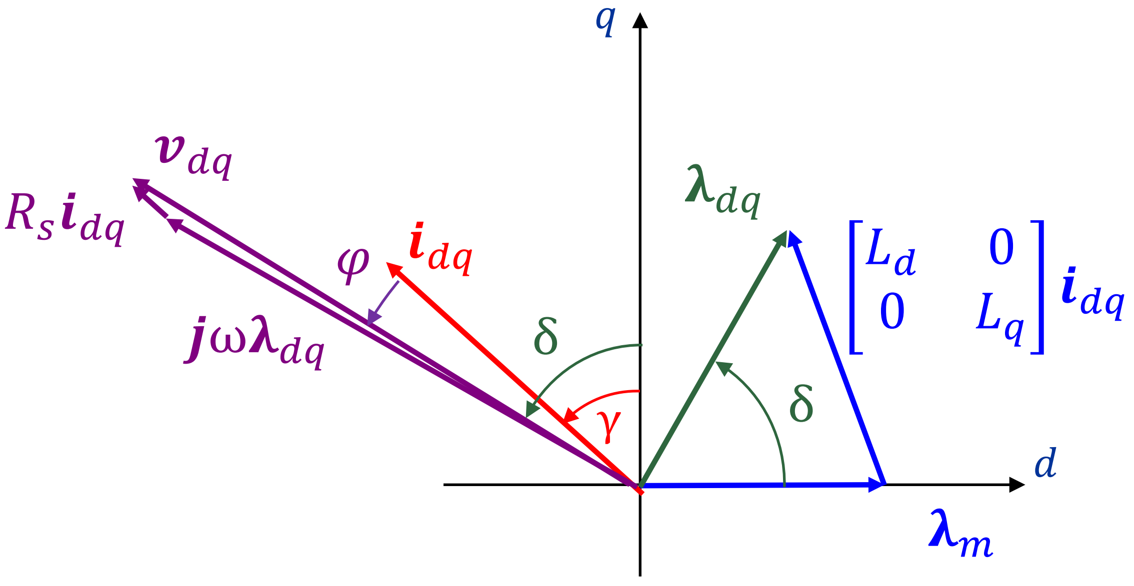

The current angle is defined after the q and d current components

$$\gamma = \text{atan}\left(\frac{-N_s i_d}{N_s i_q}\right)$$

The flux linkage components and angle follows from the lumped-parameter model

$$\delta = \text{atan}\left(\frac{\lambda_q/N_s}{\lambda_d/N_s}\right)$$

Neglecting the resistance voltage, the PF is calculated, independently of speed

$$\cos\varphi \cong \cos(\gamma - \delta)$$

This is NOT YET the MPTA condition, to be found at FEAfix stage

FEAfix correction of the contours

Selected FEA simulations (**16 dots**):
- To estimate MTPA angle correctly
- To correct the T and PF estimates

For each green dot:
- MTPA is searched iteratively with FEA
- Correction factors are computed

The correction factors are retrieved, to correct:
- *q* flux linkage
- *d* flux linkage divided into PM and armature components

[5] S. Ferrari and G. Pellegrino, "FEAfix: FEA Refinement of Design Equations for Synchronous Reluctance Machines," in *IEEE Transactions on Industry Applications*, vol. 56, no. 1, pp. 256-266, Jan.-Feb. 2020.

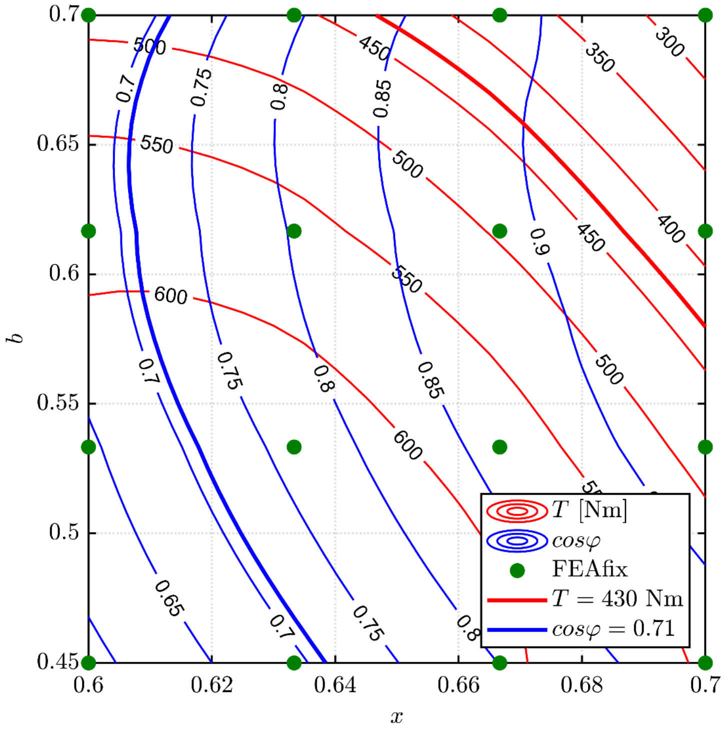

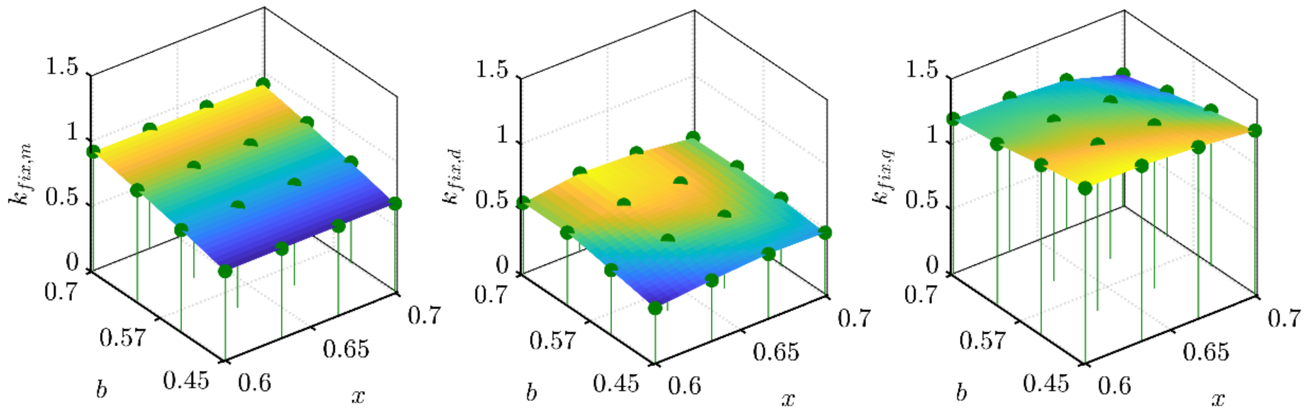

Mechanical integrity

The inner posts of each design of the plane is estimated with a simplified analytical model

Tangential ribs are constant for all the designs

Radial ribs are calculated to sustain rotating mass with no help from the tangential ribs

This is conservative, provided that the tangential ribs are reasonably set

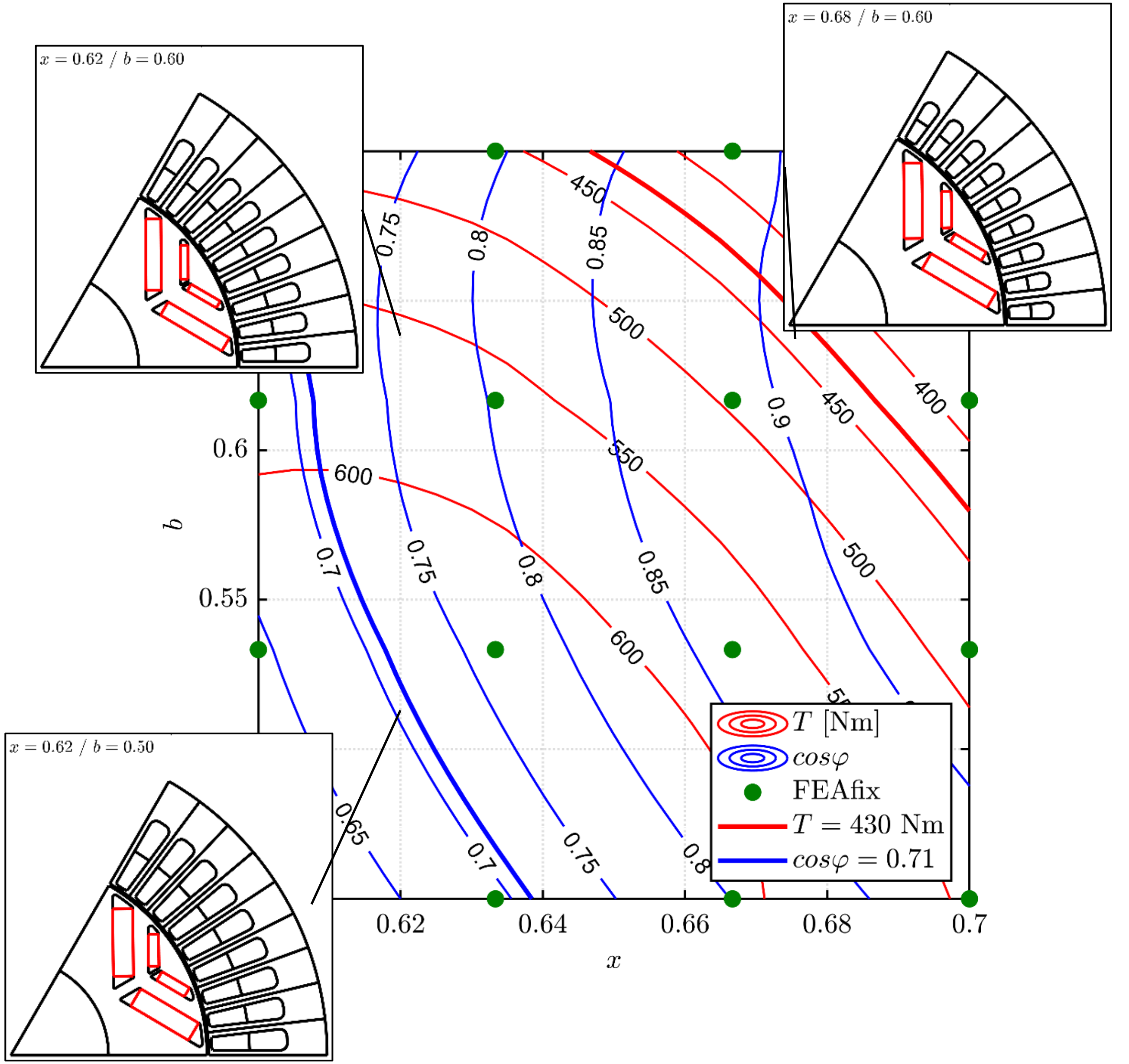

[15] M. Palmieri, M. Perta, F. Cupertino and G. Pellegrino, "High-speed scalability of synchronous reluctance machines considering different lamination materials," *IECON 2014 - 40th Annual Conference of the IEEE Industrial Electronics Society*, Dallas, TX, 2014.
[16] G. Dilevrano, P. Ragazzo, S. Ferrari, G. Pellegrino and T. Burress, “Magnetic, Thermal and Structural Scaling of Synchronous Machines,“, to be presented at *2022 IEEE Energy Conversion Congress and Exposition (ECCE)*, Detroit, MI, 2022

Design Flowchart

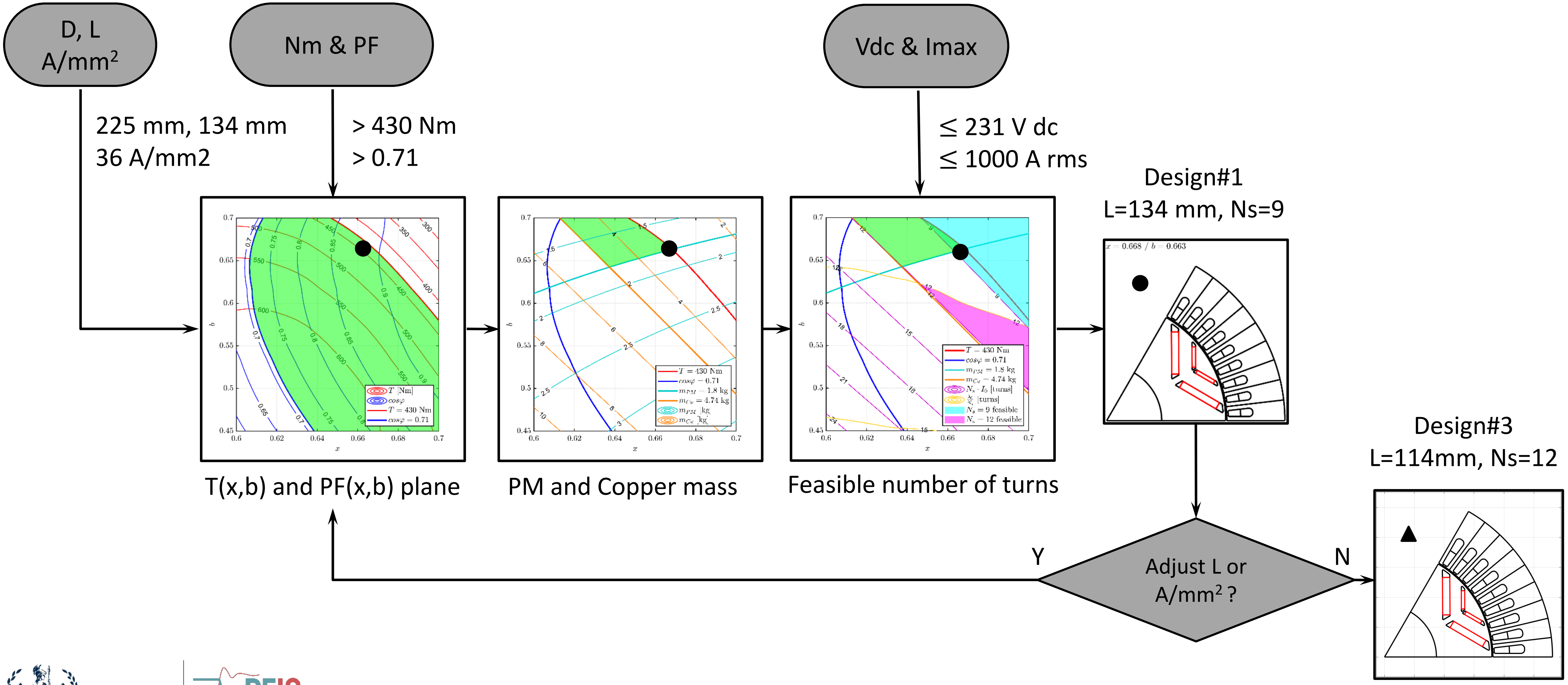

Feasible designs

The area of feasible designs is evidenced

$$T > 430\ Nm$$

$$\cos\varphi > 0{,}71$$

Opposite trends:

- Torque decreases towards the up-right corner
- PF decreases towards the down-left corner

How to pick up the optimal design?

Torque and PF curves

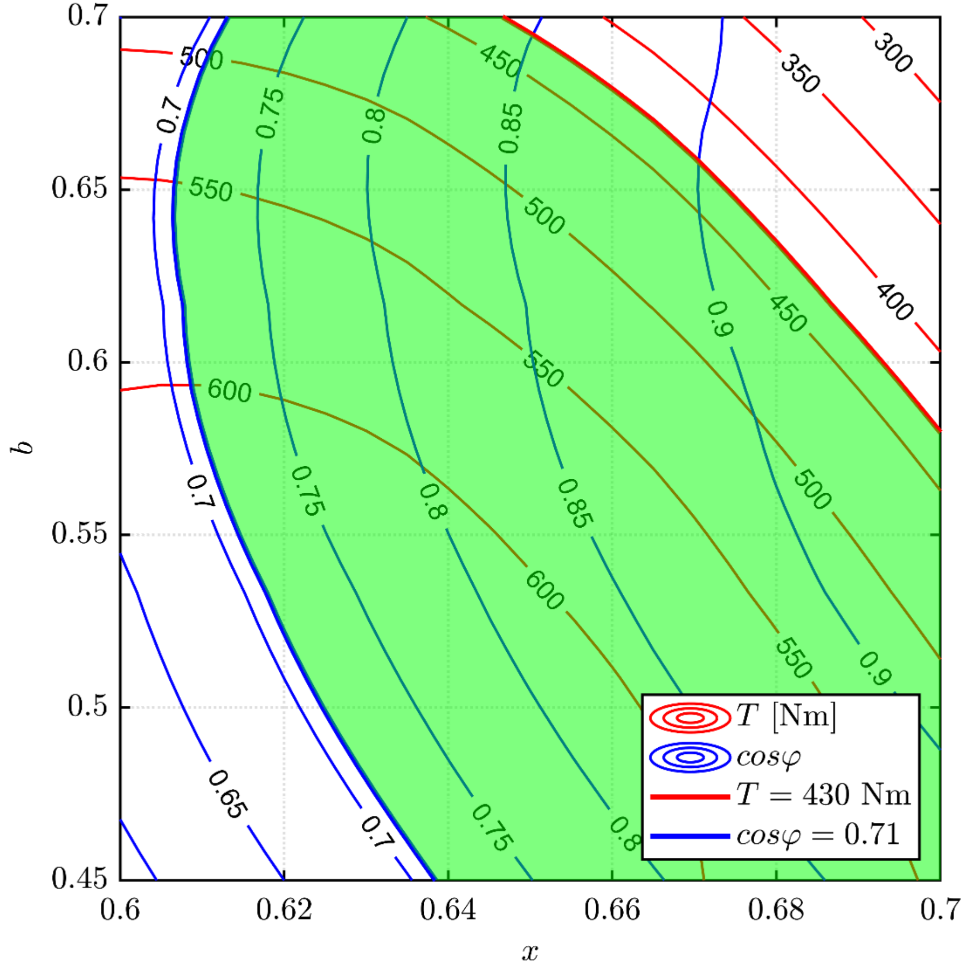

Guidelines

The closer to the up-right corner, the better

- Smaller slots → better heat rejection, less copper cross-section and thus electric loading, lower copper mass
- Higher power factor → flatter power curve

Other quantities will be considered to drive the selection of the optimal design

- PM mass
- Copper mass
- Feasible number of turns

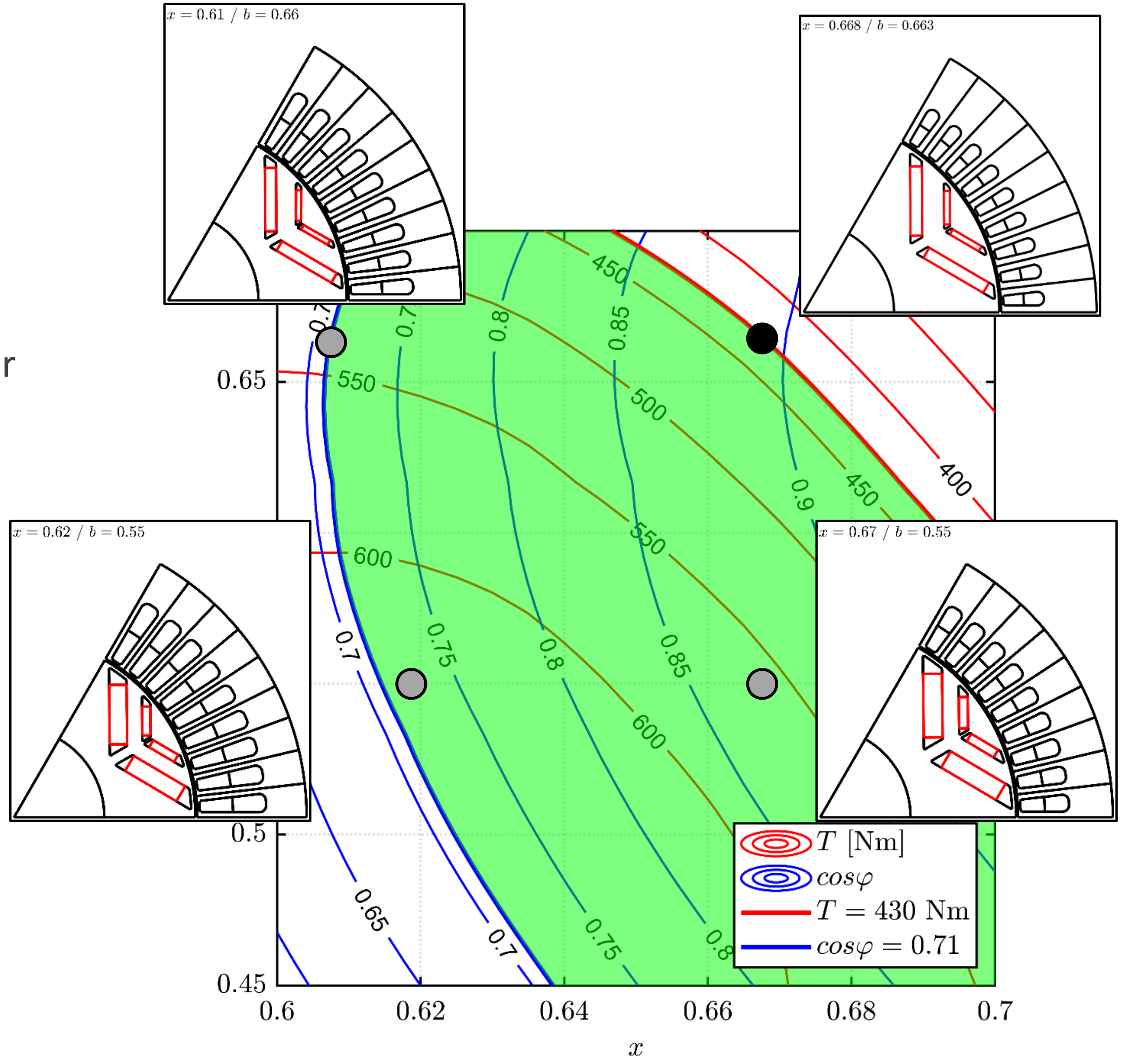

PM mass

The PM mass of the demo model is used as boundary

$$m_{PM} < 1{,}8\ kg$$

The PM mass contours are evidenced, and the are of feasible designs is correspondingly limited

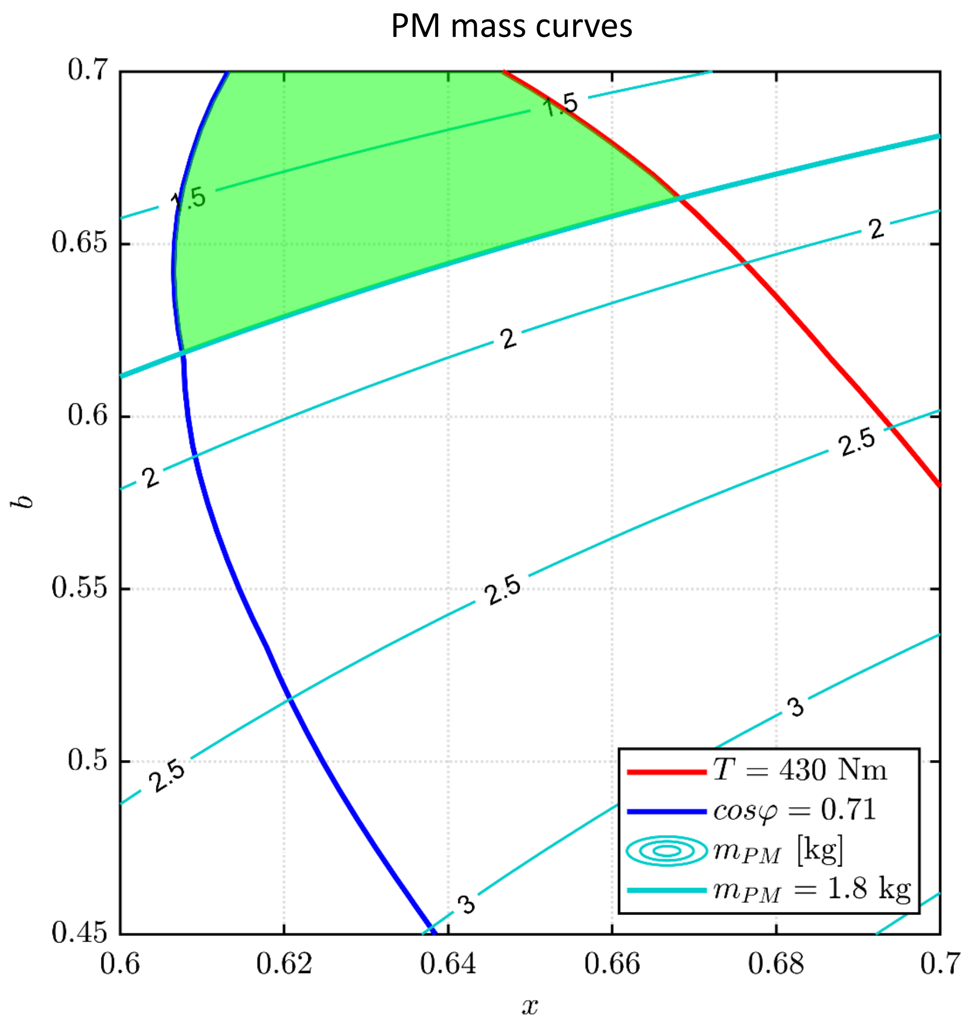

Copper mass

Similarly, the copper mass is evaluated on the plane, and the value of the demo model is used as a reference

$$m_{Cu} < 4{,}74\ kg$$

This further restricts the area of feasible designs

Copper mass curves

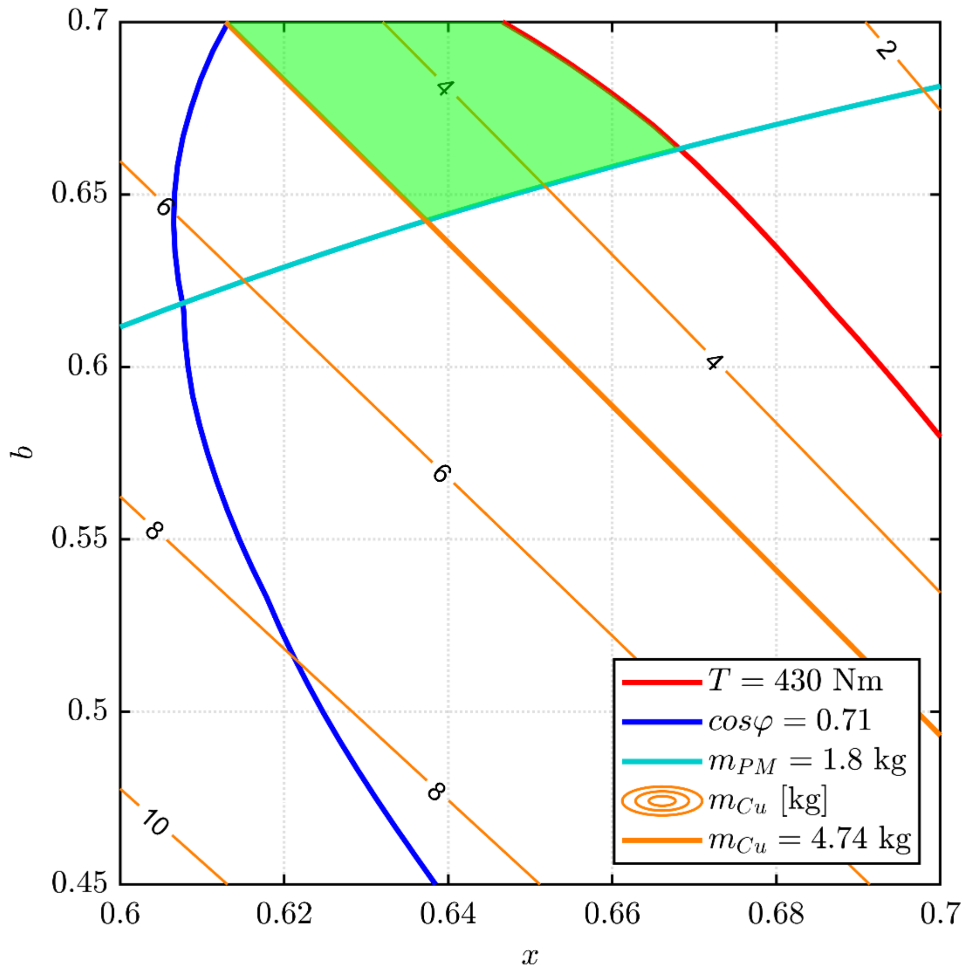

Number of turns according to the current limit

Designs respect the current limit when

$$N_s I_0 \leq N_s I_{max}$$

The inverter current limit $I_{max} = 1414$ Apk is associated to feasible numbers of turns $N_s = 9, 12, 15, 18 \ldots$

The example shows the area of respect of the current limit with $N_s = 9$

The valid area is above the limit line

The larger N_s, the larger the area

Number of turns according to current

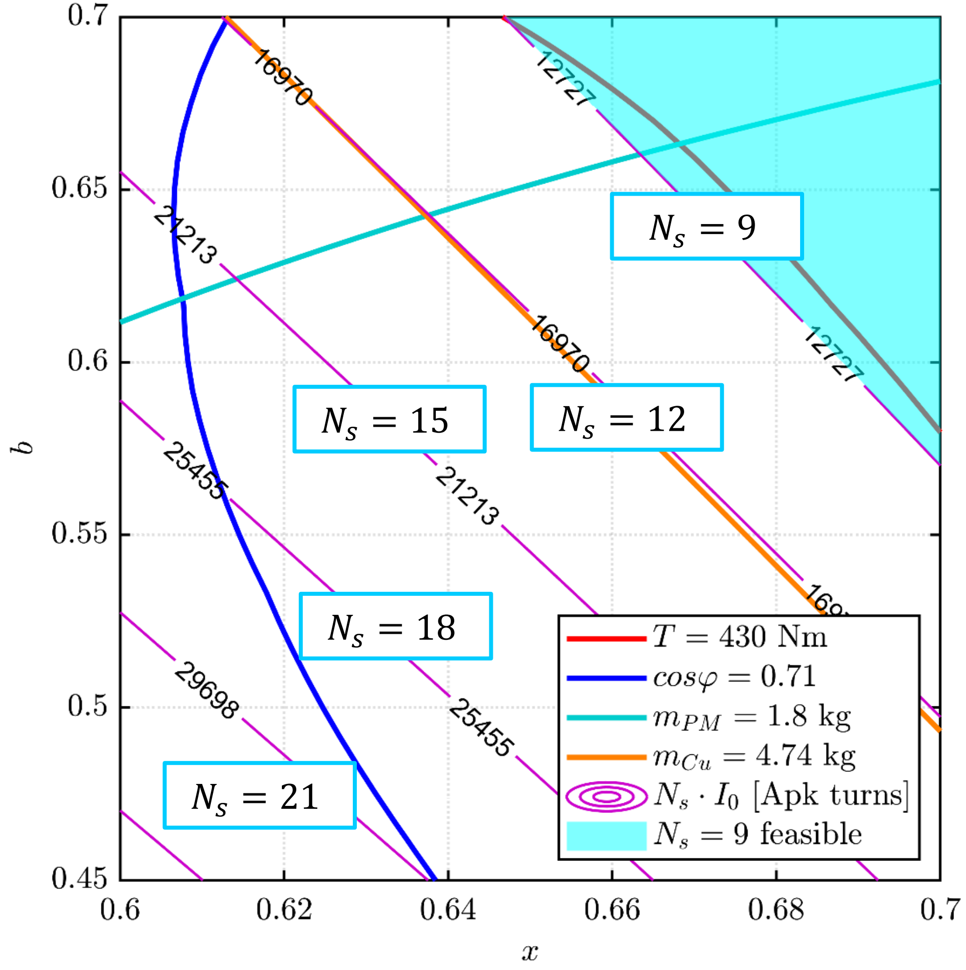

Number of turns according to the voltage limit

$N_s = 9$

Simplified voltage equation at base speed

$$p\frac{\pi}{30} \cdot n_{base} \cdot \lambda_0 \leq \frac{V_{dc}}{\sqrt{3}}$$

It defines the base flux linkage limit

$$\lambda_0 \leq \frac{V_{dc}}{\sqrt{3} \cdot p\frac{\pi}{30} \cdot n_{base}} = 996\ \mathrm{mVs}$$

The λ_0/N_s contours are reported for feasible values of N_s, the area of respect of the voltage limit for $N_s = 12$ is highlighted

The valid area is the below the line

The smaller N_s, the larger the area

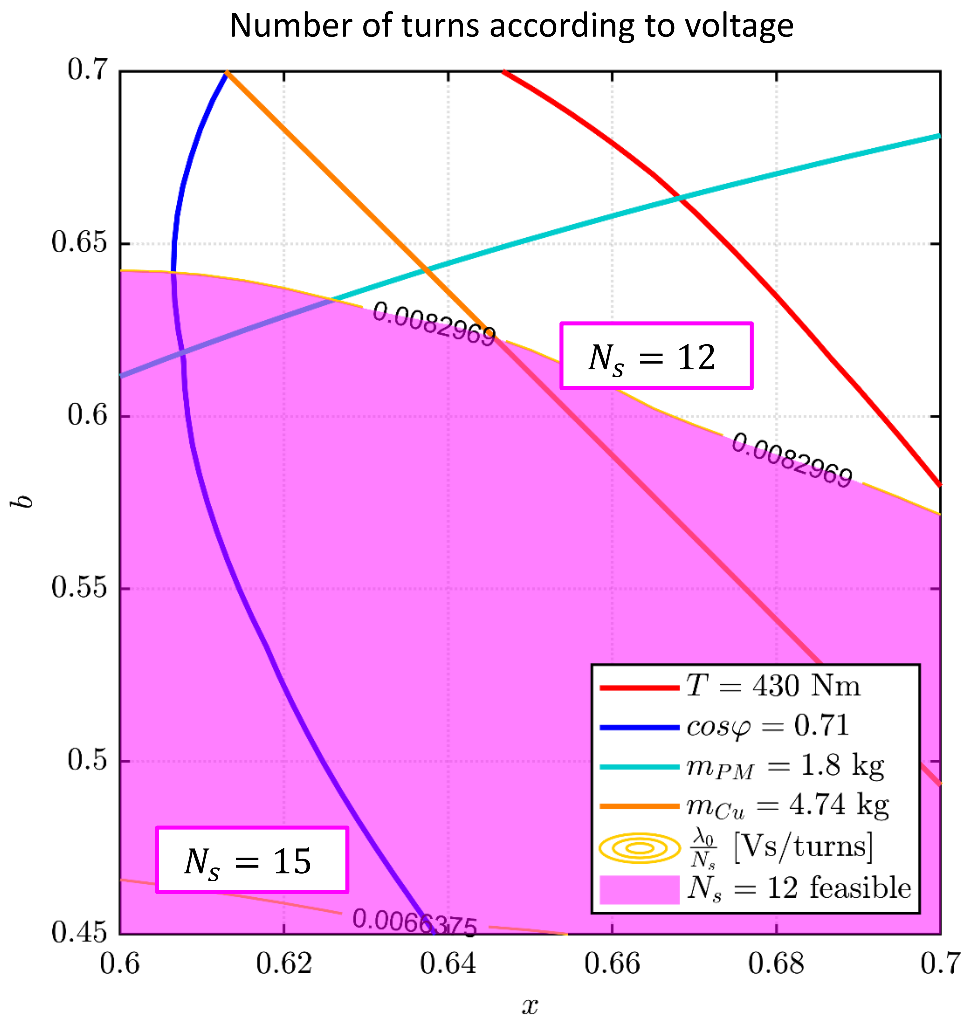

Feasible numbers of turns

The current and voltage constraints are crossed for the feasible numbers of turns

Feasible solutions are $N_s = 9$ and $N_s = 12$

- The area of respect of $N_s = 9$ is in light blue
- The area of respect of $N_s = 12$ is in magenta

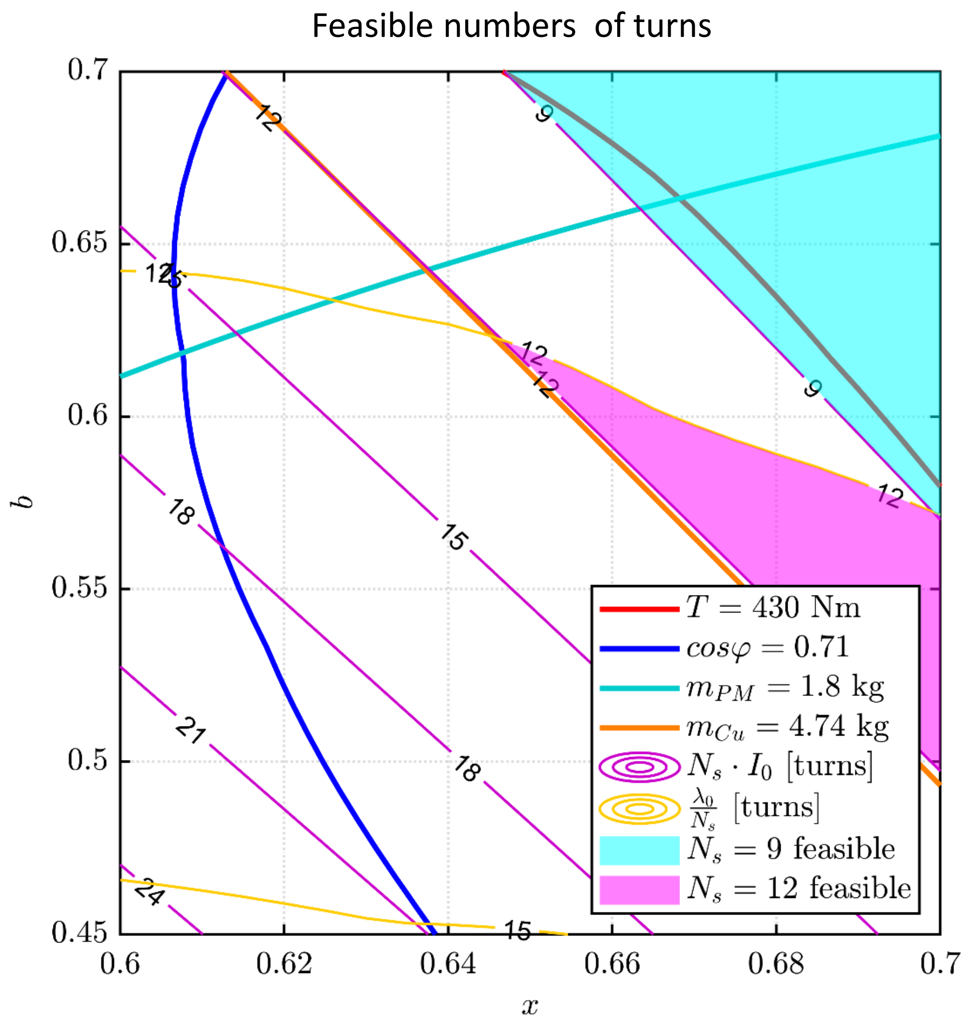

Number of turns selection

Intersecting the feasibility area of each number of turns with the sweet spot previously defined:

- $N_s = 9$ can **fulfill all constraints**
- $N_s = 12$ is **outside the sweet spot** because it cannot beat the PM mass limit

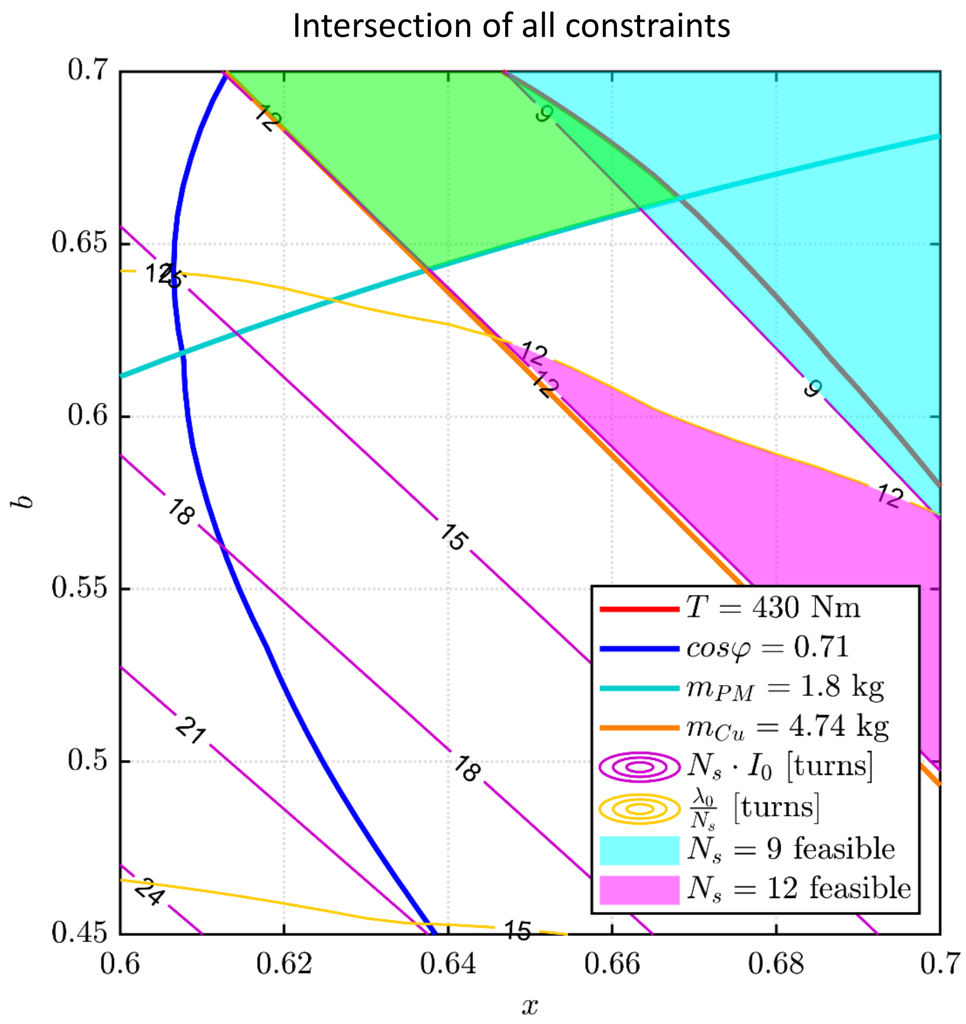

Design#1

The motor is selected at the crossing of the torque and PM mass limits

A little margin is noticed w.r.t. the current limit

Copper mass way lower than the limit

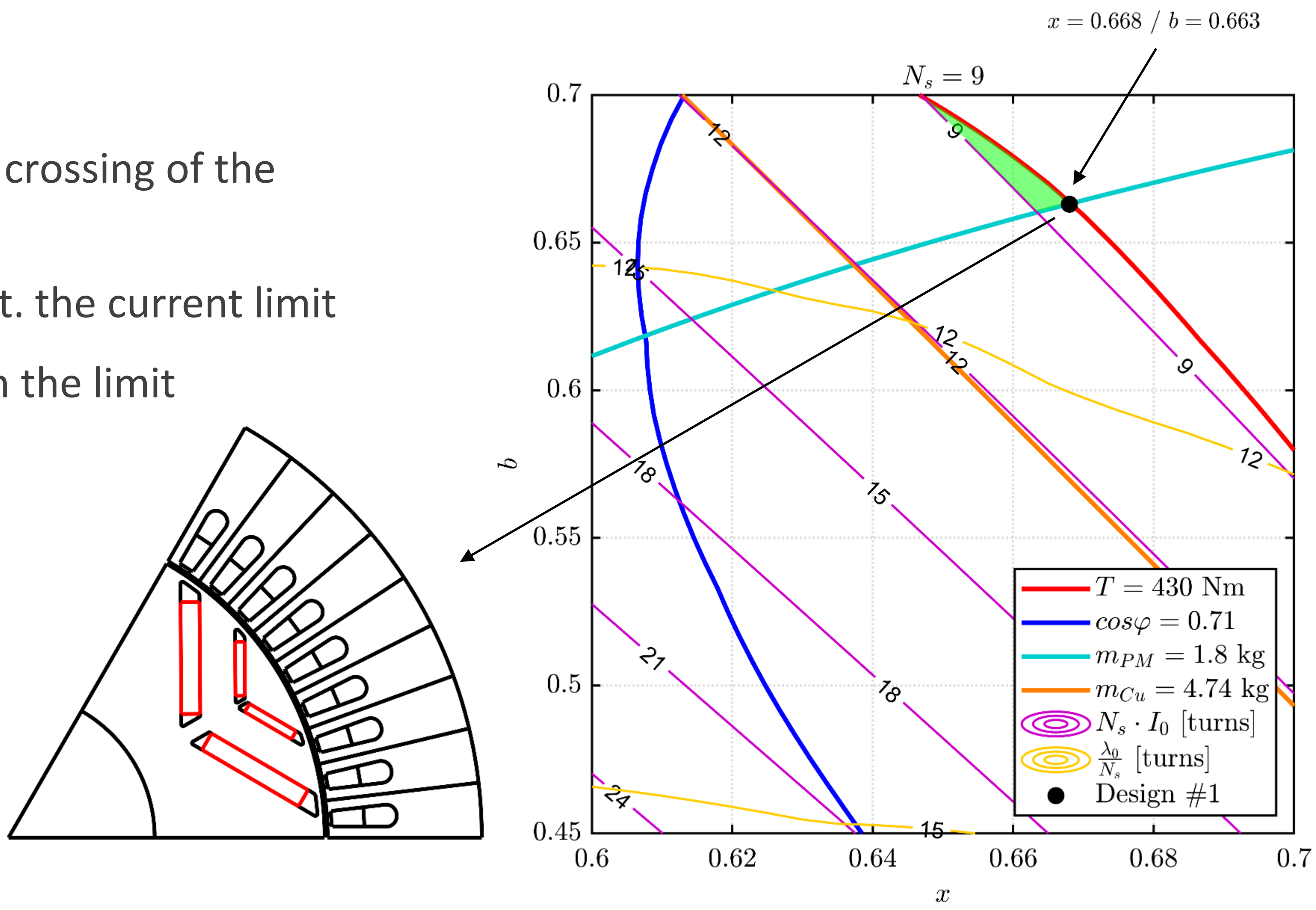

Motor Analysis – Operating Limits

The flux maps of Design#1 are FEMM evaluated and manipulated

The operating limits for this inverter tell

- Peak torque is ok
- Peak power is unnecessarily high, because
  - **$N_s = 9$ has large margin w.r.t. the voltage spec**
  - The curves refer to a lossless situation
  - The PF @ nbase criterion is pessimistic
  - The PF on the plane is circa 0.9 >> 0.71

Actions:
Reduce A/mm²?
Reduce the stack length L?

Torque and power curves of Design#1

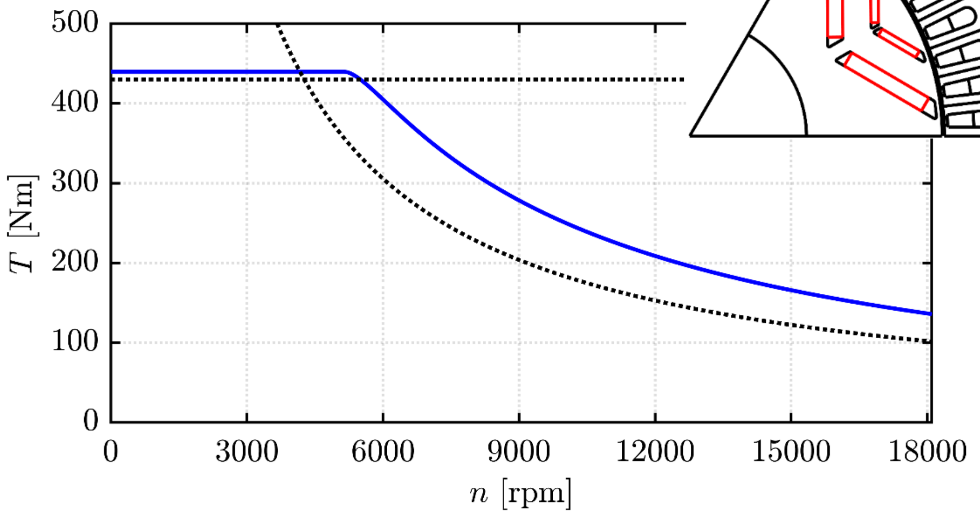

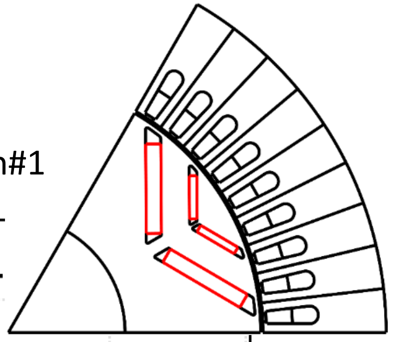

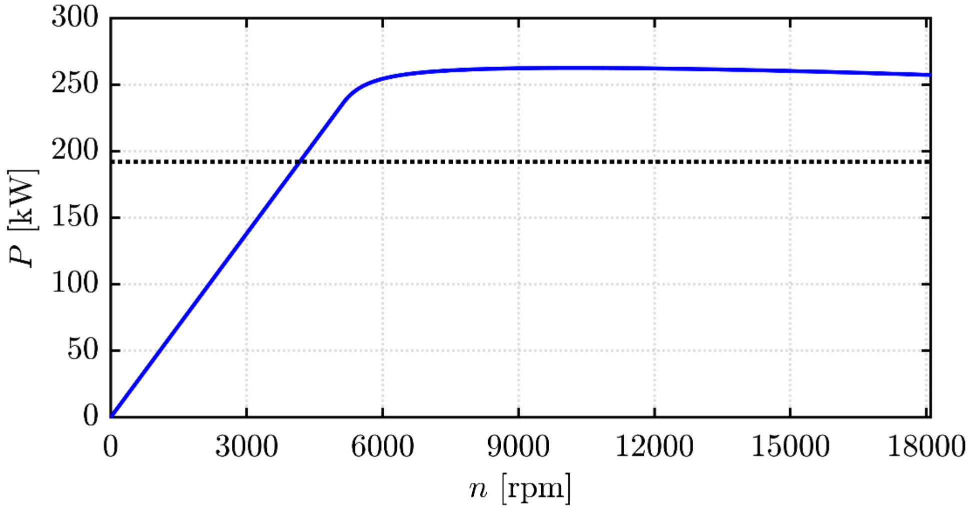

Remember the flowchart

Here we **reduce the stack length** and restart

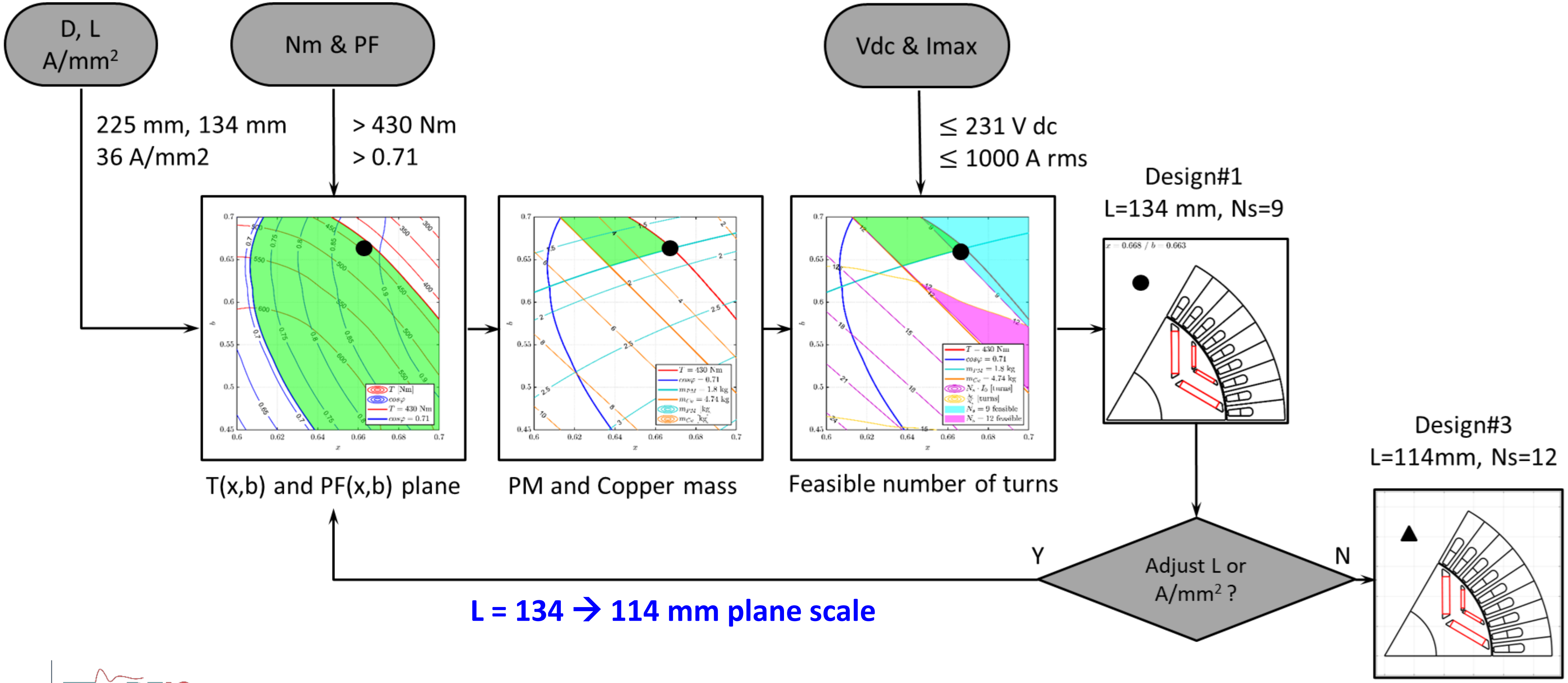

L = 134 → 114 mm plane scale

Stack length reduction

What is unchanged
- PF contour
- Ampere-turns

What has changed
- Torque contour shrinks
- PM mass and Cu mass shrink
- Voltage-driven N_s contours go up

The plane is length-adjusted, not FEA recalculated (!!)

L = 134 mm

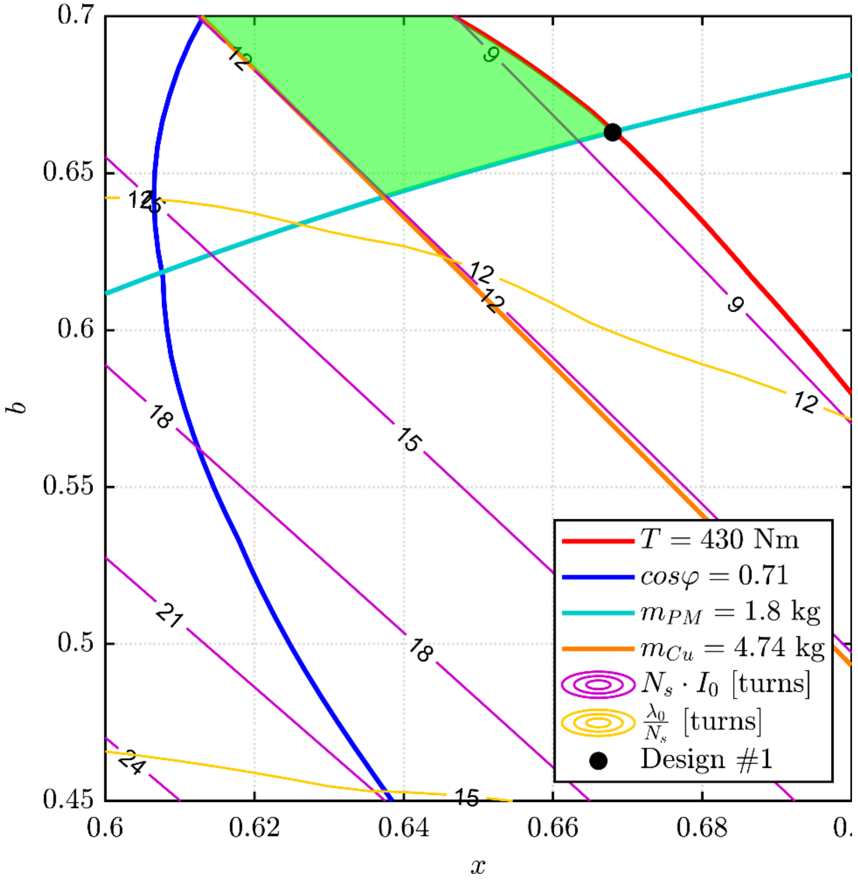

L = 114 mm

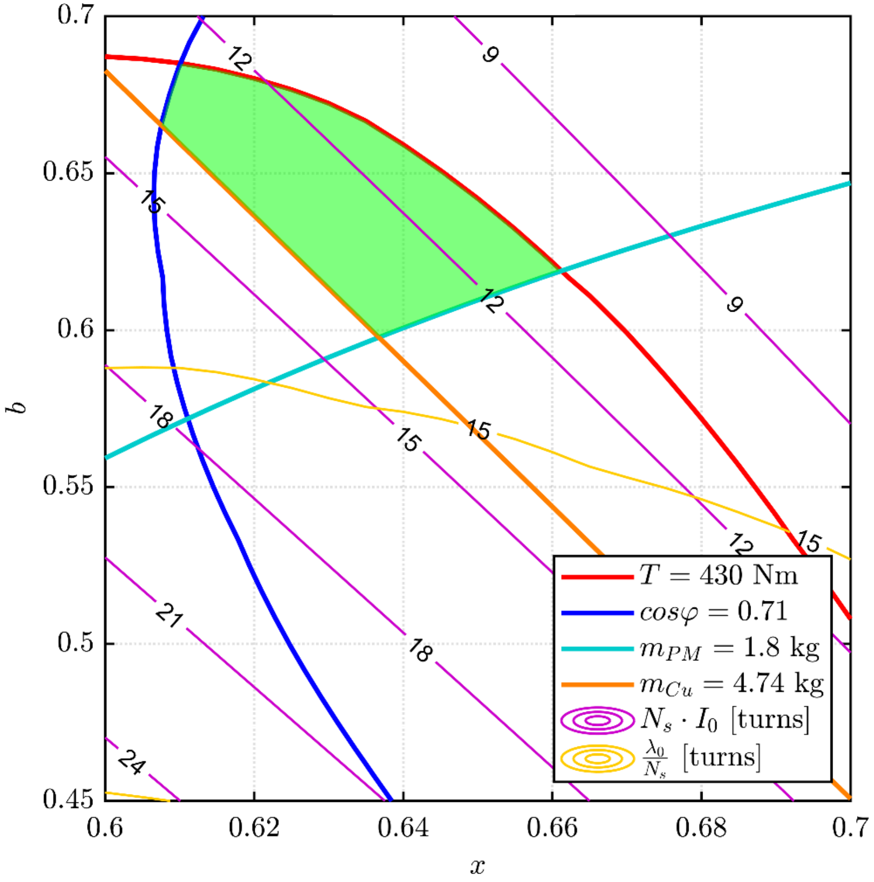

Design plane for L = 114 mm

The green area moves downwards and leftwards in the plane

Downwards means **less iron**

Leftwards means **smaller rotor, longer slots**

W.r.t. the number of turns:

- ✗ $N_s = 9$ is not feasible current wise
- ✓ $N_s = 12$ intersects the green area
- ✗ $N_s = 15$ is not feasible voltage wise

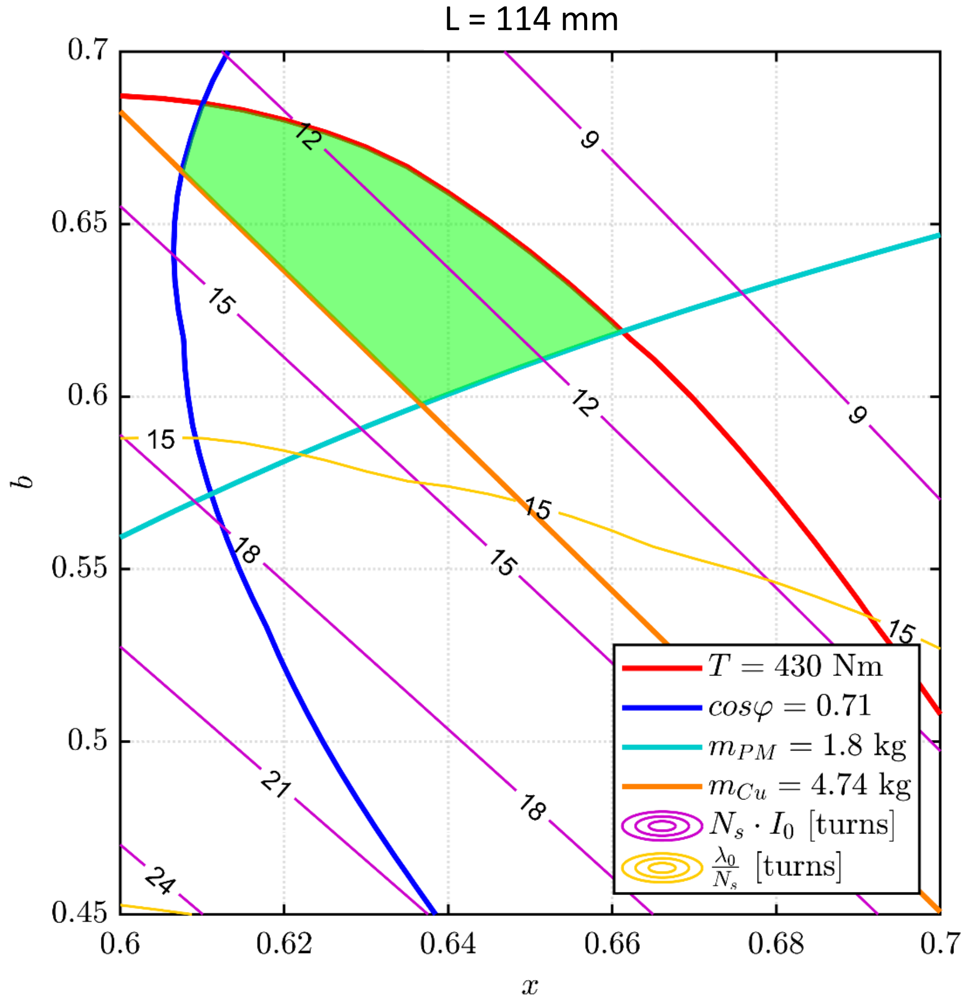

Selected 114mm motors

Two solutions are selected:

- Design#2: at the torque and PM mass limits
- Design#3: on the 12 turns current limit

$x = 0.639$ / $b = 0.640$

Design #3

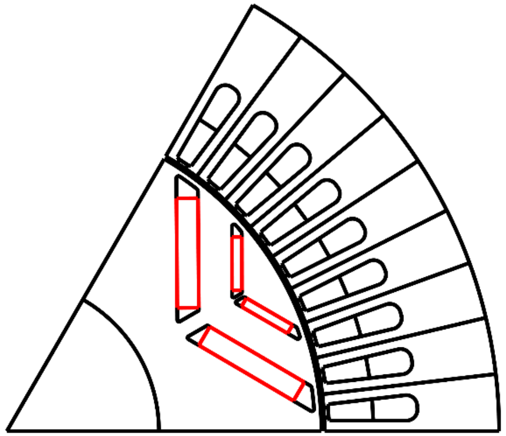

$x = 0.661$ / $b = 0.619$

Design #2

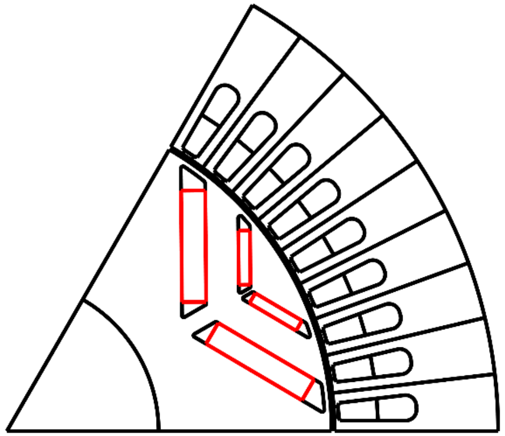

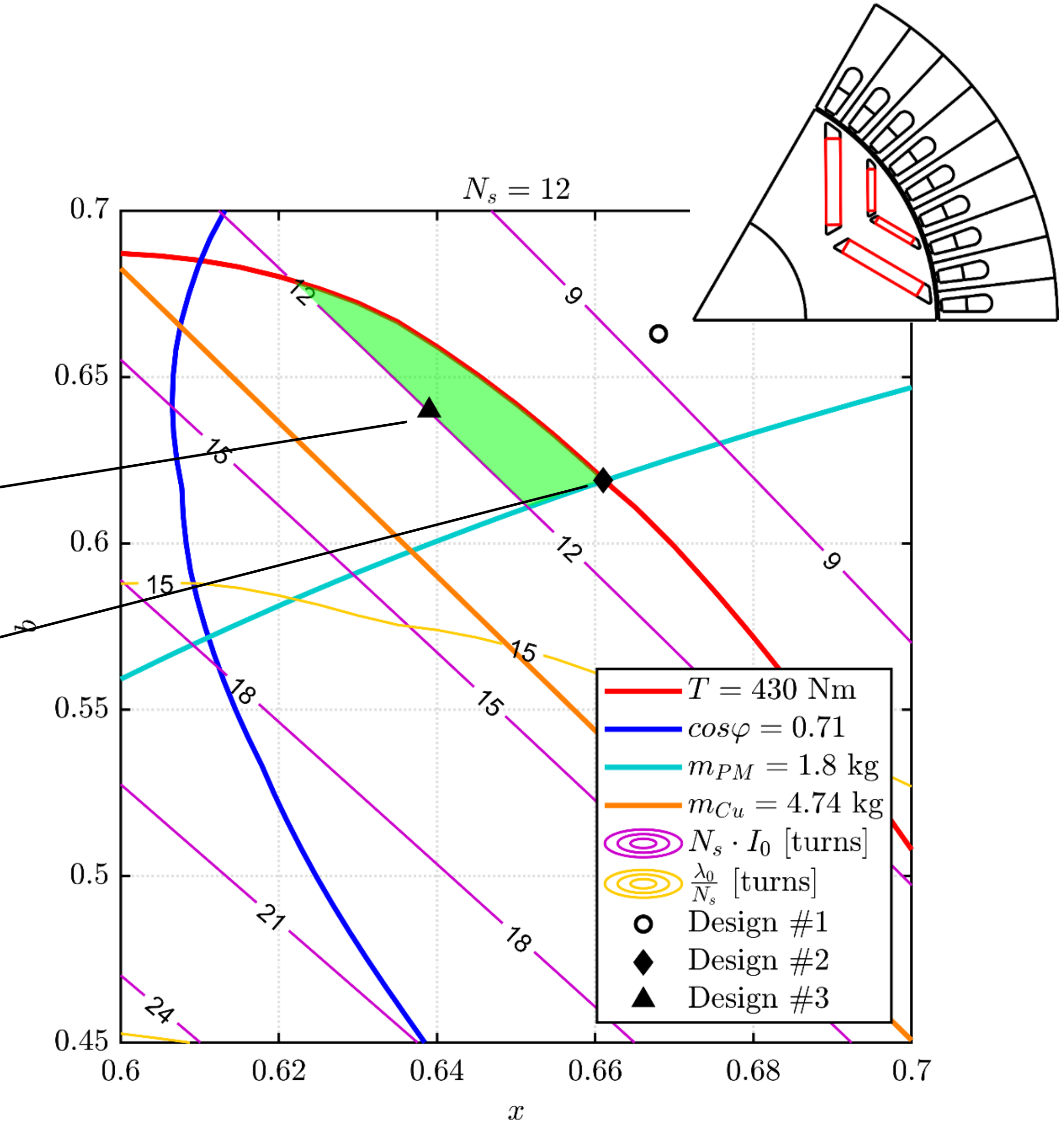

Focus on Design#3

This is considered the best candidate

The plane tells that

- 450 Nm are expected at I_{max} (> 430 Nm)
- A PF of 0,83 (> 0.71)
- PM mass 1,55 kg (< 1.8 kg)
- Cu mass 4 kg (< 4.74 kg)

Design #3

$x = 0.639$ / $b = 0.640$

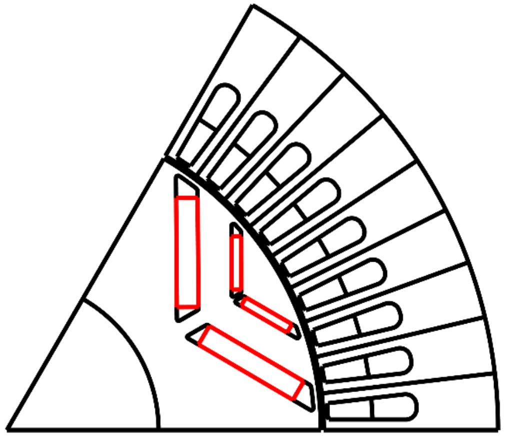

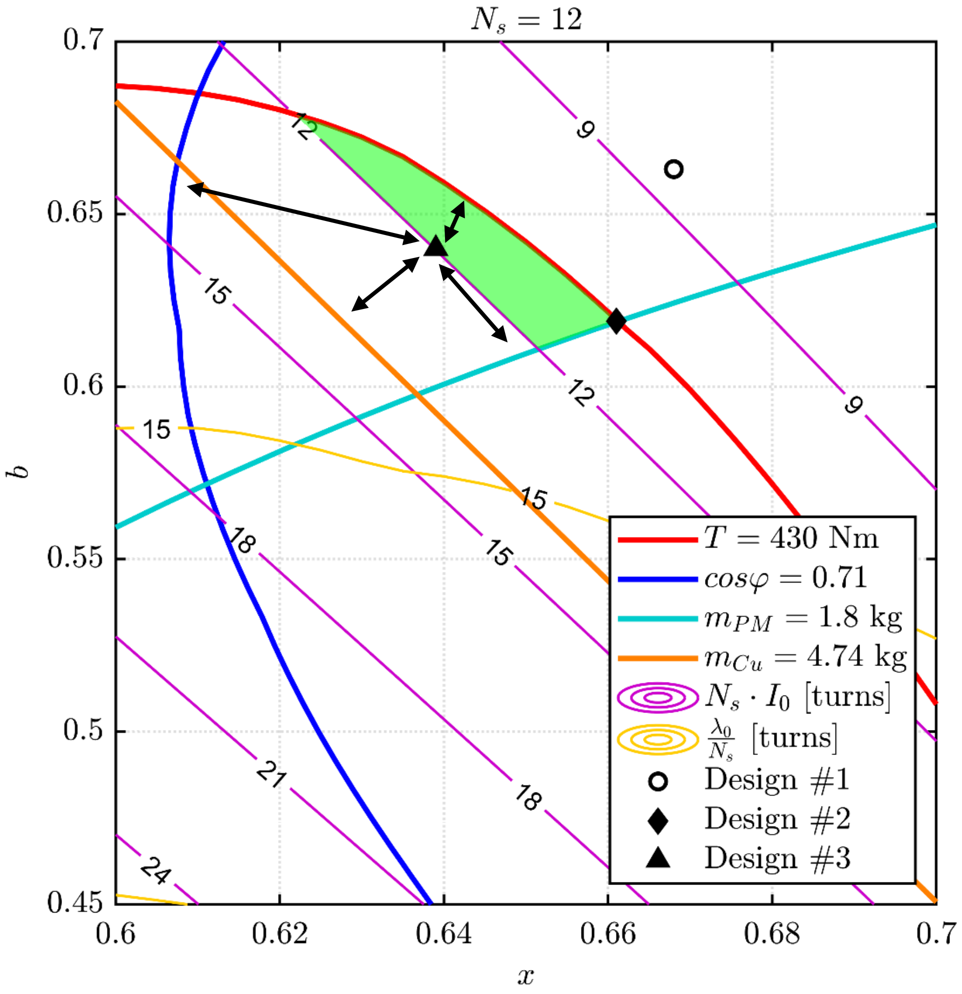

Power curves comparison

The operating limits of the three motors are compared, with the same inverter

All comply with the torque and power specs

Design#3 has **minimized stack volume AND minimized PM mass**

L = 134 mm , Ns = 9

L = 114 mm, Ns = 12

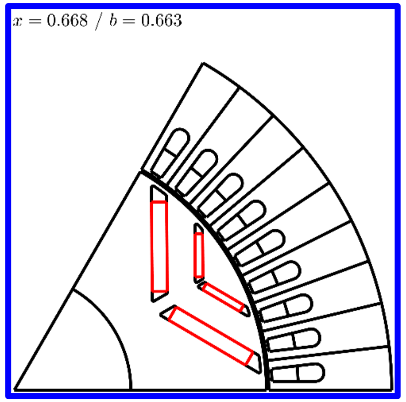

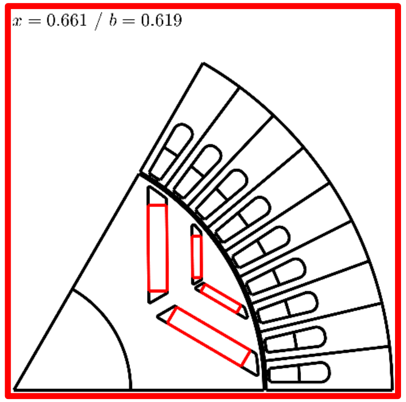

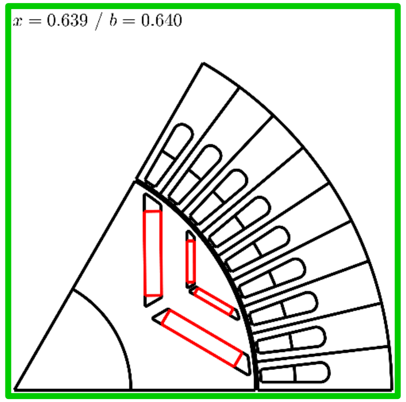

Torque curves comparison, PM at 80°C

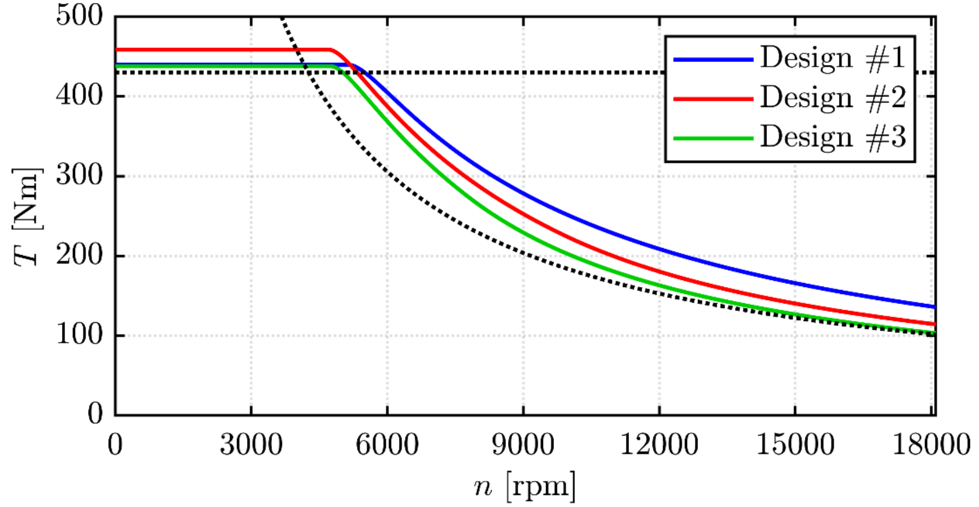

Power curves comparison

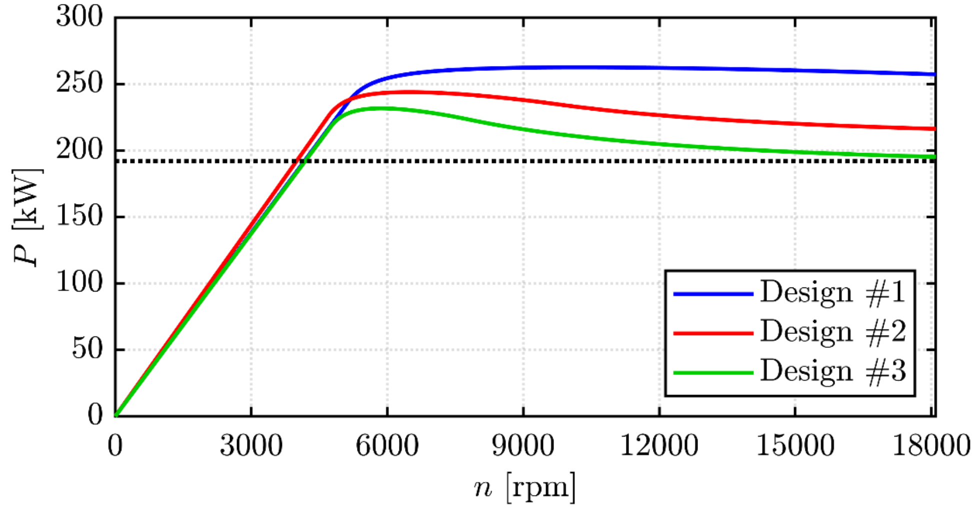

Flux Maps of Design#3

The flux map curves highlight :

- saturation of q-axis occurs
- cross-saturation more evident on d axis

Effect of PM temperature:

- d-axis flux linkage shift
  - -8% for 60°C variation (-1.3‰ /°C)
- Little effect on q-axis

Flux linkage curves at 80°C (blue and green) and 20°C (red)

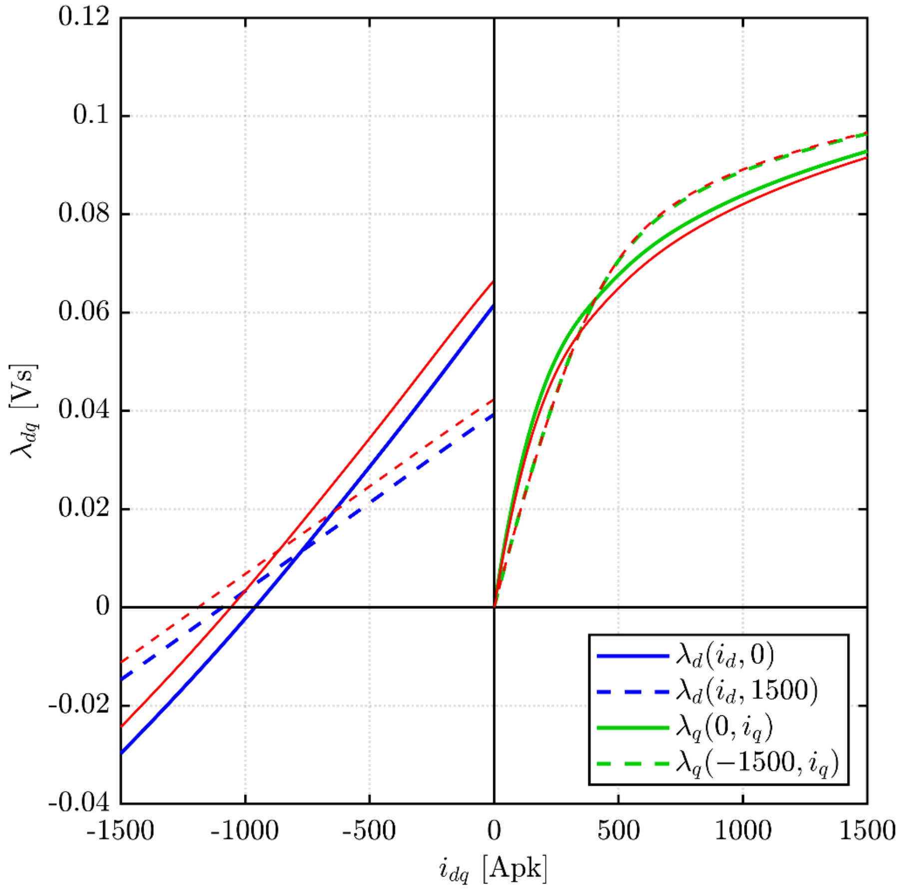

Temperature effect on torque

Torque capability under MTPA is mildly affected by temperature:

- -3% for 60°C variation (-0.5‰ /°C)

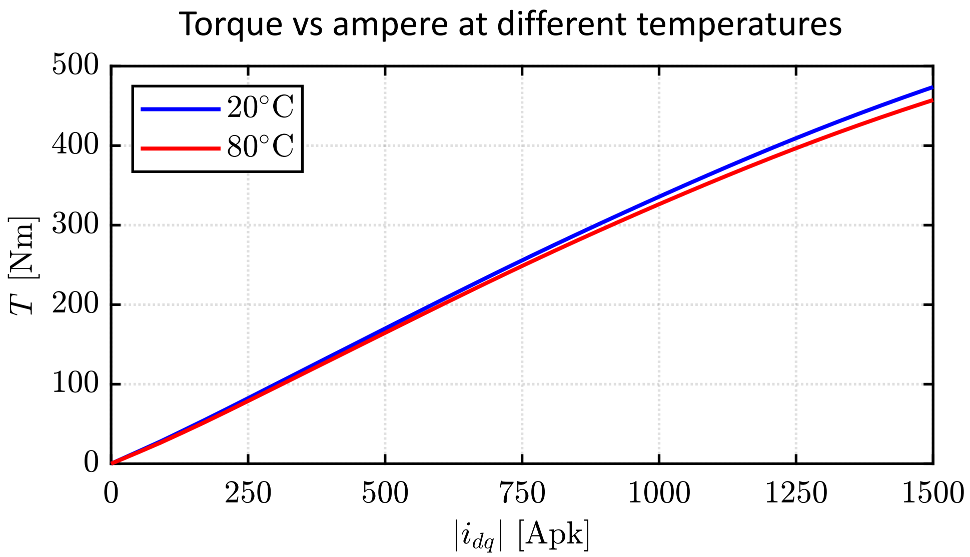

The effect on power curve at high speed is more evident

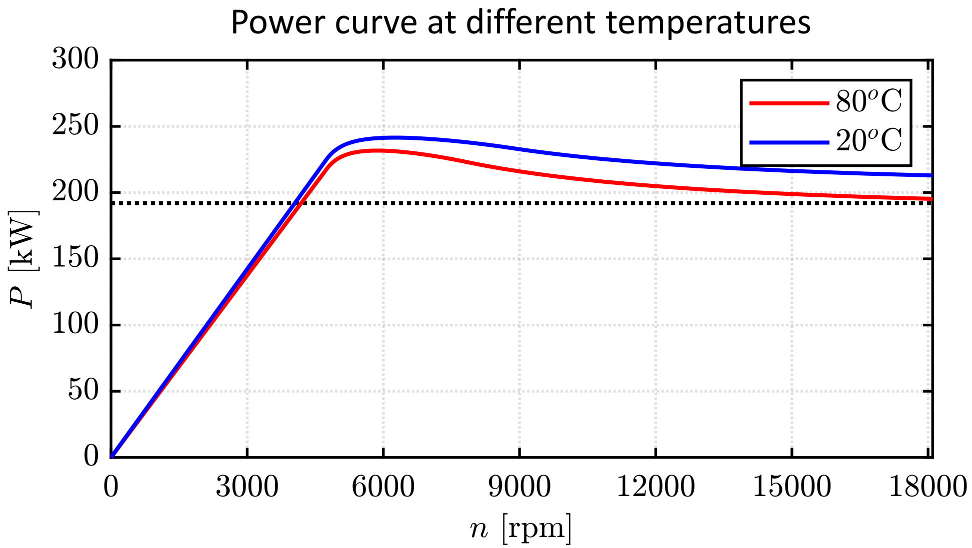

Comparison with the benchmark

Torque capability of Design#3 compared to the custom Model3:

- Comparable torque vs current curves
- Design #3 has higher peak torque and a better power curve
- Stack volume 4,5 liters vs 5,3 liters (-15%)

Tesla 3, L = 134 mm

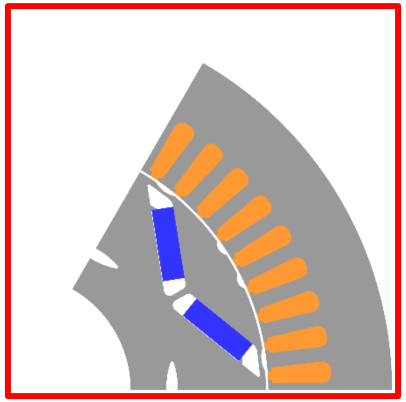

Design #3, L = 114 mm

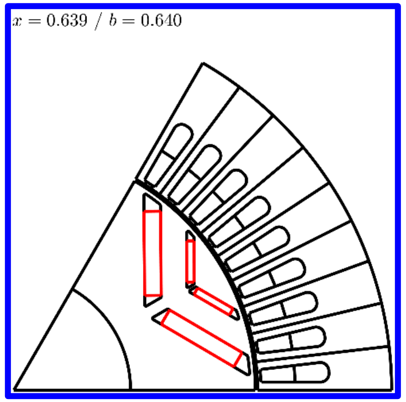

Torque vs ampere at 80°C

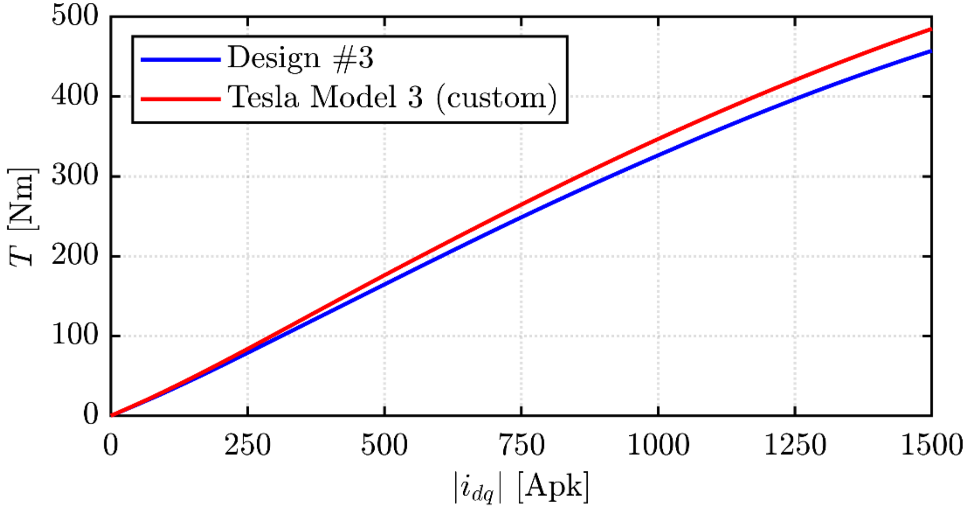

Torque vs speed at 80°C

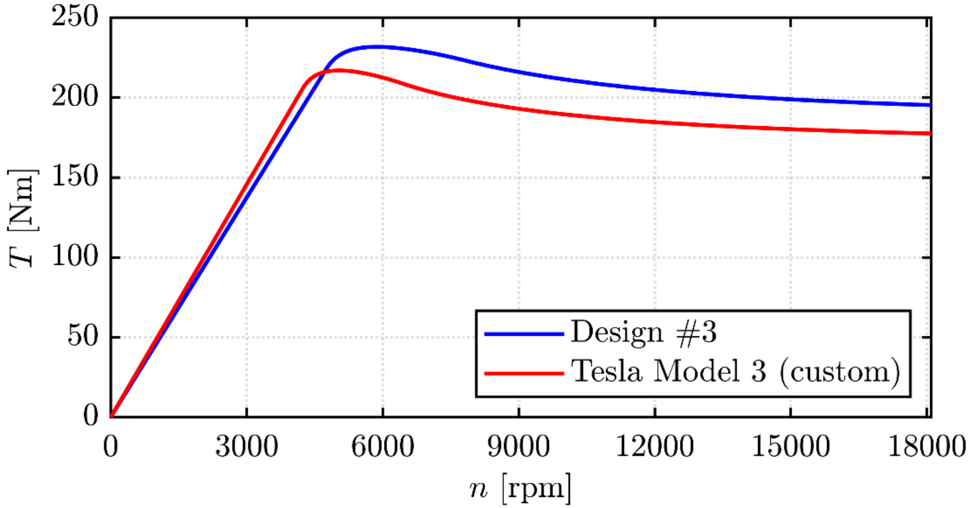

Torque ripple comparison

Design #3 is not optimized for torque ripple

Yet, the peak-peak torque envelope is under control (65 Nm pk-pk at 450 Nm) and can be further optimized

Comparison of torque waveforms shows the effect of dedicated torque ripple optimization (notches at optimal positions)

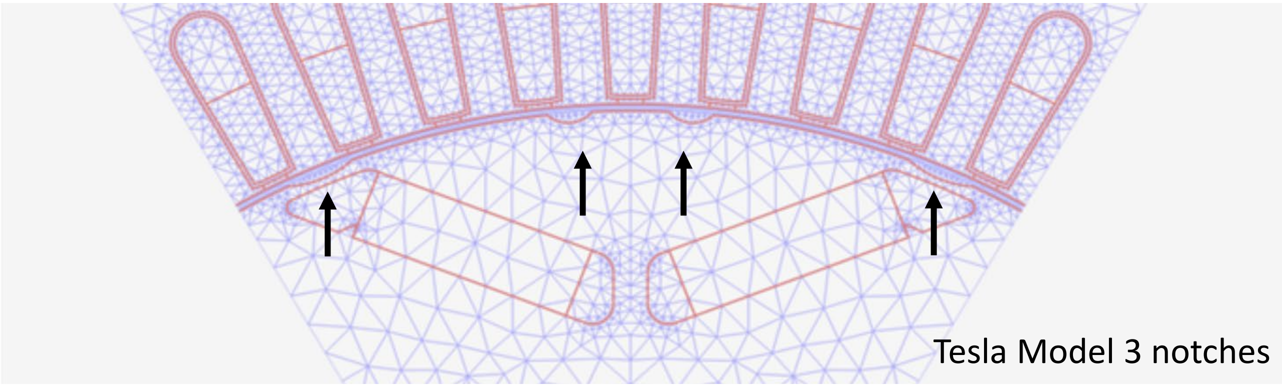

Design #3 - Torque vs ampere at 80°C, pk-pk ripple in red

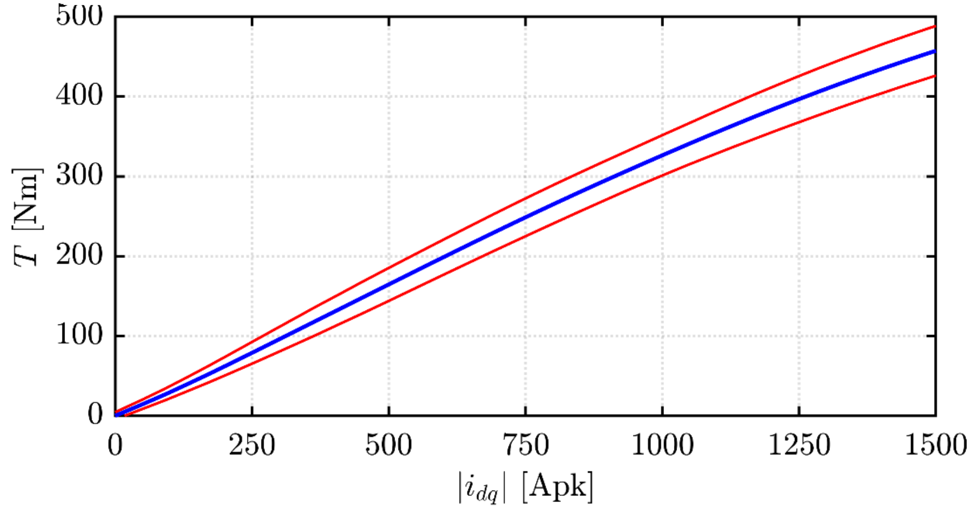

Torque waveforms comparison

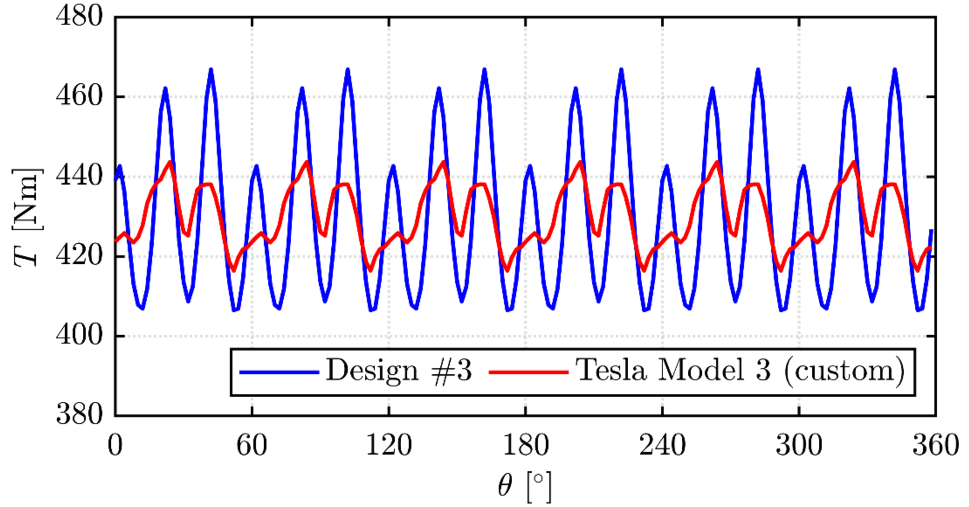

Demagnetization Limit

Demagnetization current function of PM temperature is retrieved with SyR-e automation

- Max 1% PM volume is tolerated

The demagnetization limit of Design #3 is slightly lower compared to the benchmark below 140°C of PM temperature

This relates to the smaller PM dimensions

Yet, the crossing with the maximum inverter current occurs at 140°C in both cases

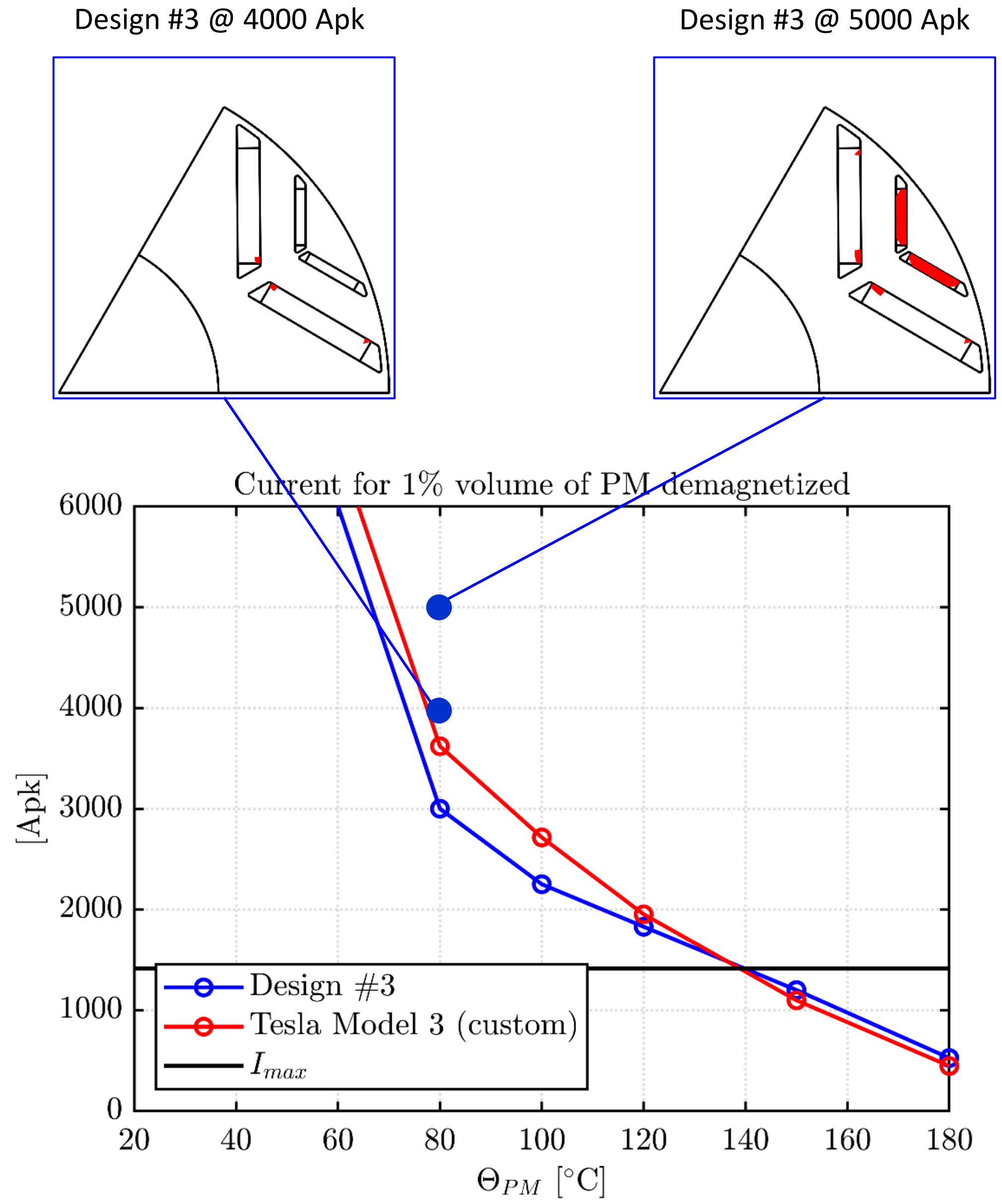

Efficiency map

Efficiency map is computed at reference temperature values PM 80°C and Cu 100°C

- DC, AC and iron loss considered
- maximum efficiency control implemented
- Sinusoidal currents (no PWM)

High-efficiency area between 3000 and 7000rpm, partial load

The maps are very similar, despite the smaller stack volume of Design#3

Design#3

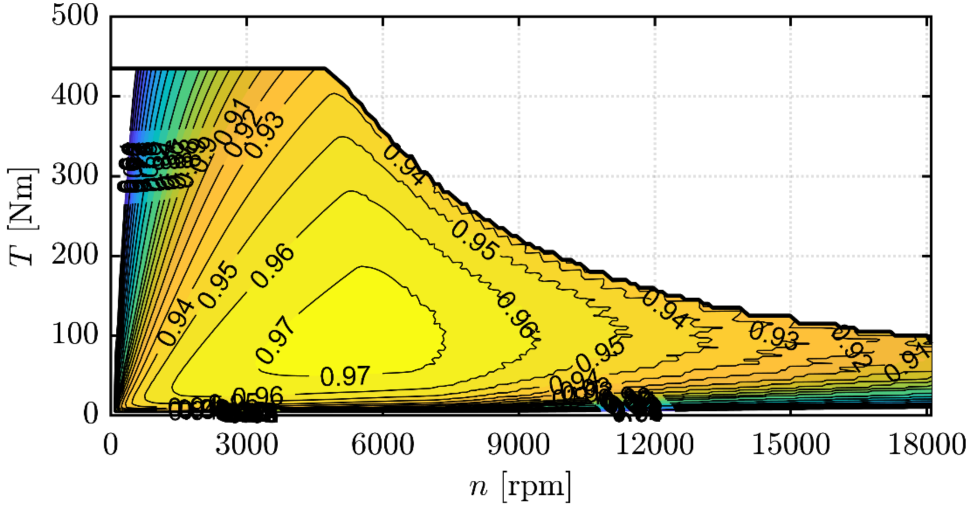

Model3 custom

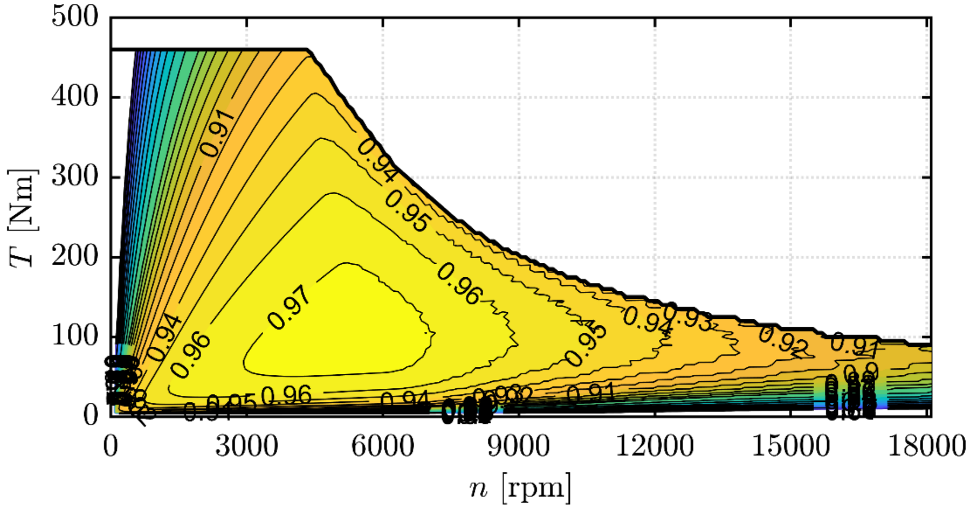

Thermal limit

Steady-state thermal limit curve computed with the same cooling system of the benchmark (10 liters/min, 45°C inlet, full potting)

- Higher loss density leads to a lower thermal limit
- Hotspot found in the inner end-winding

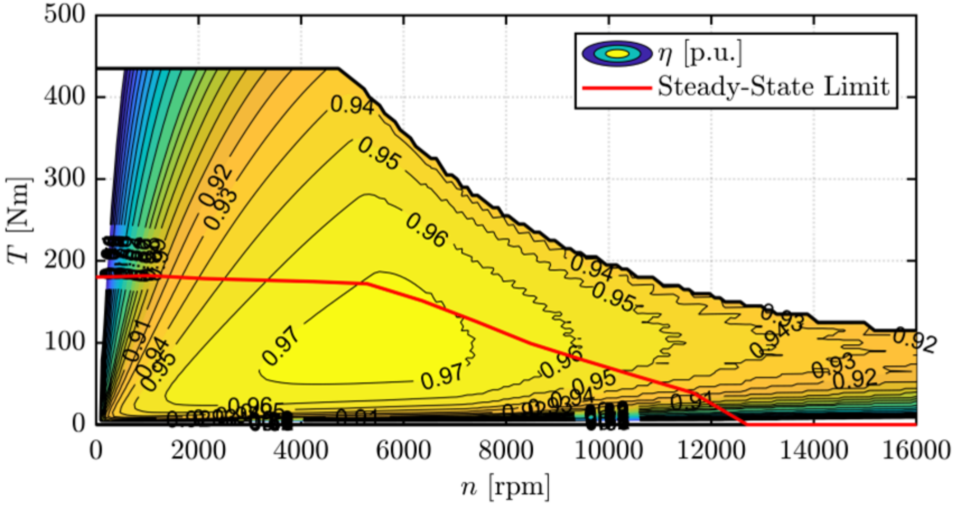

Hotspot temperature according to MotorCAD

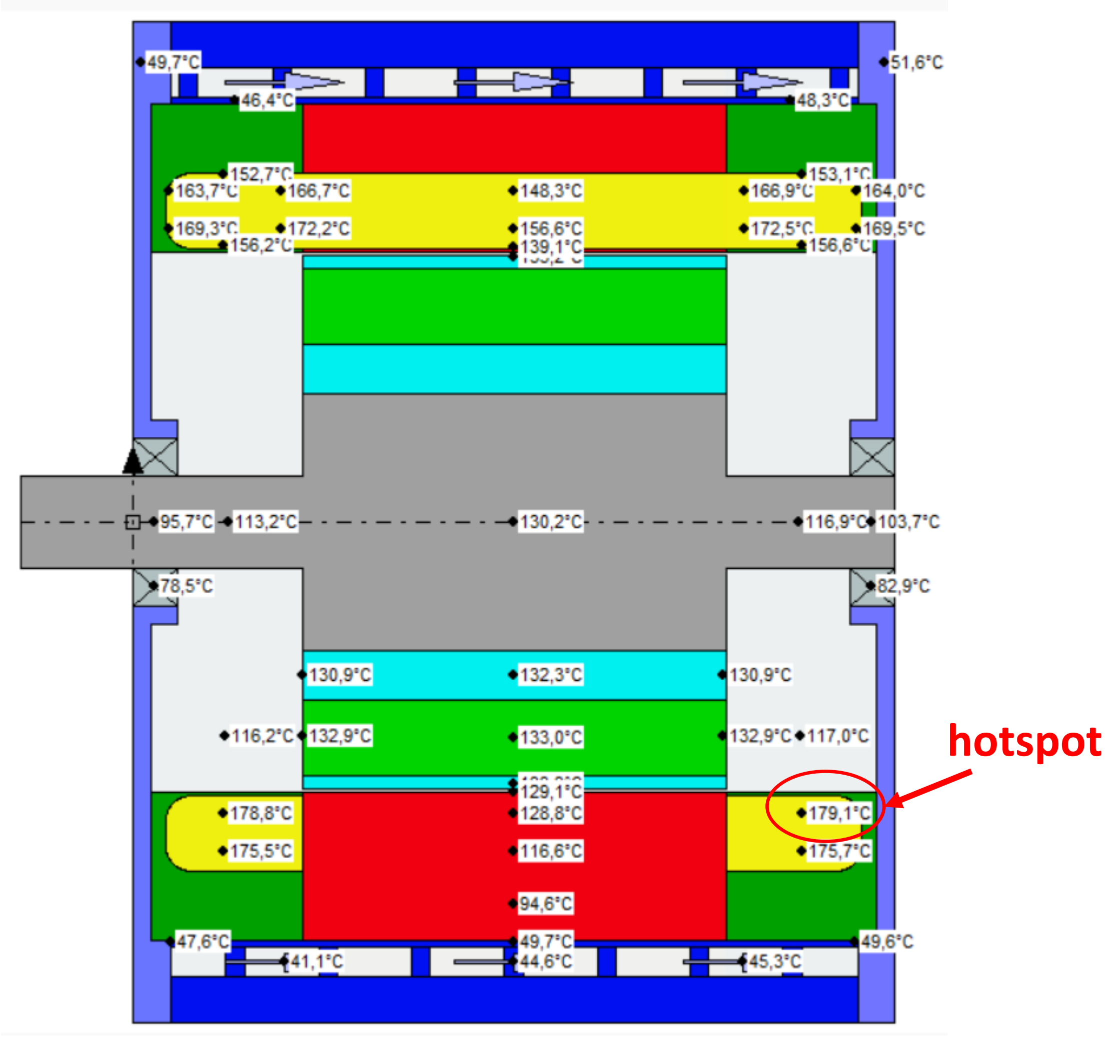

Thermal limit

Steady-state thermal limit curve computed with the same cooling system of the benchmark (10 liters/min, 45°C inlet, full potting)

- Higher loss density leads to a lower thermal limit
- Hotspot found in the inner end-winding

Hotspot temperature according to MotorCAD

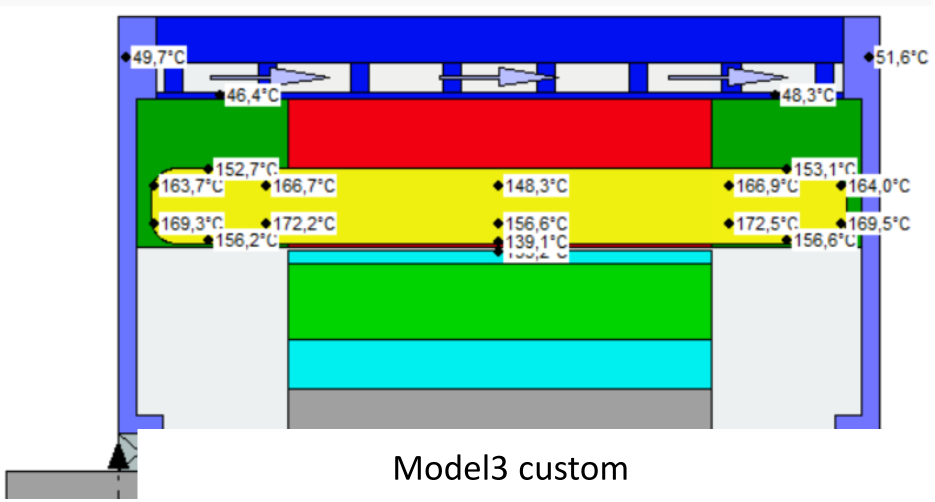

Design#3

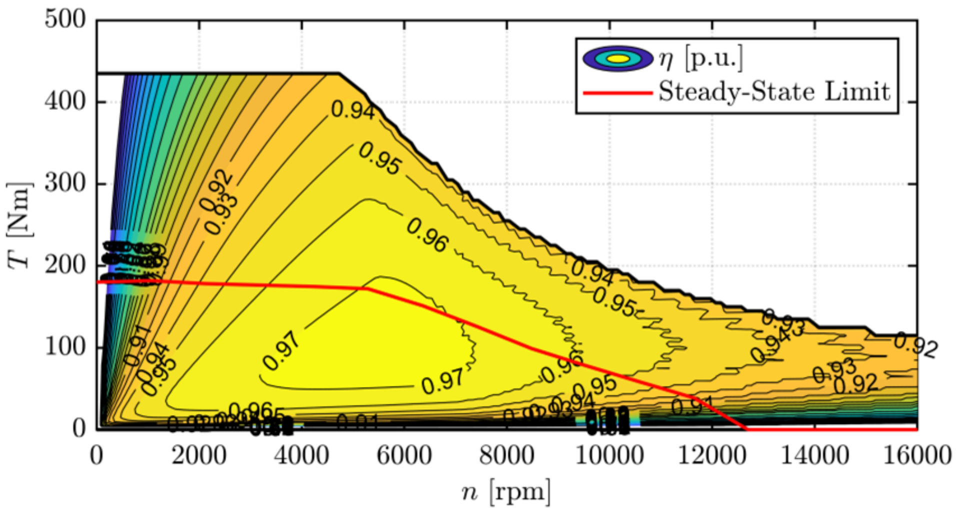

Model3 custom

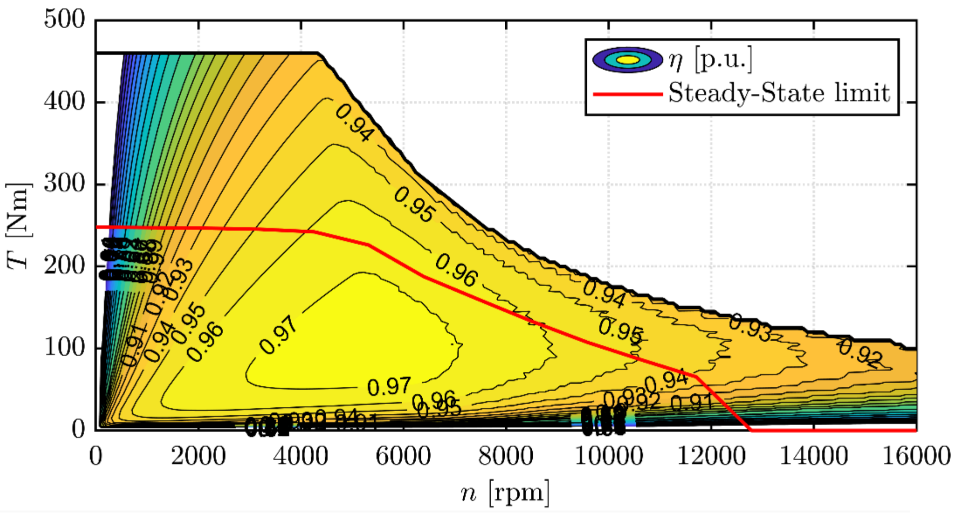

PWM waveforms and additional loss

PWM loss computed at 100Nm, 5000rpm
- Additional loss 172W (+14%)
- Mostly on the stator (eddy current term)

PM loss explodes due to PWM:
- Fine segmentation mandatory
- Refinement with transient FEA

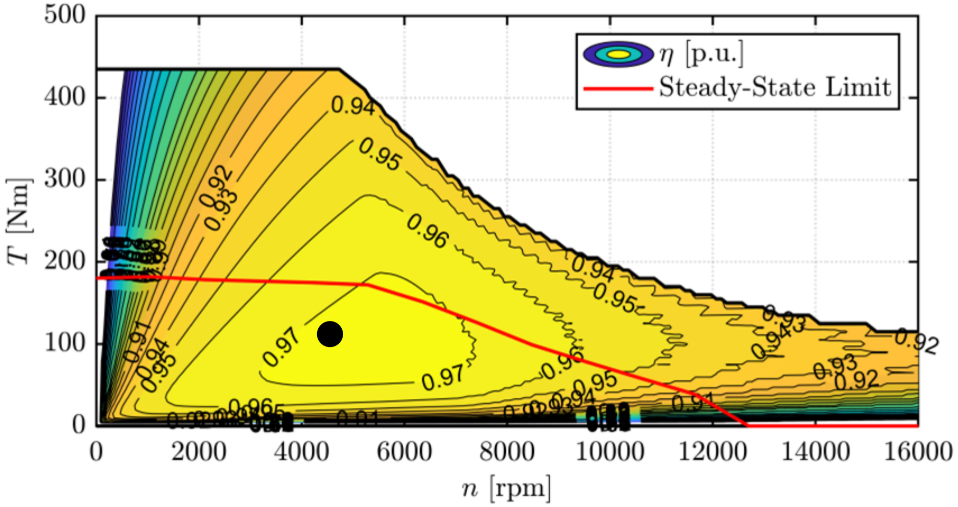

Phase currents at 5000 rpm, 10kHz PWM

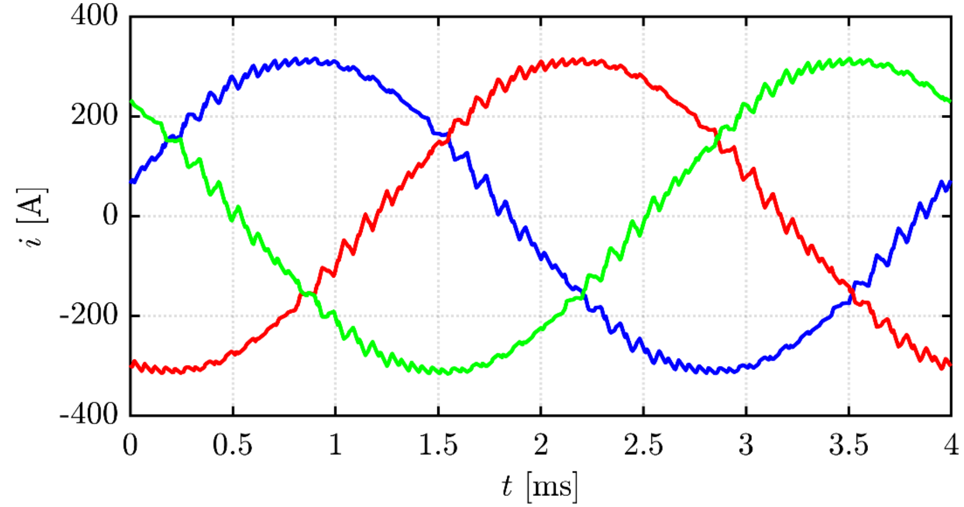

Loss breakdown

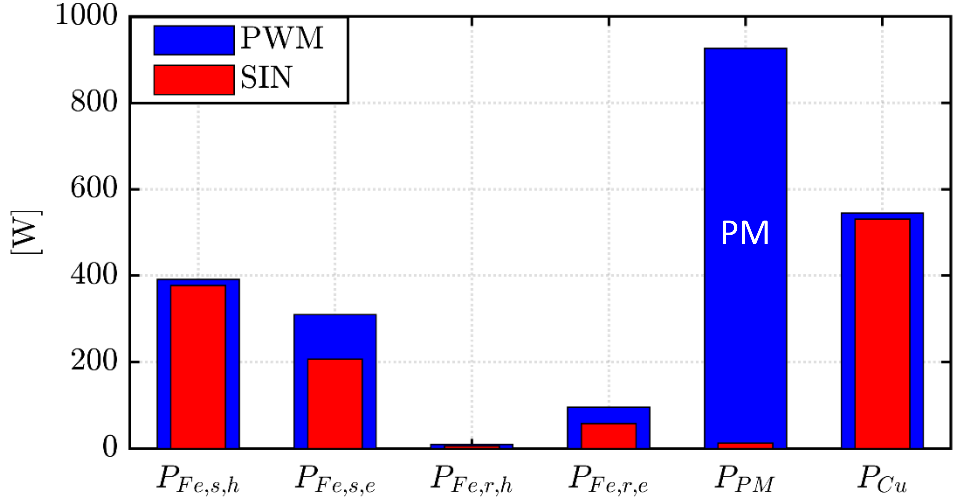

syreDrive: Control Simulation

The Simulink (and soon PLECS) model of the e-drive is automatically generated, along with floating ANSI-C control code

Different options are possible

For e-motor design, we mostly use PWM current calculation for FEM re-evaluation

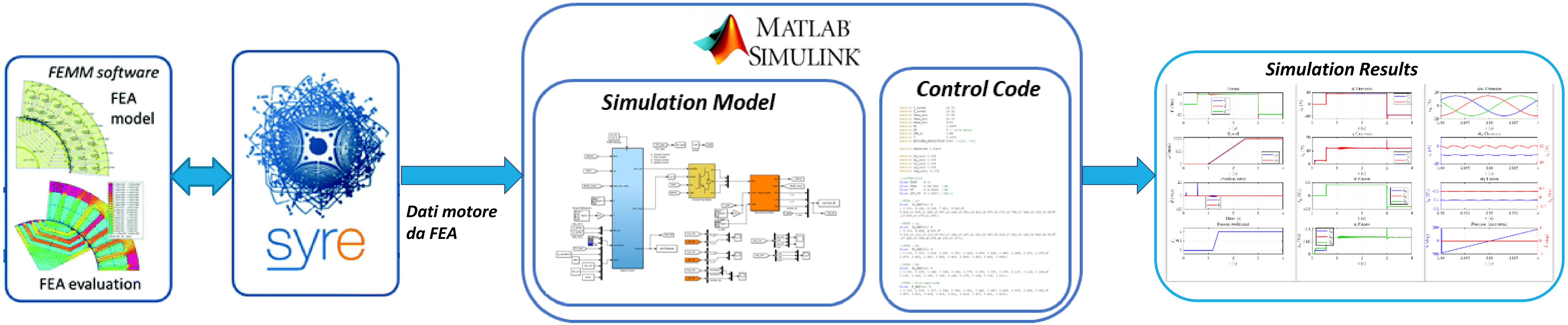

[17] A. Varatharajan, D. Brunelli, S. Ferrari, P. Pescetto and G. Pellegrino, "syreDrive: Automated Sensorless Control Code Generation for Synchronous Reluctance Motor Drives," 2021 IEEE Workshop on Electrical Machines Design, Control and Diagnosis (WEMDCD), Modena, Italy, 2021, pp. 192-197.

syreDrive tab

Main features

- Circuital motor model
- Flux-map based
  - 2D (dq) or 3D (dq-theta) maps
  - time-average or instantaneous PWM
- Discrete-time control
- Source code in ANSI-C
  - Torque control, speed control, current control
  - Sensorless control

syreDrive tab of GUI_Syre_MMM

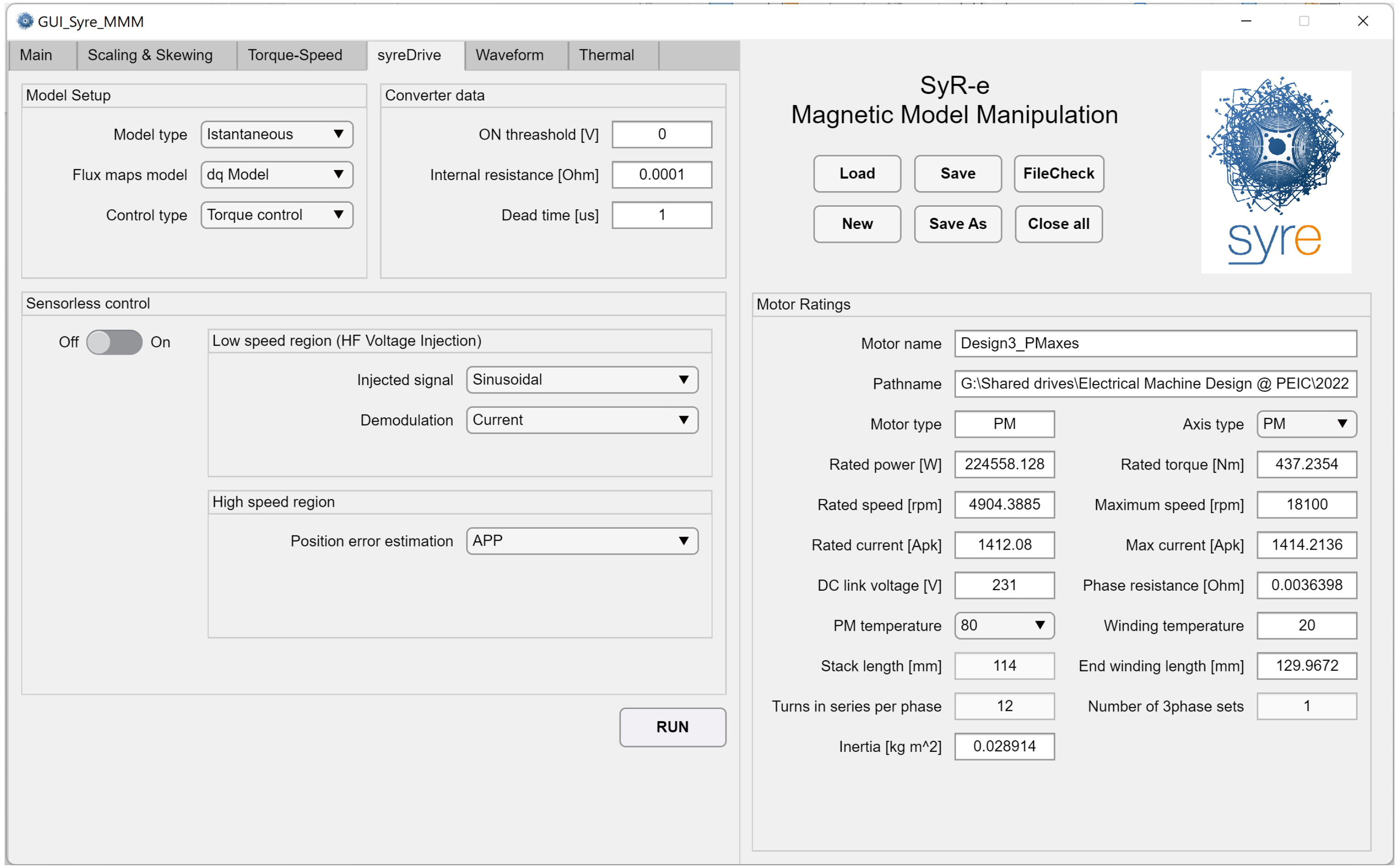

Simulink Model Overview

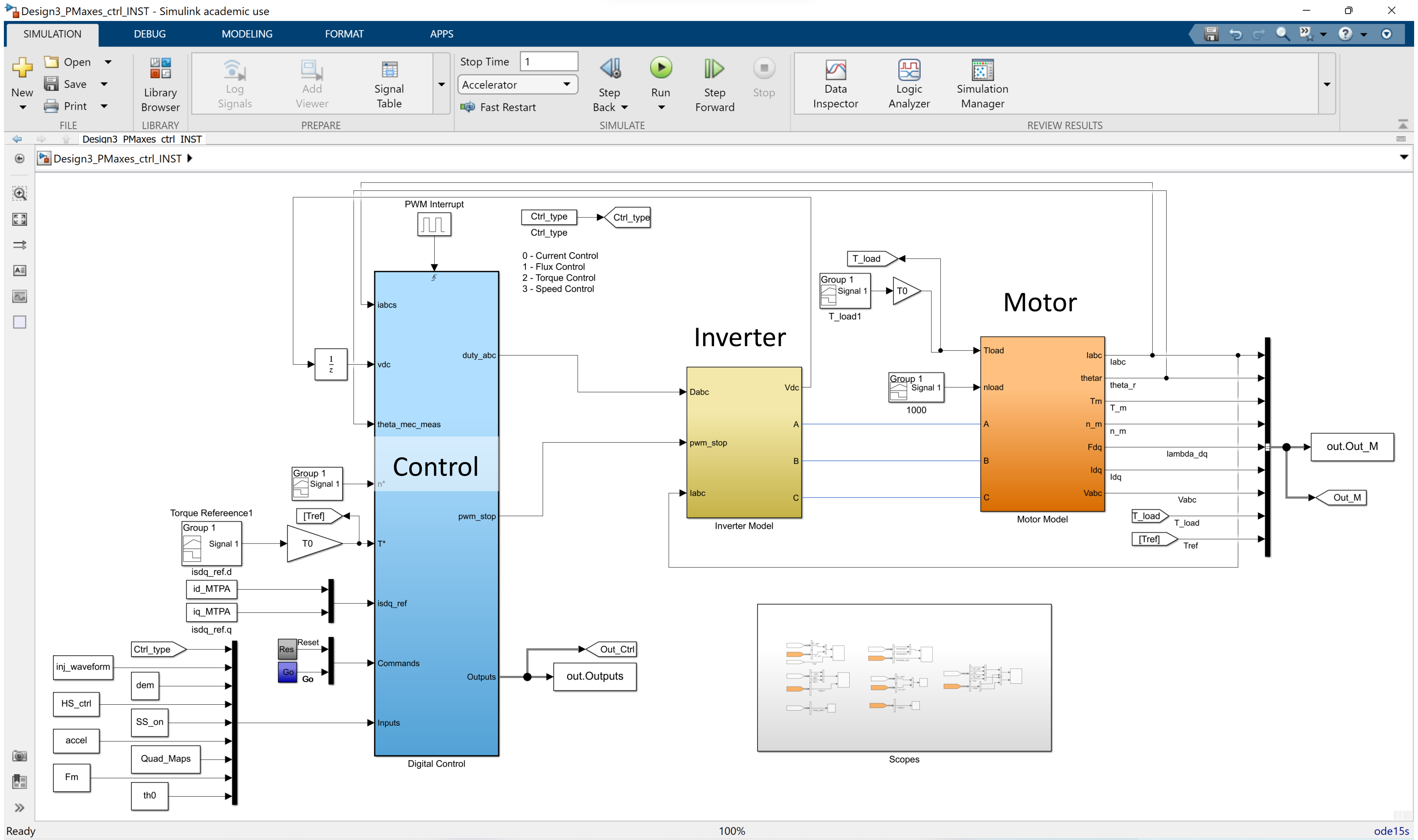

Control Subsystem

Triggered sub-system executed at sampling time Ts

C-MEX S-Function with user defined library calls

C source code

- automatically generated and calibrated using the machine params
- Accessible

The control code is portable to dSPACE and STM32 ARM based MCUs

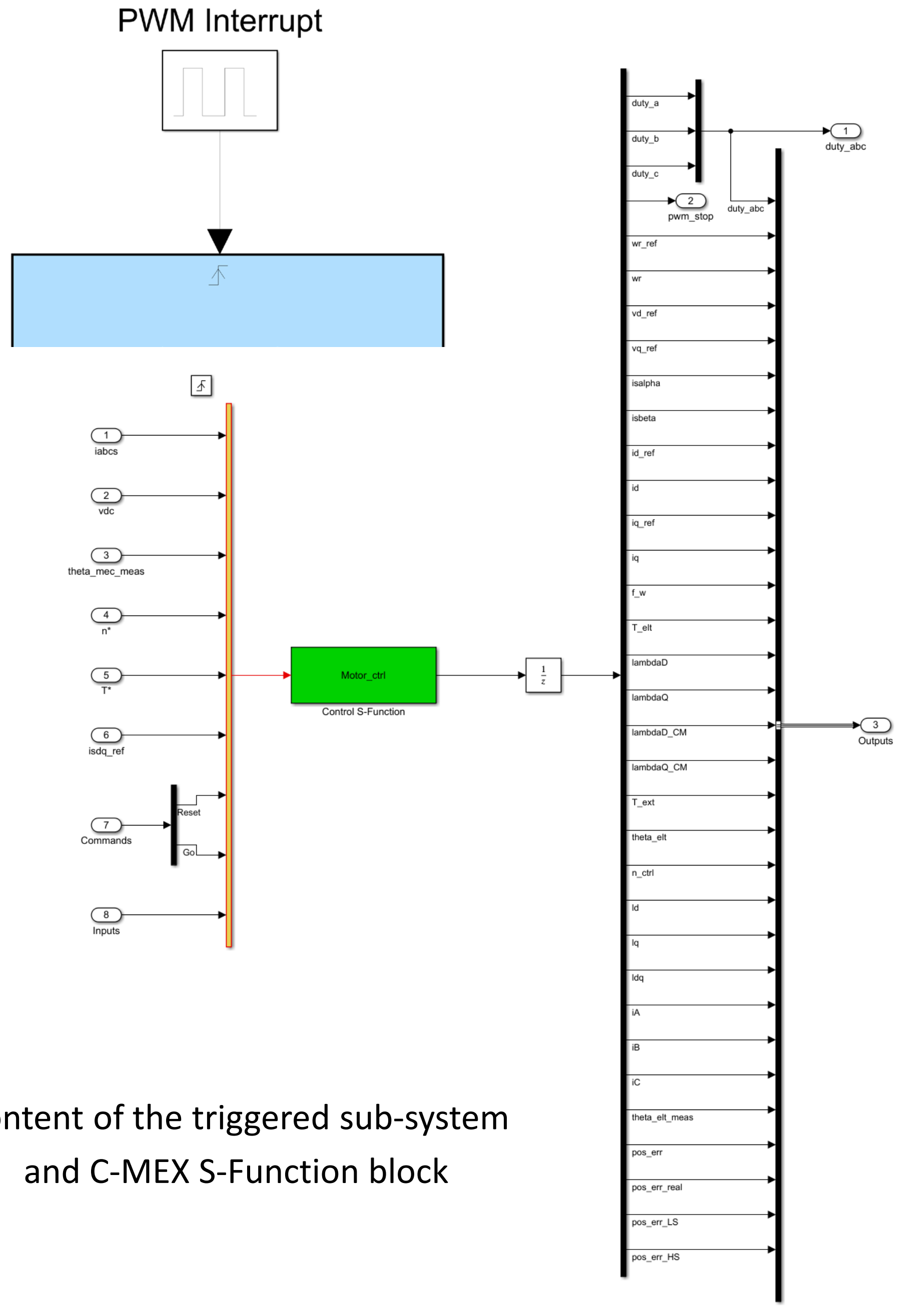

Content of the triggered sub-system and C-MEX S-Function block

Inverter Subsystem

Based on Simscape 3-ph circuital Converter

- Instantaneous or time-averaged switches
- Dead-time effect considered
- Forward voltage and R_{ON} of semiconductors

The circuital model is compatible with fault conditions

Content of the Inverter subsystem

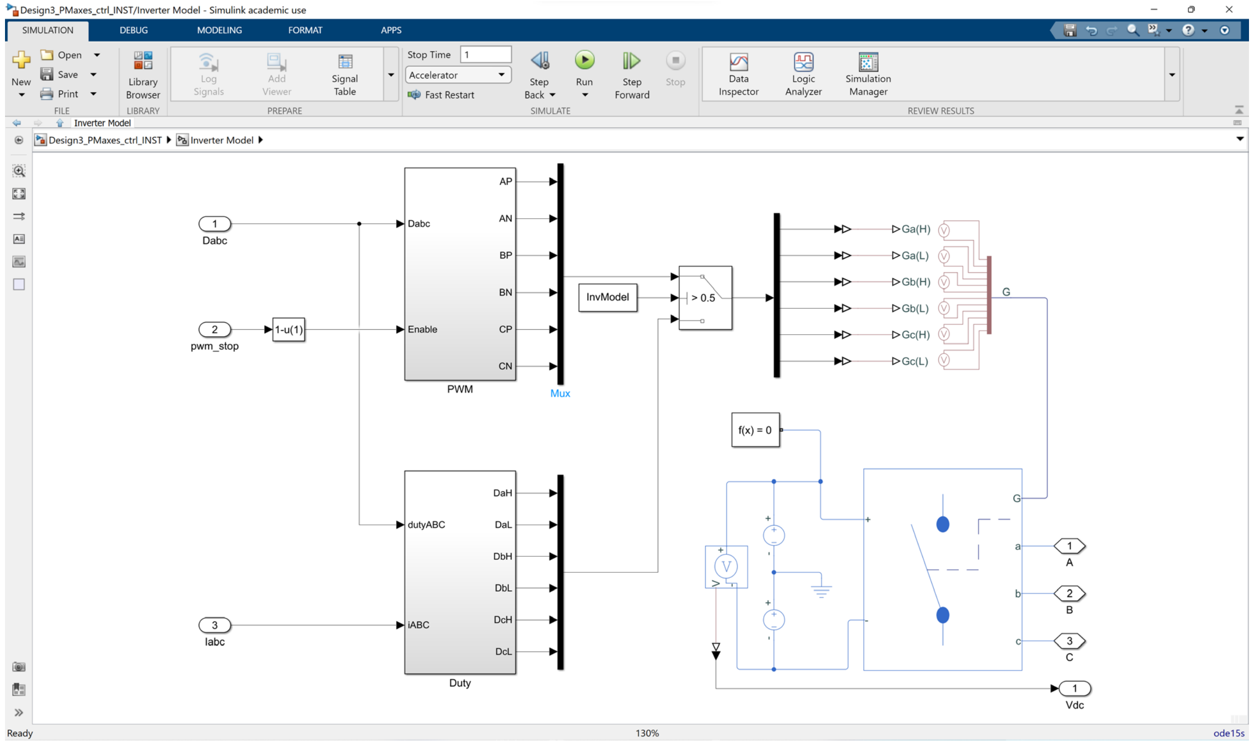

[18] A. Bojoi, "Advanced Dynamic Model of E-motor for Control Rapid Prototyping [MSc Thesis]", Politecnico di Torino, 2022, https://webthesis.biblio.polito.it/22088/1/tesi.pdf

Motor Subsystem

Controlled current generators approach

Phase currents are calculated by manipulation of current generators' voltages, using the motor parameters and flux maps

Inverse flux maps (flux input, current output)

$$i_d = f(\lambda_d, \lambda_q)$$
$$i_q = g(\lambda_d, \lambda_q)$$

Content of the Motor subsystem

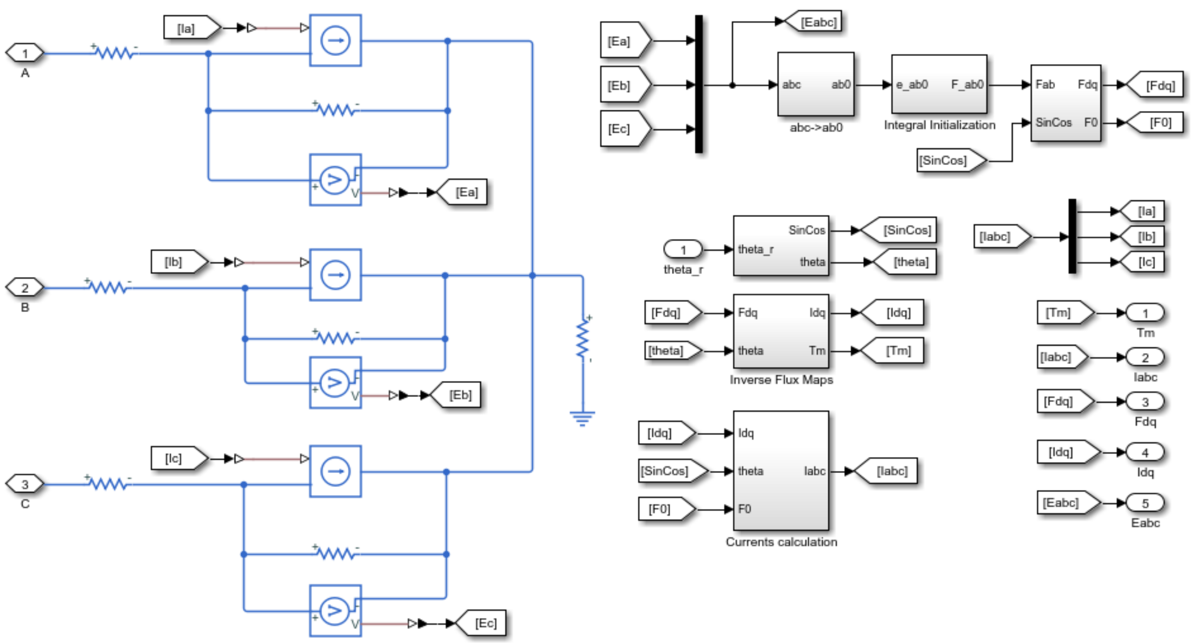

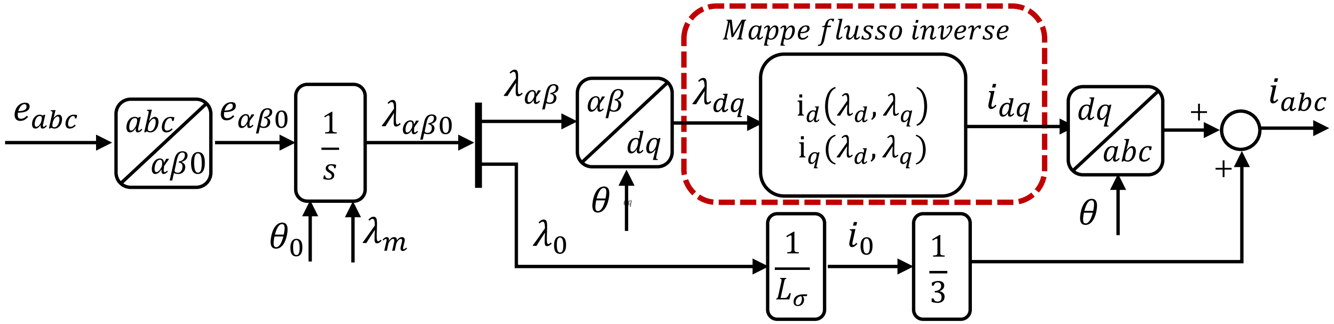

Motor Subsystem

Controlled current generators approach

Phase currents are calculated by manipulation of current generators' voltages, using the motor parameters and flux maps

Inverse flux maps (flux input, current output)

$$i_d = f(\lambda_d, \lambda_q)$$
$$i_q = g(\lambda_d, \lambda_q)$$

Controlled current generators approach

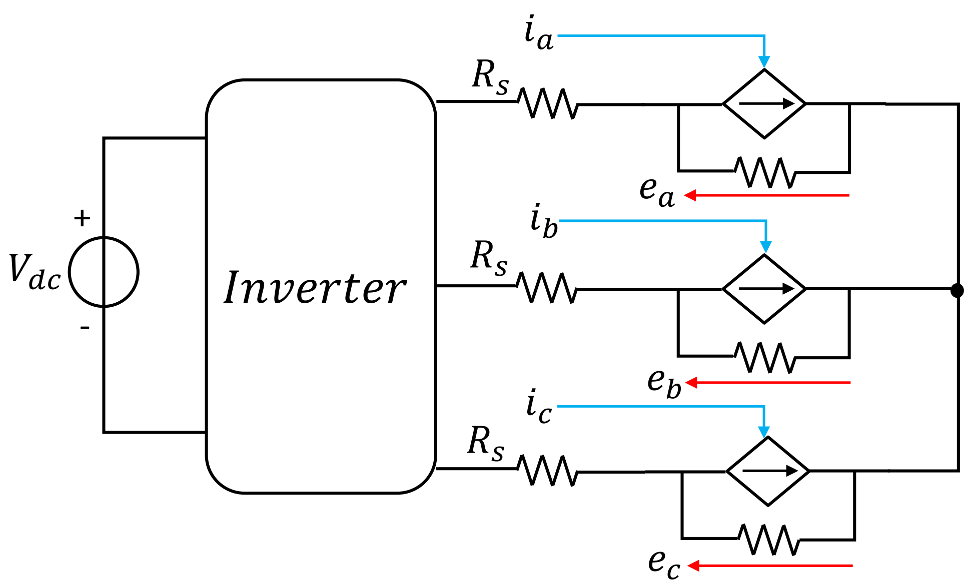

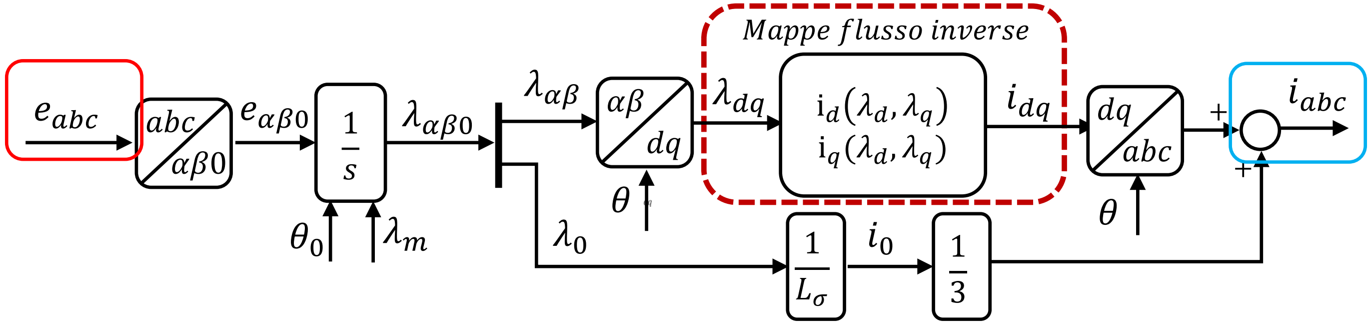

Results: torque reversal

Peak torque reversal is shown at 2000 rpm

- FOC control with MTPA id, iq references is used
- PWM time averaged model

This example uses the standard dq model of the machine (no ripple effect), based on inverse dq flux maps

Under proper current control, currents are sinusoidal, and torque is smooth

Torque reversal, **dq** model

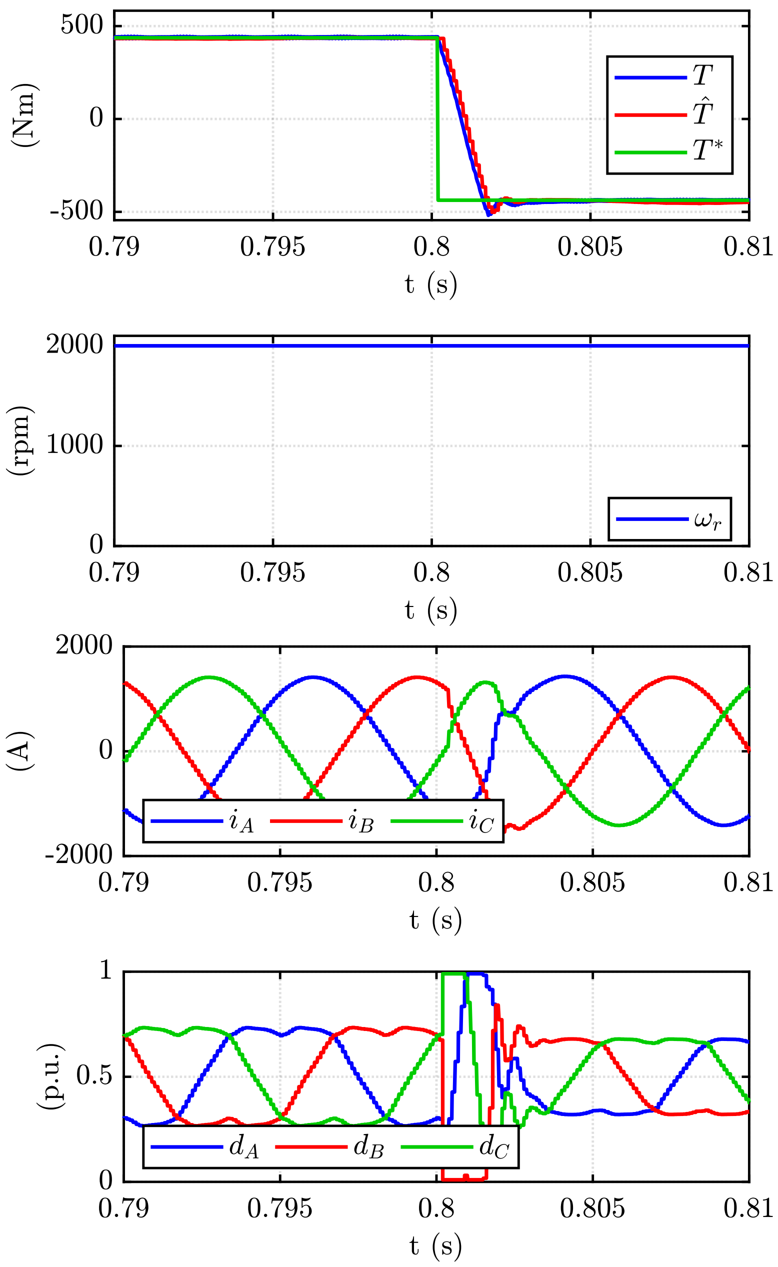

dq-theta model

Torque reversal, **dq-theta** model

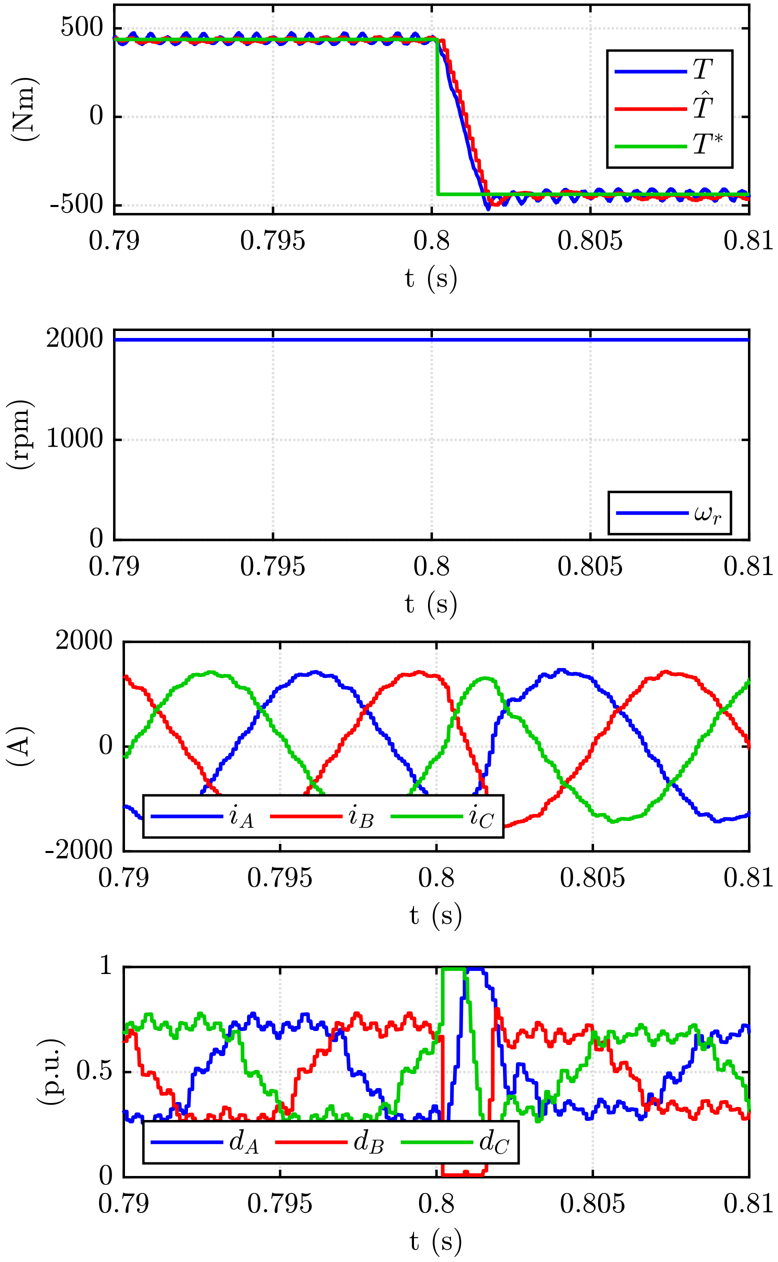

Peak torque reversal is shown at 2000 rpm

- FOC control with MTPA id, iq references is used
- **PWM time averaged model**

The **dq-theta model** of the machine is used this time, including the flux linkage and torque harmonic effects

Currents no longer sinusoidal, torque ripple is evident

High-fidelity model for better control development and better modelling overall (model-based control design, digital twin, ..)

Results: PWM ripple

4000 rpm, -430 Nm

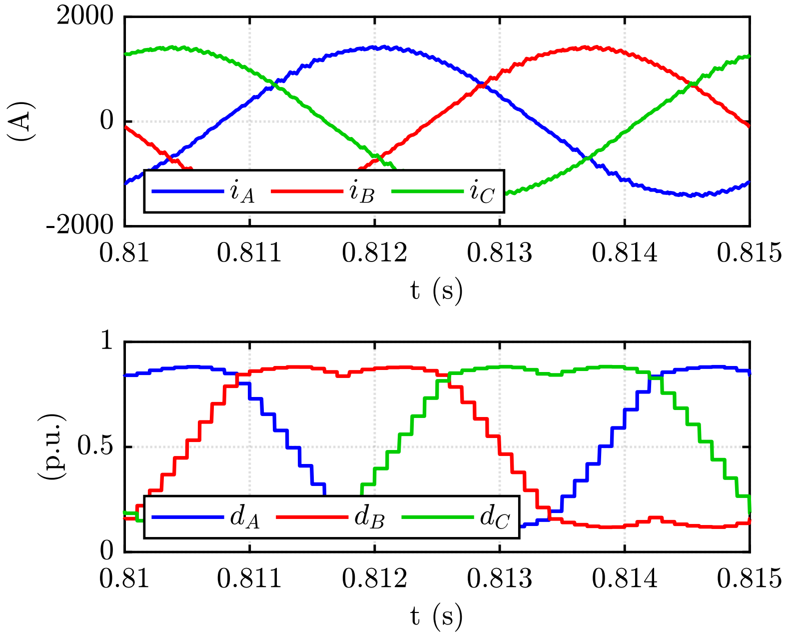

2000 rpm, -430 Nm

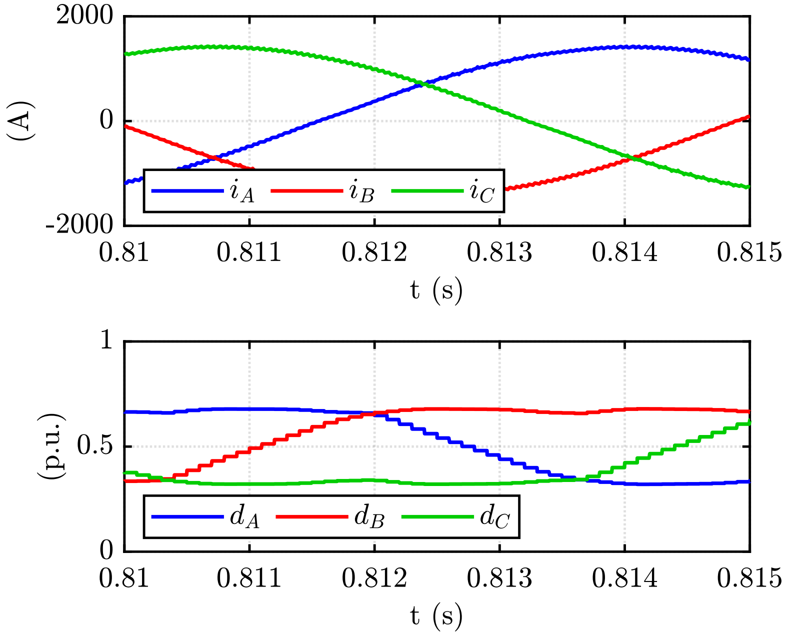

Steady-state current waveforms at 4000 rpm and 2000 rpm, under load

The PWM frequency is 10 kHz

Pk-pk current ripple is mild at all operating conditions, as its secondary effects (loss)

The worst-case dc-link voltage of 231V is best-case in this sense

Yet, 10 kHz is lower than real

Conclusion

The SyR-e approach to the design of IPM machines for traction was presented, using Tesla Model3 as reference

The FEAfix design plane covers many aspects of the design, and permits to cross design goals and constraints in graphic and insightful manner

In the example, PM and copper mass were considered as additional constraints, and the stack length was reduced with respect to the initial machine

Other aspects such as loss evaluation, thermal and structural simulation, control simulation were touched in the presentation

SyR-e is evolving under the push of the industry and the dedication of talented researchers

We invite you to try SyR-e and collaborate with us!

References

[1] A. Krings and C. Monissen, “Review and Trends in Electric Traction Motors for Battery Electric and Hybrid Vehicles,” in *2020 International Conference on Electrical Machines (ICEM)*, 2020

[2] M. Gamba, G. Pellegrino and A. Vagati, "A new PM-assisted Synchronous Reluctance machine with a nonconventional fractional slot per pole combination," 2014 OPTIM, Brasov, Romania

[3] Electric Machines Roadmap 2020 – Advanced Propulsion Center UK www.apcuk.co.uk/app/uploads/2021/09/https___www.apcuk_.co_.uk_app_uploads_2021_02_Exec-summary-Technology-Roadmap-Electric-Machines-final.pdf

[4] K. Bennion, G. Moreno, “Convective Heat Transfer Coefficients of Automatic Transmission Fluid Jets with implications for Electric Machine Thermal Management”, International Technical Conference and Exhibition on Packaging and Integration of Electronic and Photonic Microsystems, San Francisco, 2015

[5] S. Ferrari and G. Pellegrino, "FEAfix: FEA Refinement of Design Equations for Synchronous Reluctance Machines," in *IEEE Transactions on Industry Applications*, vol. 56, no. 1, pp. 256-266, Jan.-Feb. 2020.

[6] P. Ragazzo, G. Dilevrano, S. Ferrari and G. Pellegrino, “Design of IPM Synchronous Machines Using Fast-FEA Corrected Design Equations," presented at *ICEM 2022*, Valencia

[7] G. Pellegrino, F. Cupertino and C. Gerada, "Automatic Design of Synchronous Reluctance Motors Focusing on Barrier Shape Optimization," in IEEE Transactions on Industry Applications, vol. 51, no. 2.

[8] F. Cupertino, G. Pellegrino and C. Gerada, "Design of Synchronous Reluctance Motors With Multiobjective Optimization Algorithms," in IEEE Transactions on Industry Applications, vol. 50, no. 6

[9] S. Ferrari, P. Ragazzo, G. Dilevrano and G. Pellegrino, "Flux-Map Based FEA Evaluation of Synchronous Machine Efficiency Maps," 2021 IEEE Workshop on Electrical Machines Design, Control and Diagnosis (WEMDCD), 2021

[10] S. Ferrari, G. Dilevrano, P. Ragazzo and G. Pellegrino, "The dq-theta Flux Map Model of Synchronous Machines," *2021 IEEE Energy Conversion Congress and Exposition (ECCE)*, Vancouver, BC, Canada, 2021

[11] Pellegrino, G., Jahns, T.M., Bianchi, N., Soong, W. and Cupertino, F., The Rediscovery of Synchronous Reluctance and Ferrite Permanent Magnet Motors Tutorial Course Notes.

[12] P. Ragazzo, S. Ferrari, N. Riviere, M. Popescu, and G. Pellegrino, “Efficient Multiphysics Design Workflow of Synchronous Reluctance Motors,” in *2020 International Conference on Electrical Machines (ICEM)*, Gothenburg, Sweden, Aug. 2020

[13] S. Ferrari, P. Ragazzo, G. Dilevrano and G. Pellegrino, "Flux and Loss Map Based Evaluation of the Efficiency Map of Synchronous Machines," under review.

[14] MotorXP, Performance Analysis of the Tesla Model 3 Electric Motor using MotorXP-PM. VEPCO, Jun. 2020, https://motorxp.com/wp-content/uploads/mxp analysis TeslaModel3.pdf

[15] M. Palmieri, M. Perta, F. Cupertino and G. Pellegrino, "High-speed scalability of synchronous reluctance machines considering different lamination materials," *IECON 2014 - 40th Annual Conference of the IEEE Industrial Electronics Society*, Dallas, TX, 2014.

[16] G. Dilevrano, P. Ragazzo, S. Ferrari, G. Pellegrino and T. Burress, “Magnetic, Thermal and Structural Scaling of Synchronous Machines,“, to be presented at *2022 IEEE Energy Conversion Congress and Exposition (ECCE)*, Detroit, MI, 2022

[17] A. Varatharajan, D. Brunelli, S. Ferrari, P. Pescetto and G. Pellegrino, "syreDrive: Automated Sensorless Control Code Generation for Synchronous Reluctance Motor Drives," 2021 IEEE Workshop on Electrical Machines Design, Control and Diagnosis (WEMDCD), Modena, Italy, 2021, pp. 192-197.

[18] A. Bojoi, “Advanced Dynamic Model of E-motor for Control Rapid Prototyping [MSc Thesis]”, Politecnico di Torino, 2022, https://webthesis.biblio.polito.it/22088/1/tesi.pdf

Thank you!

Questions are very welcome

gianmario.pellegrino@polito.it and simone.ferrari@polito.it

www.peic.polito.it